TECHNISCHE UNIVERSITÄT MÜNCHEN

Lehrstuhl für Tierhygiene

Up-regulation of sterol regulatory element binding protein 2 (Srebp2)-mediated cholesterol biosynthesis in prion infected cells

Christian Erich Bach

Dedicated to my parents

for all their help and support

Table of contents

Summary

English version

Prion diseases are fatal neurodegenerative diseases that affect mammals including humans. While the prion disease pathology in the central nervous system is well documented, the host response to prion infection and changes within the cell caused by prions remain obscure. Understanding the host cell response to prion infection is important for unraveling the mechanisms that contribute to the propagation of TSEs agents. Knowledge of cellular metabolic pathways altered by the prion infection might lead to new strategies to activate cellular clearance mechanisms or to prevent infection and cell death.

To determine the differential gene expression of prion and mock infected cells cDNA microarray analysis was performed. Previous studies by other groups used the entire prion infected mouse brain or specific brain areas or cell culture models like microglia and neuronal cell lines. Transcriptome analysis of prion infected animals and cell cultures suggested alterations in several cellular pathways. However, no conclusive interpretation of the role of specific pathways altered by prion infection could be drawn. This might at least in part be due to a) different microarray platforms, b) different prion strains, c) different sampling time points during the course of infection or d) mixed cell populations.

To avoid these possible side effects a very susceptible cell clone to prion infection out of the murine neuroblastoma cell line N2a was used in this thesis. Additionally for microarray analysis a 22L and mock infected cell population with identical passage history (18 passages) after infection was used. Cells were kept under identical cell culture conditions before mRNA extraction, resulting in a highly controlled genome-wide cDNA microarray analysis and the detection of over 100 differentially expressed genes in prion infected cells compared to mock cells. These genes were linked to several metabolic pathways, such as ATP binding, cell cycle, cytoskeleton, DNA binding, mRNA processing, protein binding, transport and binding proteins and cholesterol metabolism. The most affected pathway found within differentially regulated genes belonged to the cholesterol metabolism. Nine genes of the whole cholesterol pathway were found significantly up-regulated including the genes for the regulatory proteins HMGCoA-reductase and the transcription factor Srebp2 (sterol regulatory element binding protein 2) in prion infected cells. Therefore, the cholesterol pathway was chosen for more detailed analysis. A significant up-regulation of the cholesterogenic genes coding for Srebp2, the LDL receptor (Ldlr) and C-4 methyl sterol oxidase (Sc4mol) was found in another neuronal cell line (GT1) infected with the RML prion strain but not in prion exposed BV-2

glia cells. On protein level a higher amount of the Srebp2 precursor protein and also a higher transcriptional activity caused by prion infection was determined. Additionally, significantly higher levels of free and total cholesterol were detected in prion infected cells. Moreover, a reduction in the total amount of PrP^{Sc} due to transient down-regulation of the cholesterol synthesis using siRNA against Srebp2 could be shown in the absence of external cholesterol sources. Finally, in primary hippocampal neurons exposed to 22L prions the genes for Srebp2, Ldlr and Sc4mol were found significantly up-regulated, whereas in sharp contrast the expression of these genes was not found altered in prion-exposed primary astrocytes. These results demonstrate that prion propagation not only depends on the availability of cholesterol, but that neuronal cells themselves respond to prions with specific up-regulation of cholesterol biosynthesis. Overall, these findings provide new insights into the reaction of neuronal cells to prion infection and point to the cholesterol metabolisms as the most affected up-regulated pathway in neuronal cells. This finding could probably be used as a new target for prion disease therapy.

Deutsche Version

Prion-Erkrankungen sind tödlich verlaufende, neurodegenerative Erkrankungen in Säugetieren, inklusive dem Menschen. Der Krankheitsverlauf im zentralen Nervensystem ist bereits weitgehend untersucht, wogegen die Reaktionen des Wirtes auf und die Veränderungen in der Zelle durch Prionen noch weitgehend unbekannt sind. Das Verständnis der Reaktion der Wirtszelle auf eine Prion-Infektion ist wichtig, um Mechanismen zu finden, die an der Vermehrung der Prionen beteiligt sind. Die Kenntnis über zelluläre Stoffwechselwege, die durch eine Prion-Infektion verändert werden, könnte zu neuen Strategien führen, um z.B. zelluläre Mechanismen zur Beseitigung des Agens zu aktivieren oder die Infektion und damit das Sterben der Zelle zu verhindern.

Um die unterschiedliche Genexpression in Prion- und Mock-infizierten Zellen zu bestimmen wurde in dieser Arbeit eine cDNS Microarray-Studie durchgeführt. In Untersuchungen anderer Gruppen wurden bisher entweder das gesamte Mausgehirn bzw. spezifische Gehirnareale, oder Zellkulturmodelle wie Mikrogliazellen und neuronale Zelllinien verwendet. Transkriptom-Analysen von Prion-infizierten Tieren und Zellkulturen zeigten Veränderungen in verschiedenen Stoffwechselwegen der Zelle. Allerdings konnte aus den Daten keine endgültige Aussage über die Rolle eines spezifischen, von der Prion-Infektion beeinflussten Metabolismus getroffen werden. Dies könnte, zumindest teilweise, auf Unterschiede in den a) Microarray-Systemen, b) Prionenstämmen, c) Zeitpunkten der Probenentnahme während der Infektion in den jeweiligen Studien oder d) auf die gleichzeitige Untersuchung verschiedener Zelltypen innerhalb einer Studie zurückzuführen sein.

Um diese möglichen, negativen Einflüsse zu vermeiden, wurde in dieser Doktorarbeit ein für die Prion-Infektion sehr empfänglicher Zellklon der Neuroblastomzelllinie N2a verwendet. Weiterhin wurde für die Microarray-Studie eine mit dem Prionenstamm 22L-und Mock-infizierte Zellpopulation mit gleicher Passagenzahl (Passage 18) verwendet. Die Zellen wurden vor der RNS-Extraktion unter identischen Bedingungen kultiviert, wodurch eine äußerst kontrollierte, genomweite cDNS Microarray-Studie erzielt wurde. In deren Verlauf konnten über 100 differenziell exprimierte Gene in den Prion-infizierten Zellen verglichen mit den Mock-infizierten Zellen identifiziert werden. Die Gene konnten verschiedenen funktionellen Gruppen und Stoffwechselwegen zugeordnet werden wie z.B. ATP Bindung, Zellzyklus, Zytoskelett, DNS-Bindung, mRNS-Prozessierung, Proteinbindung, Transport- und Bindeproteine und Cholesterinmetabolismus, wobei dieser der am stärksten veränderte Syntheseweg innerhalb der unterschiedlich regulierten Gene war. In den Prion-infizierten Zellen war die Expression von neun Genen, die bei der Cholesterinsynthese eine wesentliche

Rolle spielen, signifikant hochreguliert, inklusive der Gene der regulatorischen Proteine HMGCoA-Reduktase und des Transkriptionsfaktors Srebp2 (sterol regulatory element binding protein 2). Auf Grund dieser Ergebnisse wurde die Cholesterinsynthese näher untersucht. Eine signifikante Hochregulation der Gene für Srebp2, den Ldl Rezeptor (*Ldlr*) und der C-4 methyl sterol oxidase (*Sc4mol*) wurde auch in einer weiteren neuronalen Zelllinie (GT1), die mit dem Prionenstamm RML infiziert war, gefunden, nicht aber in Prion-exponierten BV-2 Mikrogliazellen. Auf Proteinebene konnte, verursacht durch die Prion-Infektion, eine größere Menge des Srebp2-Vorläuferproteins und eine erhöhte transkriptionale Aktivität von Srebp2 nachgewiesen werden. Zusätzlich wurde eine signifikant erhöhte Menge an Gesamt- und freiem Cholesterin in den Prion-infizierten Zellen gefunden. Desweitern konnte eine Reduktion der PrP^{Sc}-Menge durch die vorübergehende Herabsetzung der Cholesterinsynthese mittels siRNA gegen Srebp2, in Abwesenheit einer externen Cholesterinquelle, gezeigt werden. Schließlich wurde auch in Prion-exponierten primären Neuronen des Hippocampus eine signifikante Erhöhung der Genexpression von *Srebf2*, *Ldlr* und *Sc4mol* gefunden, wogegen in Prion-exponierten primären Astrozyten keine Unterschiede in der Regulation dieser Gene nachzuweisen war. Die Untersuchungen belegen, dass die Vermehrung von Prionen nicht nur von der Verfügbarkeit des Cholesterins abhängig ist, sondern zeigen auch, dass neuronale Zellen auf eine Prion-Infektion mit einer spezifischen Hochregulierung der Cholesterinbiosynthese reagieren. Zusammenfassend geben die Ergebnisse neue Einblicke in die Reaktion von neuronalen Zellen auf die Prion-Infektion und verweisen auf den Cholesterinmetabolismus als den am stärksten veränderten Metabolismus in neuronalen Zellen. Diese Erkenntnisse könnten möglicherweise zur Entwicklung neuer Therapieansätze gegen Prion-Erkrankungen führen.

1. Introduction

Prion diseases, also called transmissible spongiform encephalopathies (TSEs), which can occur in mammals including humans, cause fatal neurological disorders in the central nervous system (CNS) and can under certain circumstances be transmitted within or even between species (Weissmann *et al.* 1996; Prusiner 1998). Prion diseases are already known for many decades as, scrapie of sheep and goats was described as early as 1732 (McGowan 1914; McGowan 1922). But only in the last 20 years, as a new form of TSE, the variant Creutzfeldt-Jakob disease (vCJD) arose in humans, prion diseases attracted public interest. The key event was the occurrence of the bovine spongiform encephalopathy (BSE) in the early 1980s and the linkage of this animal disease to vCJD in humans (Will *et al.* 1996; Collinge and Rossor 1996; Will 1998). Over 180.000 clinical BSE cases in the UK and also 411 in Germany were detected until November of 2008 (Homepage of the Federal Ministry of Food, Agriculture and Consumer Protection; http://www.bmelv.de/cln_044/nn_752016/DE/07-SchutzderTiere/Tierseuchen/BSE/BSE-FaelleDeutschland.html__nnn=true). The transmission of BSE to humans demonstrates the importance of detection and understanding of the nature of prion diseases to protect the human population.

In humans prion disorders were described in the 1920s (Creutzfeldt 1920; Jakob 1921) without the knowledge of the causative agent. As TSEs can have a very long incubation time, these diseases were initially described as slow-virus infections (Gajdusek 1977). Unlike common virus diseases an immune response to the infectious agent was missing and no virus could be isolated out of patient material. Further experiments showed that the causative agent could not be inactivated by commonly used inactivation procedures that destroy nucleic acids through UV-radiation. Only the use of processes that destroy proteins through denaturation or hydrolysation could reduce the infectivity (Alper *et al.* 1966; Alper *et al.* 1967). In 1967 Griffith hypothesized that the causative agent might be a protein (Griffith 1967). In 1982 a protease-resistant glycoprotein was isolated from infected hamster brains by Prusiner and colleagues. This glycoprotein was found to be the main component of the infectious fraction in the hamster brains (Prusiner 1982; Prusiner *et al.* 1984). After identifying this protein Prusiner postulated the "protein-only" hypothesis which implicates that the causative agent for prion diseases propagates in the absence of nucleic acids and consists only of protein. As this feature characterizes a new class of infectious agent different from pathogens like viruses he suggested the new term "**prion**" for "**pro**teinaceous **in**fectious particle" (Prusiner 1982). Stanley Prusiner was awarded with the Nobel Prize for medicine in 1997 for proposing,

elucidating and confirming the protein-only hypothesis. Intensive investigations on the new pathogen revealed that mammalian prions are abnormally folded isoforms, termed PrP^{Sc} (Bolton *et al.* 1982), of a cellular prion protein PrP^{C} encoded by the host (Oesch *et al.* 1985). In the infected individual PrP^{Sc} accumulates predominantly in the CNS leading to activation of glia cells (Prusiner *et al.* 1984), neuronal cell death (Prusiner 1982) and spongiform lesions (Prusiner *et al.* 1990) (**Figure 1**).
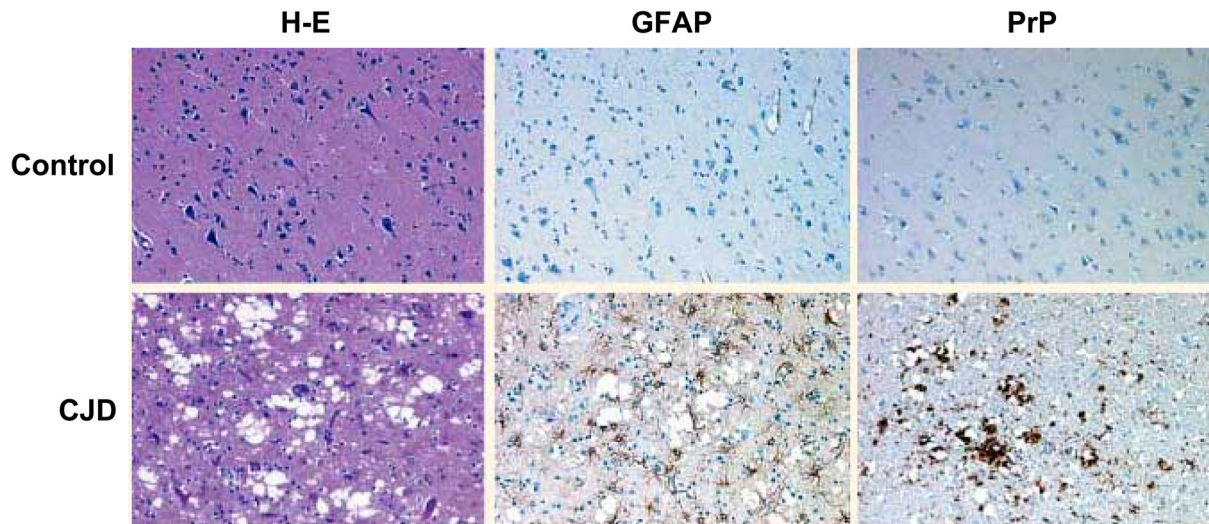
Figure 1: Neuropathological changes in TSE affected individuals. Frontal cortex brain slices of a healthy control (upper row) and a patient suffering from Creutzfeldt-Jacob disease (CJD; lower row). Staining with haematoxylin-eosin in the left panels shows neuronal loss and prominent spongiosis. Gliosis caused by strong proliferation of reactive astrocytes (middle panels) and perivacuolar prion protein deposits (right panels) are visible using antibodies against glial fibrillary acidic protein (GFAP) and the prion protein, respectively (taken from (Aguzzi *et al.* 2001)).

During the next years the possible existence of a new infectious agent consisting only of a pathogenic protein isoform was controversially discussed in the scientific community. Several recent studies as for example the in vitro generation of infectious prion protein out of brain-derived PrP^{C} (Castilla *et al.* 2005) and the infectious nature of misfolded recombinant PrP in some transgenic mouse models (Legname *et al.* 2004) strongly support the prion-only hypothesis. The auto-catalytic propagation of specific protein isoforms has also been demonstrated for some fungi proteins, termed later yeast prions (Wickner 1994).

1.1 Prion diseases in animals

Table 1: Prion diseases in animals

Host	Disease	Acronym	Cause
Cattle	Bovine spongiform encephalopathy	BSE	• Ingestion of prion contaminated food (meat-and-bone meal) • Spontaneous conformational change from PrP^C to PrP^{Sc}?
Cats and big cats	Feline spongiform encephalopathy	FSE	Ingestion of prion contaminated food
Deer and elk	Chronic wasting disease	CWD	• Ingestion of prion contaminated food • Vertical and horizontal transmission
Mink	Transmissible mink encephalopathy	TME	Ingestion of prion contaminated food
Sheep and goat	Scrapie	N/A	Vertical and horizontal transmission

The best known TSE in animals is scrapie appearing in sheep and goats. The first written description of the disease appeared in 1732 (McGowan 1914; McGowan 1922). The disease is termed "scrapie" due to the excessive scratching of the infected animals. Scrapie can be transmitted horizontally between individuals within a flock and also vertically from a dam to its child (Brotherston *et al.* 1968; Dickinson *et al.* 1974).

Further animal TSEs are feline spongiform encephalopathy (**FSE**) of cats and big cats (Wyatt *et al.* 1991), transmissible mink encephalopathy (**TME**) (Burger and Hartsough 1965) and of greater interest for human economy and/or health: Chronic wasting disease (**CWD**) in deer and elk and bovine spongiform encephalopathy (**BSE**) in cattle.

Chronic wasting disease (CWD) infections occur in white-tailed deer, Rocky Mountain elk, mule deer (Williams and Miller 2002), and moose (Williams 2005). In Northern America CWD is of great concern as it now occurs endemic in states like Colorado, Nebraska and Wyoming and is also spreading to other parts of America, including Canada. In the beginning the disease was found in the Midwest but was recently also detected in New York State (Williams 2005; Aguzzi and Sigurdson 2004). White tailed deer are mostly susceptible to CWD and the disease is located in areas with large populations of these animals. There was a great discussion about the possibility of transmission of CWD from deer to humans as three young deer hunters from these areas died of CJD (Belay *et al.* 2004). Although there was no direct link found between these CJD cases and CWD, as no extensive amyloidosis characteristics typical for vCJD or CWD (Liberski *et al.* 2001) could be detected via autopsy, the possibility of transmission has to be closely monitored, especially as CWD, similar to BSE, is also transmissible to human PrP^C expressing mice (Tamguney *et al.* 2006), nonhuman primates (Marsh *et al.* 2005) and high titers of prions can be detected in peripheral parts like muscle and salvia in CWD infected deer (Angers *et al.* 2006; Mathiason *et al.* 2006). In Europe CWD surveillance has been more limited. The test of 7300 cervids, both free-ranging and captive, in Germany for CWD has shown no signs of infection (Schettler *et al.* 2006). As the prion sequence of Reindeer or caribou from Northern America or Northern Europe is highly homologous compared to mule deer, it is very likely that they are also susceptible to CWD (Jewell *et al.* 2005).

Bovine spongiform encephalopathy (BSE) appeared 1986 in the UK and spread rapidly in the following years in Europe and worldwide (Wilesmith *et al.* 1988). The symptoms of BSE are similar to scrapie except scratching. Transmission of sheep scrapie, endemic in the UK and many other countries, to cattle via contaminated feed rendered from carcasses was widely attributed as the origin of BSE (Wilesmith *et al.* 1988; Smith and Bradley 2003). A second hypothesis raises the possibility that recycling of rare sporadic BSE cases for feed production was the source for epidemic BSE. As meat and bone meal rendered from sheep or cattle was already used before as feed for cattle without leading to the occurrence of BSE, the key event for the spread of infection is thought to be a change in the production protocol for meat and bone meal by which the prions from sheep and cattle were no longer inactivated (Wilesmith *et al.* 1988; Prusiner 2001). Despite its epidemic dimension and negative economic consequences BSE primarily caused public concern as in the 1990s the occurrence of the new form of Creutzfeldt-Jakob disease (CJD) in humans, variant CJD, made it obvious that BSE

can be transmitted to humans. As a consequence the European Union declared that all meat from cattle older than 30 months has to be tested for BSE before being sold to consumers.

1.2 Human prion diseases

In humans TSEs can have three different origins: sporadic, inherited and infectiously acquired. An overview of all three ways, the diseases and their probable cause is given below (**Table 2**). The course of each disease can vary but most of the patients suffer from characteristic symptoms like weight loss, insomnia, depression, ataxia, lack of coordination and a very rapid progressive dementia. Caused by the progressive neuronal degeneration the patients loose their ability to move or speak in the latest stage of the disease.

Table 2: Overview of prion diseases in humans

Etiology	Disease	Acronym	Causation
Sporadic	sporadic CJD	sCJD	• Spontaneous conformational change from PrP^C to PrP^{Sc} • Somatic mutations in *PRNP* (?)
Inherited	• Fatal Familial Insomnia • Familial CJD • Gerstmann-Sträussler-Scheinker-Syndrom	FFI fCJD GSS	Germline mutations in *PRNP*
Acquired	• Kuru	N/A	Ritualistic cannibalism
	• Iatrogenic CJD	iCJD	Contaminated blood, tissue or surgery instruments
	• Variant CJD (vCJD)	vCJD	BSE contaminated food

Sporadic Creutzfeldt-Jakob disease (sCJD) is characterised by a long incubation time and a very short clinical phase. Usually, patients show the first symptoms at the age of 45 – 65 and die within half a year after first onset of symptoms. With a rate of 85-90 % of all TSE cases in humans, sCJD is by far the most frequent prion disease with an incidence of 0.6 - 1.2 : 1.000.000 worldwide (Ladogana *et al.* 2005). Investigation of the amino acid

sequence of the *PRNP* gene of sCJD patients compared to healthy individuals revealed no disease causing mutations. Based on this, somatic mutations in *PRNP* or a spontaneous conformational change in PrP^C to PrP^{Sc} is discussed as the causative event for developing the disease (Collinge 1997).

Insertions, nonsense and missense mutations in the *PRNP* gene inherited via autosomal dominant traits lead to the familial forms of CJD. The proline (P) to leucine (L) substitutions at position 102 in the *PRNP* gene causes the Gerstmann-Sträussler-Scheinker (GSS) syndrome. It was first described by Gerstmann and colleagues in 1936 (Gerstmann *et al.* 1936). Affected individuals typically show the first symptoms at a mean age of 45 years and die within 2 to 17 years. In 1981 GSS was experimentally transmitted to apes and was therefore accepted as a TSE (Masters *et al.* 1981). A very rare and more recently described inherited TSE is the Fatal Familial Insomnia (FFI) (Lugaresi *et al.* 1986). This disease is mainly caused by an aspartic acid (D) to asparagine (N) point mutation at codon 178 of the prion protein. A naturally occurring polymorphism at codon 129 in the *PRNP* gene, either coding for valine or methionine at this position, modulates the occurrence of FFI or Familial CJD (fCJD). A combination of a D178L mutation and a valine encoded at position 129 of the same allele leads to the development of FFI. With a methionine instead of a valine at codon 129 patients come down with fCJD.
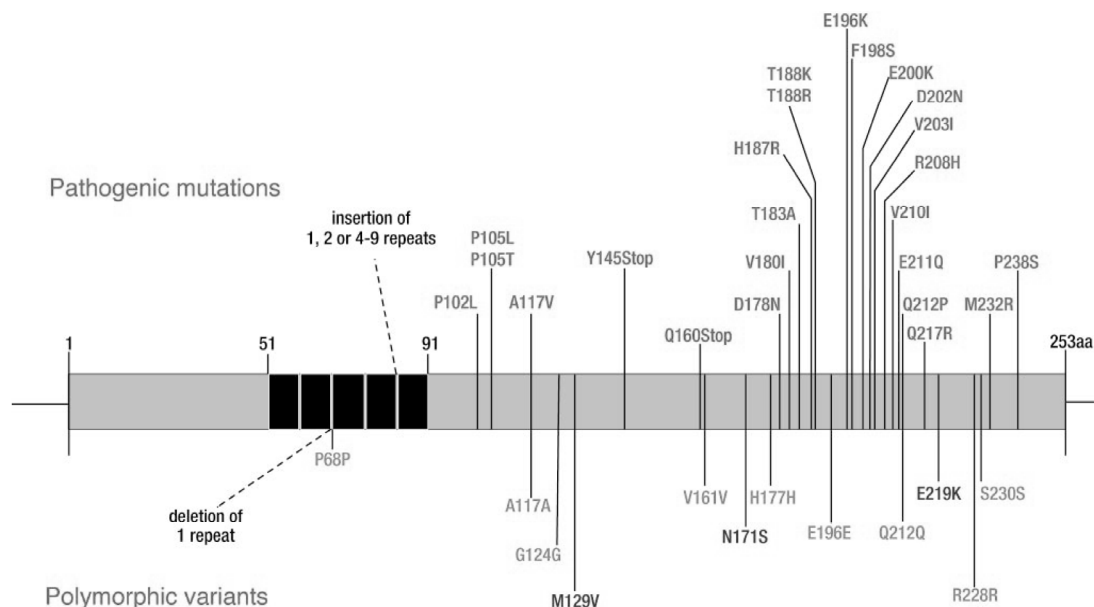
Figure 2: Schematic overview of pathogenic mutations (upper part) and polymorphic variants (lower part) known so far in the human prion protein (taken from (Collinge 2001)).

Kuru, variant CJD (vCJD) and iatrogenic CJD (iCJD) belong to the group of acquired TSEs in humans. All these diseases are transmitted in humans by different sources.

Kuru was first described in 1957 by Gajdusek and colleagues (Gajdusek and ZIGAS 1957; Zigas and Gajdusek 1957) and arose only in Papua Neuguinea among the Fore people. Mainly children and women of the Fore people traditionally consumed body parts of their deceased family members (including the brain) during ritual cannibalism. By doing so they also ingested infectious prions that lead to the development of Kuru disease. The patients suffered of tremor and ataxia. Later on they were unable to sit in an upright position, to walk and speak. As disturbances in the behaviour like hilarity were often described Kuru was also called the "laughing death". This vicious cycle of infection by endocannibalism was finally interrupted in the mid 1950s as the ritual cannibalism was prohibited by the Australian government. Because of the very long incubation time of Kuru even more than 50 years after preventing cannibalism local cases of Kuru were reported (Collinge 2001).

Iatrogenic CJD was caused by either inadequately decontaminated surgery instruments and intracerebrally used EEG-electrodes or by administration of contaminated products derived from CJD infected human cadavers (e.g. transplants of dura mater grafts or the cornea and the use of the growth hormones derived from the pituitary gland) (Davanipour *et al.* 1985; Lueck *et al.* 2000; Head *et al.* 2003). With several hundred cases of iCJD reported in the last decades it amounts to one of the largest catastrophes in medicine history (Brown *et al.* 1992).

As mentioned before a new form of animal TSE appeared in the 1980s in the UK, the Bovine Spongiform Encephalopathy (BSE). Fearing the transmission from the animal to humans the government in Great Britain monitored intensively new CJD cases. Then in 1995, first located mainly in the UK, but later also in other European countries a new form of CJD appeared (Will *et al.* 1996; Collinge and Rossor 1996). The new cases showed a very characteristic difference to sCJD: mainly teenager and younger people were affected with a mean age of 29 years. Other characteristics were a so far unusual long clinical phase of two to three years. In contrast to sCJD the patients mainly suffer from ataxia and psychiatric symptoms but develop only dementia in the later stage of disease (Zeidler *et al.* 1997; Belay 1999; Hill *et al.* 1999). According to these findings the new form of CJD was termed variant CJD (vCJD). Beyond the known alterations found in a sCJD infected brain like spongiform lesions caused by neurodegeneration and astrocytic gliosis, vCJD has its own histopathologically characteristics that are used to distinguish between sCJD and vCJD (**Figure 3**): amyloid PrP plaques, surrounded by spongiform vacuoles, the florid plaques (Wadsworth and Collinge 2007).

A) sporadic CJD
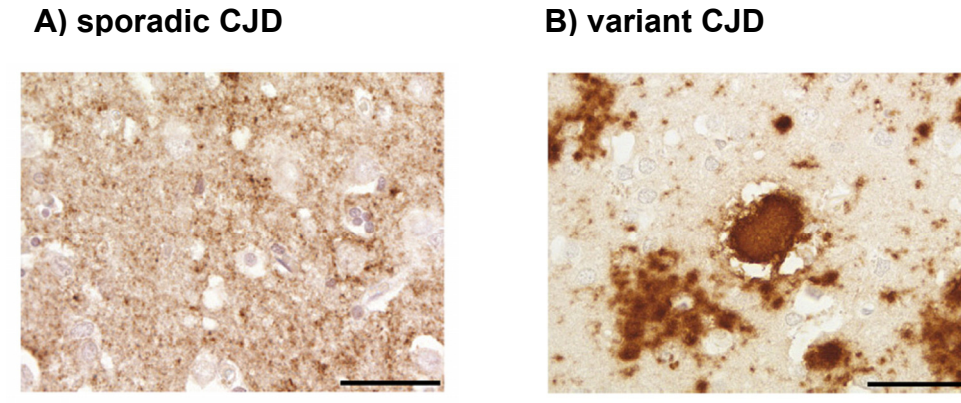
B) variant CJD

Figure 3: Immunohistochemistry detection of abnormal PrP accumulation in brain slices of patients with sporadic CJD (A) or variant CJD (B) showing a distinct pattern for each CJD form: More diffuse synaptic staining of abnormal PrP deposition in sporadic CJD brain whereas in variant CJD brain florid PrP plaques can be found (pictures taken from (Wadsworth and Collinge 2007)).

Monitoring the areas of vCJD cases and of the new BSE disease in cattle revealed a very likely connection between the occurrence of both TSEs. Moreover, the comparison of the plaques found in vCJD and those found in the brain of BSE infected macaques showed high similarity. This similarity together with a link between the area of infected bovines and the appearance of vCJD were the first hints that a transmission of BSE to humans may be the cause for vCJD. Further biochemical and histopathological evidence like molecular strain typing showed that BSE and vCJD have identical patterns of un-, mono- and diglycosylated PrP^{Sc} (Collinge *et al.* 1996b) and also transmission studies of BSE and vCJD to transgenic mice (Bruce *et al.* 1994; Hill *et al.* 1997) and later on to macaques (Lasmezas *et al.* 1996) supported this theory. Nowadays it is widely accepted that BSE is the causing agent of vCJD and that the disease is transmitted from bovines to humans by the oral route through BSE contaminated meat. Until now over 200 vCJD cases are known worldwide (http://www.prionforschung.de/html/page_entry.php?eof=0&sub=1&sel=5&id=7) all showing so far one characteristic in the *PRNP* gene: at codon 129 all patients were homozygote for methionine (Collinge *et al.* 1996a), arguing that this genetic background modulates the onset of vCJD. On the other hand further investigations are needed to assess whether methionine/valine heterozygosity or valine homozygosity at this position provide real protection against vCJD or just delay the onset of clinical signs. This may cause problems as PrP^{Sc} is not only found in the brain of vCJD patients but also in lymphatic tissue like spleen, lymph nodes and the blood (Wadsworth *et al.* 2001). Contaminated blood products from presymptomatic patients or unaffected carriers may be a potential risk factor for the lateral spread of vCJD. The description of at least five lateral transmissions of vCJD via blood

transfusions and blood products between 2004 and 2005 support this hypothesis (Llewelyn *et al.* 2004; Peden *et al.* 2004).

1.3   The cellular prion protein PrP^C

The gene coding for the cellular prion protein PrP^C is located on the short arm of the chromosome 20 in humans and chromosome 2 in mice (Robakis *et al.* 1986; Sparkes *et al.* 1986). It is evolutionary highly conserved between different species like mammals, birds, amphibians and fishes (Schatzl *et al.* 1995; Wopfner *et al.* 1999; Rivera-Milla *et al.* 2003) and codes for a protein of approx. 250 amino acids depending on the species. The PrP^C gene in hamsters and humans span over 2 exons whereas those of mice, cattle and sheep contain 3 exons (**Figure 4**) (Lee *et al.* 1998). A single open reading frame is encoded by the last exon of all PrP genes thus alternative splicing unlikely leads to different proteins (Basler *et al.* 1986; Westaway *et al.* 1994). The gene promoter consists of GC-rich regions including transcription factor binding sites for proteins of the SP-family and AP-1. A typical TATA-box is missing (Basler *et al.* 1986). Several insertions like retrotransposons have been described within the *Prnp* gene and its promoter region (Lee *et al.* 1998).
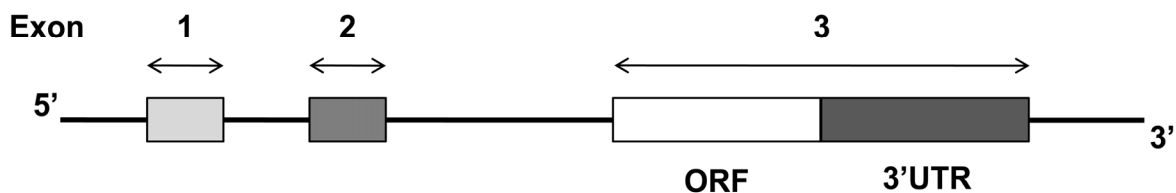
Figure 4: Schematic structure of the murine PrP gene *Prnp*. The gene consists of three exons. The open reading frame (ORF) is encoded by the third exon with its long un-translated region (UTR) at its 3'-end.

Prnp is present as a single copy gene in the mammalian genome. Transcription of mRNA is developmentally regulated during embryogenesis. PrP is constitutively expressed in the adult animal (Manson *et al.* 1992) in many tissues (Bendheim *et al.* 1992; Dodelet and Cashman 1998) but the highest expression level can be found in the CNS and there especially in neurons (Kretzschmar *et al.* 1986). After translation of the mRNA PrP^C has a primary sequence of 253 amino acids (aa) in humans and 254 aa in mice. **Figure 5** gives an overview of the primary structure of the human PrP^C with its posttranslational modifications.
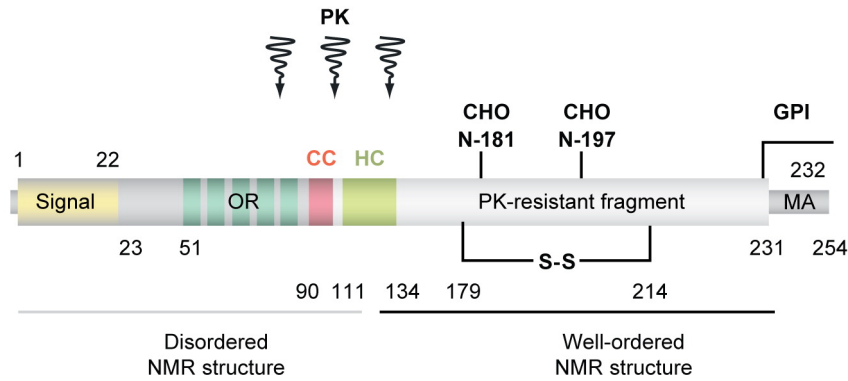
Figure 5: Schematic overview of the primary structure of human PrP^C with its posttranslational modifications. The numbers describe the positions of the respective amino acids. The primary structure consist of the amino-terminal secretory signal peptide followed by the octapeptide repeat region (OR), the charged cluster (CC), the hydrophobic core (HC), the PK-resistant fragment with its single disulfide bond (S-S), the two glycosylation sites (CHO) and the membrane anchored signal sequence (MA), which is posttranslationally replaced by a glycosyl phosphatidyl inositol (GPI) anchor. Amino acids 1 to 111 comprise the disordered and 134 to 231 the ordered part of PrP^C as assessed via NMR analysis. The region of arrows indicates the approx. PK processed area in PrP^{Sc} (taken from (Aguzzi *et al.* 2008)).

The first 22 aa at the N-terminus act as a signal peptide leading to translocation into the endoplasmatic reticulum (ER). There, this N-terminal signal peptide is cleaved off by a signal peptide peptidase (Oesch *et al.* 1985). Another signal peptide (amino acids 232 to 254) at the C-terminus promotes posttranslational addition of a glycosyl phosphatidyl inositol (GPI) anchor (Stahl *et al.* 1992). Linkage of carbohydrate molecules can occur at two asparagines residues at amino acids positions 181 and 197 (in human) or 180 and 196 (in mouse), resulting in three different mature forms of PrP^C: un-, mono- and diglycosylated. From the ER the protein transits via the Golgi/Transgolgi network to the plasma membrane of the cell, where it gets integrated into membrane microdomains, rich in cholesterol and sphingolipids, the so called lipid rafts (**Figure 6**). This integration is triggered by the GPI anchor at the C-terminus of PrP^C (Taraboulos *et al.* 1995; Vey *et al.* 1996; Simons and Ikonen 1997). The internalisation of PrP^C from the cell surface into early endosomes appears to occur in neurons mostly through clathrin-mediated endocytosis (Sunyach *et al.* 2003) but also the caveolin-dependent pathway has been described for PrP^C internalisation (Prado *et al.* 2004). From the early endosomes two fates for PrP^C are possible: the lysosomal degradation or the recycling of PrP^C leading to re-incorporation into the plasma membrane (Vey *et al.* 1996).
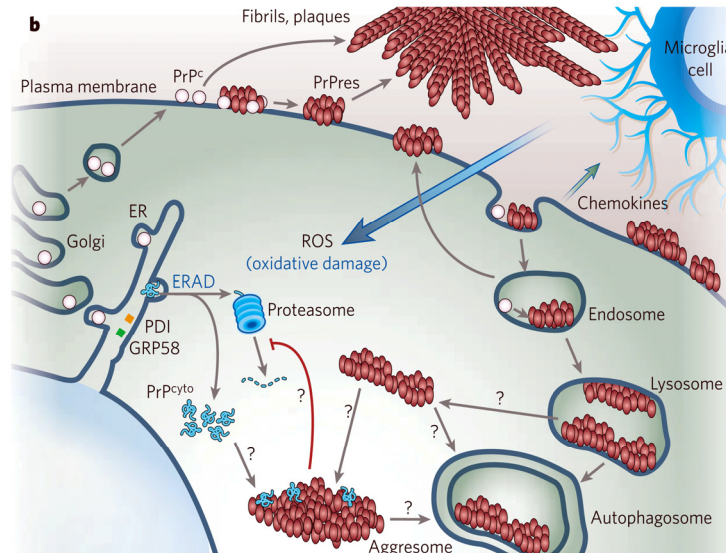
Figure 6: Trafficking of PrP^C and PrP^{Sc}. PrP^C (white circles) normally traverses from the endoplasmatic reticulum (ER) through the Golgi/trans-Golgi network to the plasma membrane, where it gets incorporated into lipid rafts via its GPI-anchor. For recycling PrP^C is endocytosed and either degraded via the edosomal/lysosomal pathway or shuttled back to the plasma membrane. Refolding of PrP^C to PrP^{Sc} could possibly occur either on the cell surface or in endosomes/lysosomes. As PrP^{Sc} has a longer half life time and is partially resistant to proteolysis it accumulates and aggregates within the cell. Misfolded PrP^C can also be subjected to the ER-associated degradation pathway (ERAD) or form cytosolic PrP^C (blue) upon proteasome inhibition. This PrP^{cyto} can also form aggregates and shows cytotoxic effects (taken from (Caughey and Baron 2006)).

After decades of experiments and the availability of PrP knockout mice since 1992 (Bueler *et al.* 1993) a distinct role and function of PrP^C in the cell remains still a mystery. PrP knockout mice do not show a distinct phenotype but are resistant to prion infection and do not replicate PrP^{Sc} (Bueler *et al.* 1993).

To get further insights into the role of PrP^C different methods like yeast two-hybrid screens and co-immunoprecipitations were performed by different groups to find possible binding partners of PrP. A list of putative prion interactors is given in **Table 3**. Copper was found to bind to the octapeptide repeat region of PrP^C (Brown *et al.* 1997a; Burns *et al.* 2003) leading to the hypothesis of a role of PrP in copper homeostasis. PrP^C could bind copper at the cell surface and release it inside the cell in acidic endosomatic vesicles. This is in line with findings, that the binding of copper to PrP^C is weaker in environment with lower pH and that copper stimulates the internalisation of PrP (Lee *et al.* 2001; Miura *et al.* 1999; Pauly and Harris 1998). A function in the control of the sleep-wakefulness cycle (Manetto *et al.* 1992), in memory retention (Nishida *et al.* 1997), protective role of PrP^C against oxidative stress (Brown *et al.* 1997a; Brown *et al.* 1997b; Herms *et al.* 1999; Klamt *et al.* 2001; Wong *et al.*

2000), in the glutamatergic system (Coitinho *et al.* 2002) and in protecting cells from apoptosis (Kuwahara *et al.* 1999; Bounhar *et al.* 2001; Roucou *et al.* 2005; Li and Harris 2005) has also been discussed. The anti-apoptotic effect of PrP^C appeared to be specific to Bax mediated apoptosis as no protection against neuronal apoptosis induced by Bak, t-Bid, staurosporin or thapsigargin could be found by Roucou *et al.* (Roucou *et al.* 2005). As the prion protein gets integrated into lipid rafts on the cell surface it has been suggested that PrP^C could play a role in transmembrane cell signalling either constitutively or by interaction of PrP^C with specific ligands. For example, the cross-linking of PrP^C on the cell surface of a neuroectodermal cell line (1C11) by prion specific antibodies resulted in a higher activity of fyn, a non-receptor tyrosine kinase (Mouillet-Richard *et al.* 2000) leading to production of reactive oxygen species, stimulation of NADPH oxidase and extracellular regulated kinases (ERKs) (Schneider *et al.* 2003).

Table 3: Putative PrP interactors with their typical cellular localization and function (Table taken from (Westergard *et al.* 2007) with modifications)

Putative interactor	Function	Localization	Reference
Grb2	Signal transduction (adaptor protein)	Cytoplasm	(Spielhaupter and Schatzl 2001)
Pint1	Unknown	Cytoplasm	(Spielhaupter and Schatzl 2001)
Synapsin 1b	Synaptic vesicle trafficking	Cytoplasm	(Spielhaupter and Schatzl 2001)
TREK-1	Two-pore K$^+$ channel	Plasma membrane (transmembrane)	(Azzalin *et al.* 2006)
Tubulin	Microtubule subunit	Cytoplasm (cytoskeleton)	(Nieznanski *et al.* 2005)
NRAGE (Neurotrophin receptor-interacting MAGE homologue)	Activator of apoptosis	Cytoplasm	(Bragason and Palsdottir 2005)
Laminin receptor precursor (LRP)	Extracellular matrix interactions	Cytoplasm (plasma membrane?)	(Gauczynski *et al.* 2001)
STI-1 (stress-inducible protein 1)	Heat-shock protein	Cytoplasm and plasma membrane	(Zanata *et al.* 2002)
Hsp60	Chaperone	Cytoplasm	(Edenhofer *et al.* 1996)
N-CAM	Cell adhesion	Plasma membrane (transmembrane and GPI-anchored forms)	(Schmitt-Ulms *et al.* 2001)

Bcl-2	Multi-domain anti-apoptotic regulator	Cytoplasm (mitochondria, ER)	(Kurschner and Morgan 1995)
Caveolin-1	Caveolar coat	Plasma membrane (hairpin loop)	(Mouillet-Richard *et al.* 2000)

Despite from its role in the CNS a role of PrP^C in the immune system has been hypothesised and supported for example by the finding that self-renewal of long-term hematopoietic stem cells under stressful conditions is altered by PrP^C expression (Zhang *et al.* 2006). PrP^C might also help balancing phagocytic response of macrophages towards apoptotic cells, as macrophages of PrP$^{-/-}$ mice showed a higher activity in phagocytosis than those in WT mice (de Almeida *et al.* 2005).

1.4 Structural and biochemical features of PrP^C and PrP^{Sc}

Pan *et al.* (Pan *et al.* 1993) showed that PrP^{Sc} is an isoform of PrP^C with identical primary structure and posttranslational modifications but an abnormal 3D structure resulting in different biochemical features. The 3D structure of PrP^C has been determined by nuclear magnetic resonance or spectroscopic analysis (Riek *et al.* 1996; Riek *et al.* 1997; Hornemann *et al.* 1997; Riek *et al.* 1998) whereas the high resolution structure of PrP^{Sc} is still a unresolved. The mature human PrP^C protein has a tertiary structure of three α-helices at residues 144-154, 173-194 and 200-228 interspersed by two β-strands corresponding to aa 128-131 and 161-164 (**Figure 7**). These α-helices and the anti-parallel β-pleated sheet form the globular domain of PrP^C. A single disulfide bond can be found between cysteine residues 179 and 214. The amino-terminal region of approximately aa 23-124 and the C-terminal domain of residues 229-230 are the flexible ends of PrP^C (Zahn *et al.* 2000). Although the amino-terminus of PrP^C appears to be unstructured it contains two conserved regions: the first one consists of four to five repetitions of an octameric amino acid sequence (Riek *et al.* 1997). This octapeptide repeat region is thought to be important for copper binding and amplification of the octapetide repeats has been found in vCJD and GSS patients (Brockes 1999; Owen *et al.* 1989; Collinge *et al.* 1989). The second region (termed trans-membrane region or hydrophobic core domain; downstream relative to the first region) is highly hydrophobic and conserved.
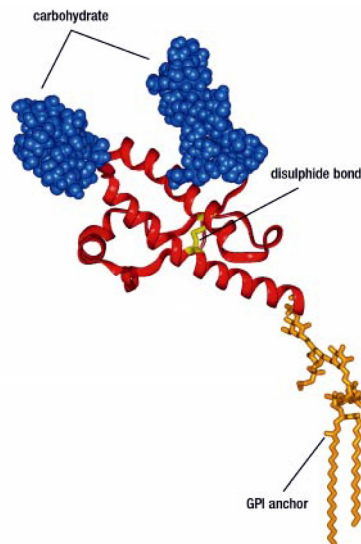
Figure 7: Structural model of mature PrP^C. NMR analysis revealed that PrP^C consists mainly of three α-helices with two short β-sheets (both given in red). The protein structure is stabilized by a disulphide bond (yellow) between α-helix 2 and 3 and can be post translationally modified with carbohydrates (blue) at two glycosylation sites linked to asparagines. With the glycosylphosphatidylinositol (GPI) anchor at the C-terminus PrP^C gets attached to cellular membranes (from (Collinge 2001)).

The 3D-structure of PrP^C is mainly α-helical (about 42 %) and has a lower β-sheet content (3 %). In sharp contrast to this PrP^{Sc} mainly consists of about 45 % β-sheets and to a lesser extent of α-helices (~30 %) (Pan *et al.* 1993; Gasset *et al.* 1993; Pergami *et al.* 1996). Although detailed structural analysis of PrP^{Sc} are still missing 3D-models for it have been established by analyzing 2D-crystals in electron microscopy and computer based molecular modelling (Wille *et al.* 2002; Govaerts *et al.* 2004) (**Figure 8**). According to this it was predicted that a PrP^{Sc} monomer consists of a left-handed β-sheet region. Three PrP^{Sc} monomers can form a disc and several trimeric discs assemble to fibrils.
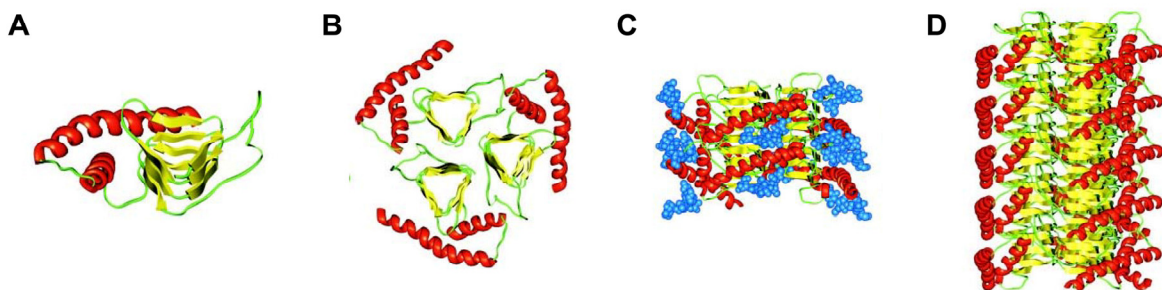
Figure 8: Predicted 3D-models of PrP^{Sc} structure and fiber formation. (A) One PrP^{Sc} monomer consisting of a left-handed β-sheet region (N-terminal truncated part; aa 89-143; yellow) and two α-helices formed by the C-terminus (aa 177-227; red). **(B)** Three PrP^{Sc} monomers forming a disc (trimeric structural model) **(C)** two trimeric discs can assemble via polar backbone interactions leaving enough space for the

stacking α-helices including the attached sugar molecules (blue) (D) model for PrP^{Sc} fiber formation through assemble of several trimeric discs (shown without sugar molecules for better clarity) (taken from (Govaerts *et al.* 2004)).

These described structural differences between PrP^C and PrP^{Sc} are supposed to be the cause for their different functional and biochemical behaviour. The most powerful tool to detect PrP^{Sc} beside its insolubility in mild detergent relates on its partial resistance to proteinase K (PK) digestion. Upon PK digestion PrP^{Sc} becomes amino-terminally truncated (aa 1-89) (Prusiner *et al.* 1984; Oesch *et al.* 1985), whereas PrP^C is totally digested. PK resistance of PrP^{Sc} can be detected e.g. by Western blot analysis where a typical banding pattern can be found (**Figure 9**):
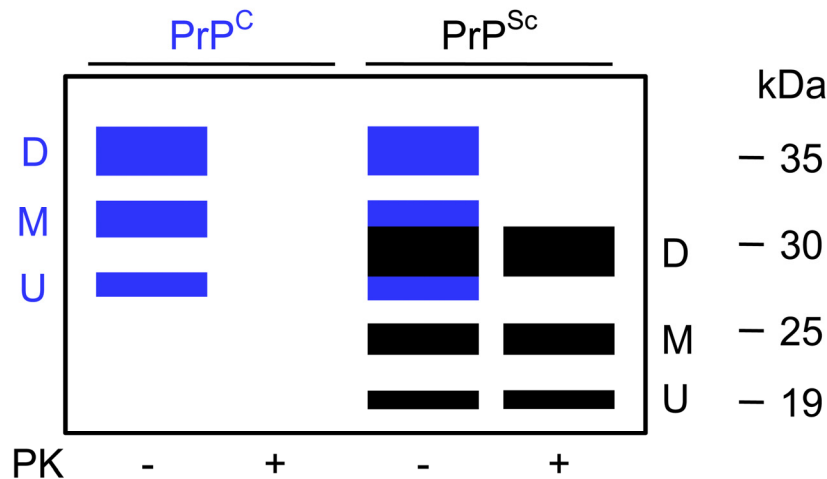
Figure 9: Banding pattern of PrP^C and PrP^{Sc} analysed by Western blot. Schematic illustration of typical detectable bands of PrP^C (blue) and PrP^{Sc} (black) by Western blot analysis with (+) and without (-) PK digestion. Both isoforms can occur as three glycosylation states (di-, mono- and unglycosylated; D,M,U) but have different molecular weights as PrP^{Sc} gets partially truncated either by intracellular or extracellular proteinases (PK digestion). Therefore six protein bands are theoretically detectable in PK untreated PrP^{Sc} samples (three of PrP^C and three of PrP^{Sc}), but in contrast after PK digestion only PrP^{Sc} can be detected.

1.5   Models for conversion of PrP^C to PrP^{Sc}

The hallmark of the prion diseases is the accumulation of PrP^{Sc} in the CNS. PrP^{Sc} is thought to be a pathogenic isoform of PrP^C that accumulates by structural refolding of PrP^C to PrP^{Sc}. Two models for this conversion step have been predicted so far that both can, although suggesting different mechanisms, explain all forms of the prion disease (**Figure 10**):

a) The **heterodimer model** proposed by Prusiner and Cohen (Prusiner *et al.* 1990; Cohen *et al.* 1994) postulates a spontaneous folding of PrP^C to PrP^{Sc} naturally prevented by a high activation energy barrier. After contact with exogenously introduced PrP^{Sc}, PrP^C will be refolded during a heterodimer step and adopts the structure of PrP^{Sc}. This folding step could be dependent on cellular factors like chaperons to overcome the high energy barrier. The newly formed homodimer dissociates and the released PrP^{Sc} monomers can refold new PrP^C molecules.

b) The **nucleation-polymerisation or "seeding" model** initially postulated by D. C. Gajdusek and later refined by Jarrett and Caughey (Jarrett and Lansbury, Jr. 1993; Caughey *et al.* 1995) is nowadays the most accepted conversion model. Here a reversible thermodynamic equilibrium of PrP^C and PrP^{Sc} in the cells is postulated strongly favouring the PrP^C structure. Only if two or more PrP^{Sc} monomers get into contact the PrP^{Sc} structure stabilizes and PrP^{Sc} molecules can form a highly ordered seed. This seed can recruit more PrP^{Sc} monomers and after reaching a critical size the amyloid can break up into several newly formed infectious seeds.

A) Heterodimer model
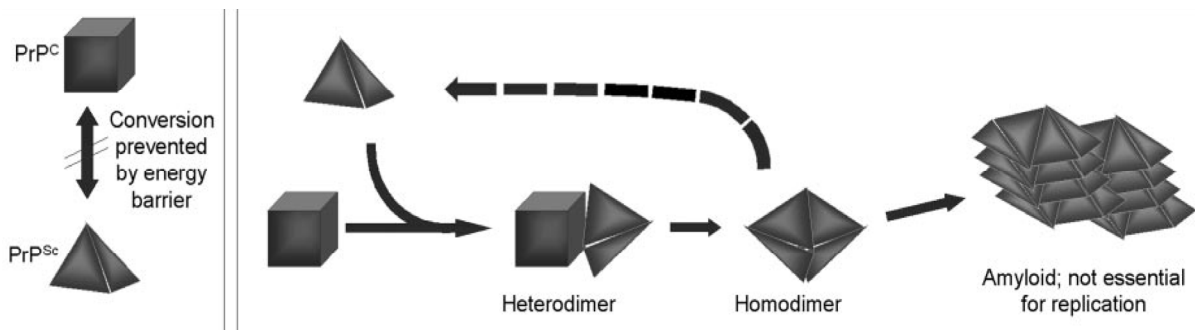
B) "Seeding" model
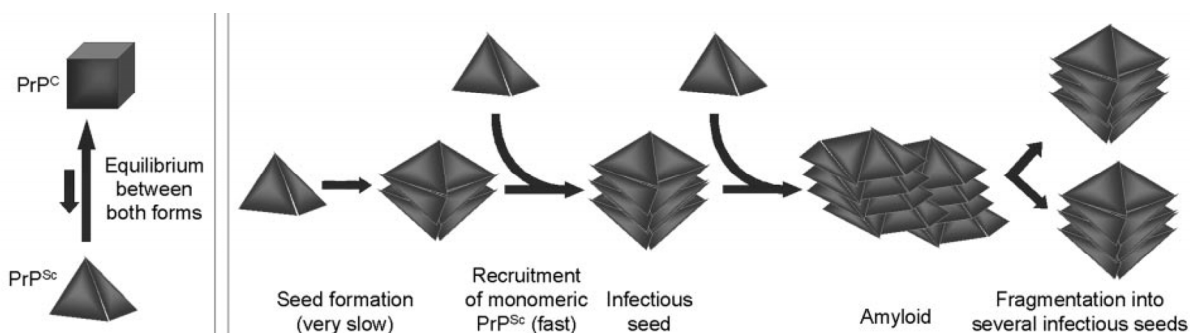
Figure 10: Models of PrP^C conversion to PrP^{Sc}. A) The heterodimer model predicts a prevention of spontaneous conversion of PrP^C to PrP^{Sc} in the cell by e.g. a high energy barrier. The conversion of PrP^C to PrP^{Sc} can only occur by direct contact of endogenous PrP^C and introduced PrP^{Sc}. B) In contrast to this

the "seeding" model postulates a reversible equilibrium of PrP^C and PrP^{Sc} within the cell. Only by contact of several monomeric PrP^{Sc} molecules, an infectious seed forms that recruits other PrP^{Sc} monomers and forms a growing amyloid. The amyloid breaks up into new infectious seeds which results in replication of PrP^{Sc}. (taken from (Aguzzi and Heppner 2000)

1.6 Prion strains and the species barrier

Propagation of distinct prion strains in inbreed mouse lines places a conundrum to the protein-only hypothesis. Strains of TSEs can in general be clearly distinguished by their stable incubation periods *in vivo* and distinct pattern of histopathologic lesions ("lesion profiles") in the brain of the same inbreed mouse line. But how can one misfolded protein cause different strains each with significant properties? Normally strains of conventionally pathogens occur by mutations in the genome of the original virus or bacteria. In TSE PrP^{Sc} is an isoform of PrP^C which does not show any difference in the primary structure. Lacking a scrapie genome Charles Weissmann postulated a "unified hypothesis" in 1991 (Weissmann 1991) where a small nucleic molecule or "coprion" was thought to be responsible for the strain characteristics. Until now nobody has ever reported the finding of such a molecule.

Another way to explain scrapie strains was the hypothesis, that the prion protein itself may encode strain specificity. This idea was supported by the experiments of Bessen & Marsh in 1992, who reported the transmission and serially propagation of two distinct TME strains in hamsters, termed hyper (HY) and drowsy (DY). Both strains showed different biochemical properties of PrP^{Sc} in the infected hamster brains (Bessen and Marsh 1992). In Western blot analysis the banding patterns of HY and DY PrP^{Sc} implicated different amino-termini upon PK digestion and therefore different PrP^{Sc} conformations for each strain (Bessen and Marsh 1994). Furthermore, different human PrP^{Sc} types associated with different CJD phenotypes have been identified (Parchi *et al.* 1996) that differ in individual fragment sizes detected by Western blot analysis after PK digestion. After inoculation of human and bovine prions in wild-type mice murine PrP^{Sc} was isolated with similar size and glycosylation pattern as the original inoculum. Such results were also reported for BSE in cattle and in other species (Collinge *et al.* 1996b). These findings suggest that differences in PrP^{Sc} and conformations may lead to scrapie strain variations.

The "species barrier" describes the restriction of transmission of TSEs between different species and is associated with prolonged disease incubation times after transmission between different species. After the first infection round in the new species prions have likely adapted to the new host and will cause a faster disease progression than the original ones, so that

almost all newly infected animals will develop the disease. So the species barrier can be overcome by repeated incubation rounds in the new host or if it is a very substantial barrier, like e.g. between hamsters and mice, by generating transgenic animals expressing the prion protein of the original host (Prusiner *et al.* 1990). In addition, mice expressing human PrP are to 100 % susceptible to classical CJD prions (Collinge *et al.* 1995), but on the other hand are much less affected by vCJD prions as wild-type mice (Hill *et al.* 1997). These findings implicate that the transmission barrier depends on the protein-protein interaction between PrP^C and PrP^{Sc} that is affected by the PrP amino acid sequence and 3D-structure of the glycosylated prion proteins. Only if the particular PrP^{Sc} conformation is thermodynamically permissible PrP^C can be turned into the pathogenic form and disease progression can occur (Collinge and Clarke 2007).

1.7   Prion cell culture models

The selection or even creation of cell lines that are permissive to prions and can actively propagate the TSE agent was one of the most important steps in the prion science field to gain deeper knowledge on the nature of prion infections through *in vitro* experiments. Also possible anti-prion compounds could now be more easily and rapidly tested. In the early 1970s the prion replication in a mouse brain-derived cell line, the SMB cell line, was reported (Clarke and Haig 1970), but until the beginning of the next century only few cell lines with susceptibility only to rodent-adapted prion strains, could be established. Then in 2001 a rabbit epithelia cell line (RK13), showing non-detectable endogenous PrP^C expression, was modified to express the ovine PrP^C genotype 136V154R171Q associated with high susceptibility to sheep scrapie (Hunter 1997). These cells could now be successfully infected with the original sheep scrapie agent (Vilette *et al.* 2001). Until now many different cell lines derived from different organisms and tissue are in use. Most common is the mouse neuroblastoma cell line N2a (Race *et al.* 1987a; Butler *et al.* 1988). These cells are susceptible to 22L and RML mouse-adapted prion strains and were used for different approaches aimed to understand the cell biology of PrP^C/PrP^{Sc} e.g. studying the rate of synthesis, degradation and localization (Borchelt *et al.* 1992; Nunziante *et al.* 2003; Gilch *et al.* 2006). A disadvantage of this cell line is the lack of any cytopathic effect upon prion infection e.g. neurodegeneration through apoptosis. By contrast the murine hypothalamic cell line GT1, established by Schätzl et.al in 1997, show an apoptotic phenotype after prion infection and propagation (Schatzl *et al.* 1997; Nishida *et al.* 2000; Arjona *et al.* 2004). Other neuronal cell

lines that can propagate prions are for example the PC12 rat pheochromocytoma cell, that can be differentiated into neuronal-like cells (Rubenstein *et al.* 1984) and the mouse cholinergic septal neuronal cell line SN56 (Baron *et al.* 2006). Recently, it was also shown, that hippocampal-derived HpL3-4 cells out of a PrP knock-out mouse can be susceptible to prion infection upon reconstitution with mouse PrP^C (Maas *et al.* 2007). Despite from neuronal cell lines also a microglial (MG20; (Iwamaru *et al.* 2006)), a skeletal myoblast (C2C12; (Dlakic *et al.* 2007)) and fibroblast cell lines (L fibroblasts (Clarke and Millson 1976), 3T3 and L929 (Vorberg *et al.* 2004)) are susceptible to prion infection. With these cell lines the prion infection and propagation in neuronal and non-neuronal tissues can be investigated *in vitro*, but up to date no models for BSE are available.

1.8   Cellular response (in vivo and in vitro) upon prion infection

A lot of studies were accomplished *in vivo* using prion mouse models and also *in vitro* using prion susceptible cell lines to define the effect of prion infection on neuronal cells. However, neurotoxicity upon prion infection was only detectable *in vivo* or in primary cells, as in most neuronal cell lines, except the GT1 cells ((Schatzl *et al.* 1997), the prion infection has little to no effect on cell viability. To date the questions how PrP^{Sc} or neurotoxic PrP causes neuronal loss and what are the contributing cellular pathways are still unsolved. Several possible explanations for the neurotoxic effect are discussed in the science field mainly that neurotoxicity may occur by modification of cellular processes due to a loss of function of PrP^C or gain of function of PrP^{Sc} or by a toxic effect of PrP^{Sc} *per se*. Cell death caused by an altered PrP^C functionality has already been published. For example Solforosi *et al.* reported an induction of neuronal apoptosis through cross linking of PrP^C by antibodies *in vivo* (Solforosi *et al.* 2004) and several other studies showed neurotoxic effects if aberrant conformers of PrP^C instead of PrP^C were expressed in transgenic mice (Muramoto *et al.* 1997; Shmerling *et al.* 1998; Ma *et al.* 2002; Li *et al.* 2007). The cytotoxic effect is not limited to altered PrP^C conformers present in the secretory pathway. Neurodegeneration was also detected in mice expressing PrP without the ER targeting sequence (cytoPrP), which localized to the cytosolic compartment (Ma *et al.* 2002). These data indicate that disturbance in PrP^C function, positive or negative, could lead to neuronal cell death. A neurotoxic effect of PrP^{Sc} *per se* is controversial discussed, as the presence of PrP^{Sc} does not lead to neurodegeneration (Hsiao *et al.* 1994; Lasmezas *et al.* 1997).

Knowledge of the cellular response upon prion infection is important for unrevealing the mechanisms that contribute to the propagation of TSE agents and neurotoxicity. Differential gene expression profiling was done by several groups using either the complete prion infected mouse brain and specific brain areas (Riemer *et al.* 2000; Xiang *et al.* 2004; Riemer *et al.* 2004; Brown *et al.* 2005) or cell culture systems (Baker and Manuelidis 2003; Doh-Ura *et al.* 1995; Greenwood *et al.* 2005). A big disadvantage of the mouse brain studies could be seen in the mixed cell population used for microarray experiments. It is very likely that different cell populations may react in different ways upon prion infection leading to a possible masking of the neuronal gene expression by other cells found in the infected brain. The gene expression profiles of special extracted microglia cells (Baker and Manuelidis 2003) or neuronal cell lines (Doh-Ura *et al.* 1995; Greenwood *et al.* 2005) revealed several possible altered cellular pathways in the prion infected cell for each study. However, no real overlap could be identified between all these studies so that the cellular response upon prion infection is still unclear.

Aim of this PhD thesis

Detailed information about the cell-pathogen interaction during prion infection is still missing so far. The aim of this PhD thesis was the identification of affected metabolic pathways in prion infected neuronal cells compared to mock controls in a highly controlled experimental procedure using in the beginning the cDNA microarray technology as a method of choice. Unwanted side effects should be avoided, so it was planned to use a highly prion susceptible N2a cell clone, resulting in a high infection rate within the cell population. Prion and mock infected cells should be age matched and kept under identical culture conditions. The resulting gene expression profile of the prion infected cells should be further analysed and clustered into affected metabolic pathways. The most affected one should be analysed in more detail and not only on gene expression but also on protein level using different methods. To estimate if this alteration is a cell type specific or a general response towards prion infection it was planned to repeat parts of the analysis using other cell lines or even primary murine cells. In the end the affected metabolic pathway should be further manipulated to find a linkage between this pathway and the prion propagation, if possible. All these goals could help to get a more detailed understanding of the cellular reaction towards the prion infection leading to new therapeutic strategies against TSEs.

2. Material and Methods

2.1 Materials

2.1.1 Chemicals

2log-standard	Gibco/Invitrogen, New York, USA
Agarose	Invitrogen, Karlsruhe, D
Bacillol Plus	Roth GmbH & Co, Karlsruhe, D
Bromphenole blue	Merck, Darmstadt, D
ß- Mercaptoethanol	Sigma-Aldrich Chemie GmbH, Steinheim, D
$Cy^{TM}3$ fluorescent dye	GE Healthcare, Freiburg, D
$Cy^{TM}5$ fluorescent dye	GE Healthcare, Freiburg, D
Dimethylsulfoxide	Sigma-Aldrich Chemie GmbH, Steinheim, D
Di-thiothreitol	Sigma-Aldrich Chemie GmbH, Steinheim, D
EDTA	Roth GmbH & Co, Karlsruhe
Ethanol p. a. 99%	Roth GmbH & Co, Karlsruhe, D
Ethidium bromid solution (10 mg/ml)	Invitrogen, Karlsruhe, D
5-Fluoro-2`-deoxyuridine	Sigma-Aldrich Chemie GmbH, Steinheim, D
Glycerol	Roth GmbH & Co, Karlsruhe, D
Glycine	Roth GmbH & Co, Karlsruhe, D
Guanidine hydrochloride	Roth GmbH & Co, Karlsruhe, D
HBSS (+Ca, +Mg)	Invitrogen, Karlsruhe, D
HCl 37% (w/w)	Roth GmbH & Co, Karlsruhe, D
Hoechst 33342, trihydrochloride, trihydrate	Sigma-Aldrich Chemie GmbH, Steinheim, D
Hybond-P PVDF membrane	GE Healthcare, Freiburg, D
Isopropanol p. a.	Roth GmbH & Co, Karlsruhe, D
MESA	Sigma-Aldrich Chemie GmbH, Steinheim, D
Methanol p. a.	Roth GmbH & Co, Karlsruhe, D
Nonidet P40	Sigma-Aldrich Chemie GmbH, Steinheim, D
Pefabloc SC	Roche, Mannheim, D
PBS	Invitrogen, Karlsruhe, D
Poly-L-lysine solution	Sigma-Aldrich Chemie GmbH, Steinheim, D

Potassium chloride	Sigma-Aldrich Chemie GmbH, Steinheim, D
Protogel Ultra Pure 30%,	
Acrylamide: Bisacrylamide 37, 5:1	National Diagnostics, Atlanta, USA
RNA loading buffer	Sigma-Aldrich Chemie GmbH, Steinheim, D
Safeseal tips	Biozym, Oldendorf, D
Skim milk powder	Merck, Darmstadt, D
Sodium chloride	Roth GmbH & Co, Karlsruhe, D
Sodium deoxycholate	Roth GmbH & Co, Karlsruhe, D
Sodium dodecylsulfate	Roth GmbH & Co, Karlsruhe, D
Syringe needle (Microlance; 0.9 mm)	Becton Dickinson, Heidelberg, D
TEMED	Sigma-Aldrich Chemie GmbH, Steinheim, D
Tris	Roth GmbH & Co, Karlsruhe, D
Triton-X- 100	Sigma-Aldrich Chemie GmbH, Steinheim, D
Trizol	Gibco/Invitrogen, New York, USA
Trypane Blue	Sigma-Aldrich Chemie GmbH, Steinheim, D
Trypsin- EDTA	Gibco/Invitrogen, New York, USA
Tween 20	Roth GmbH & Co, Karlsruhe, D
Uridine	Sigma-Aldrich Chemie GmbH, Steinheim, D
X-ray films Kodak Biomax MS	Becton Dickinson, Heidelberg, D
7-AminoActinomycin D (7-AAD)	Becton Dickinson, Heidelberg, D

2.1.2 Kits

Bradford Assay	Thermo Fisher Scientific, Rockford, USA
Dual-Luciferase® Reporter Assay System	Promega, Mannheim, D
ECL plus Western blotting	
detection system	GE Healthcare, Freiburg, D
Fugene 6 Transfection Kit	Roche, Mannheim, D
High range protein molecular weight marker	GE Healthcare, Freiburg, D
LightCycler FastStart DNA	
Master SYBR Green I	Roche, Mannheim, D
mi-*Taq* Mix	Metabion international AG, Martinsried, D
Lipofectamine 2000 Transfection Kit	Invitrogen, Karlsruhe, D
Plasmid Maxi Kit	Qiagen, Hilden, D
RNase free DNase Set	Qiagen, Hilden, D

RNeasy Mini Kit	Qiagen, Hilden, D
SuperScript II Reverse Transcription Kit	Gibco/Invitrogen, New York, USA
QIAquick Spin Kit	Qiagen, Hilden, D

2.1.3 Cell lines

In this work the following eukaryotic cells and cell lines were used

- Hippocampal primary neurons
- Primary astrocytes
- N2a: murine neuroblastoma line (American Tissue Culture Collection (ATCC, No. CCL-131)
- L929: murine fibroblastoma line (ATCC, No. CCL-1)
- BV-2: murine monocyte-macrophage line (Blasi *et al.* 1990)
- GT1: murine hypothalamic line (Schatzl *et al.* 1997)

Primary neurons and astrocytes were extracted from brains of C57BL/6 mice embryos and later on exposed to the mouse adapted prion strain 22L.

The N2a, GT1 and L929 cells can be permanently infected with the mouse adapted scrapie strain 22L (Race *et al.* 1987b; Butler *et al.* 1988; Schatzl *et al.* 1997).

The BV-2 macrophages can only be transiently infected by uptake and clearance of PrP^{Sc} (Gilch *et al.* 2007).

2.1.4 Cell culture media and additives

OptiMem with GlutaMAX	Invitrogen, Karlsruhe, D
DMEM with GlutaMAX	Invitrogen, Karlsruhe, D
RPMI1680	Invitrogen, Karlsruhe, D
Neurobasal Media	Invitrogen, Karlsruhe, D
FCS	Invitrogen, Karlsruhe, D
Penicillin/Streptomycin	Invitrogen, Karlsruhe, D
B27 Serum-Free Supplement	Invitrogen, Karlsruhe, D

2.1.5   Oligodeoxynucloetides

Primers for the quantitative real-time PCR (qRT-PCR) were designed using the following criteria:

- All oligodeoxynucleotides had a length of approximately 20 bases
- Forward and reverse primers annealed at a distance of at least 100 bases between and were placed within the complementary sequence of the capture probe
- No complementary ends within the primer itself or between the forward and reverse primer to avoid primer-loops or primer-dimer.
- The ratio of AT to GC was approx. 1:2

The sequence for each capture probe can be found in the LION database (https://www.lionbioscience.com/). For identification of the complementary sequence of the capture probe and for excluding the binding of the primer to no-target sequences the BLAST analysis was used (http://www.ncbi.nlm.nih.gov/BLAST/). All oligodeoxynucleotides were obtained from Metabion international AG (Martinsried, D).

Table 4: Sequences of used oligodeoxynucleotides in this thesis

Gene	Sequence forward primer	Sequence reverse primer
Cyp51	5' GGTCGACTATGCTTCGTTTA 3'	5' CTCCACACTGGCTTCTTGTT 3'
Fdft1	5' AACTGGGAGAGGAAAGGATG 3'	5' ATCCAATCAGCATTCTAGCC 3'
Ldlr	5' GACTATTTGGTGGGACTTGG 3'	5' TTTACAAGTGTCCCAGTGGG 3'
Mvk	5' GGAAGAGCACTGTGCCTTTG 3'	5' AGATCAGCCACGCTTCAATG 3'
RPII	5' GCACCACGTCCAATGATAT 3'	5' GTGCTGCTGCTTCCATAA 3'
Sc4mol	5' AGCCCCACTTCCACTGTCCA 3'	5' AACATGGCAGCTAATCTTCA 3'
Srebf2	5' TTCAACCCCACCTACTCTGC 3'	5' AGGCATATCCCCTGTTCAGT 3'
Iap	5' GGAGAAGTCCTACCTCAGGG 3'	5' GGAGAACAAAATGTCATCCATATA 3'

2.1.6   Enzymes and antibodies

2.1.6.1   Enzymes

DNase I (recombinant, RNase-free)   Roche, Mannheim, D

Proteinase K   Roth GmbH & Co, Karlsruhe, D

Trypsin-EDTA   Invitrogen, Karlsruhe, D

2.1.6.2 Antibodies

Table 5: Antibodies used in this work

Primary antibody	Specificity	Application	Dilution	Source and Reference
4H11	PrP of various species, including mouse	Western blot (Immunoblot) FACS analysis Immunofluorescence	1:1000 1:100 1:100	Mouse monoclonal (Ertmer *et al.* 2004)
ab28482	Srebp2 of various species including mouse	Western blot (Immunoblot)	1:1000	Rabbit polyclonal (Abcam plc; Cambridge; UK)
ab30532	Ldlr of various species including mouse	Western blot (Immunoblot)	1:1500	Rabbit polyclonal (Abcam plc; Cambridge; UK)
MAB374	GAPDH of various species including mouse	Western blot (Immunoblot)	1:10.000	Mouse monoclonal (Millipore/Chemicon; Billerica, USA)
MAB1987	Neurofilament N of various species including mouse	Immunofluorescence	1:200	Rabbit monoclonal (Millipore/Chemicon; Billerica, USA)
AB5040	GFAP of various species including mouse	Immunofluorescence	1:100	Rabbit polyclonal (Millipore/Chemicon; Billerica, USA)
Secondary antibody	**Specificity**	**Application**	**Dilution**	**Source and Reference**
Horseradish peroxidase – conjugated anti-IgG	Mouse IgG	Western blot (Immunoblot)	1:7500	Sheep (GE Healthcare, Freiburg, D)
Horseradish peroxidase – conjugated anti-IgG	Rabbit IgG	Western blot (Immunoblot)	1:7500	Sheep (GE Healthcare, Freiburg, D)
Cy2-conjugated anti-IgG	Mouse IgG	FACS analysis	1:400	Donkey (Dianova, Hamburg, D)
Cy2-conjugated anti-IgG	Rabbit IgG	Immunofluorescence	1:100	Donkey (Dianova, Hamburg, D)
Cy3-conjugated anti-IgG	Mouse IgG	Immunofluorescence	1:400	Donkey (Dianova, Hamburg, D)

2.1.7 Plasmids and bacterial strains

For the luciferase assay the psynSRE plasmid (**Figure 11A**; kindly provided by Dr. Osborne, Department of Molecular Biology and Biochemistry, University of California, Irvine, California) and a pGL3 renilla plasmid (**Figure 11C**; obtained from Promega, Mannheim, D) were used. psynSRE codes for a firefly luciferase under the control of a synthetic promoter harboring two Srebp2 binding motifs (sterol regulatory elements (SREs); (Dooley *et al.* 1998)). The pGL 3 renilla plasmid codes for a renilla luciferase under the control of the constitutive SV 40 early enhancer/promoter.

A)

B)
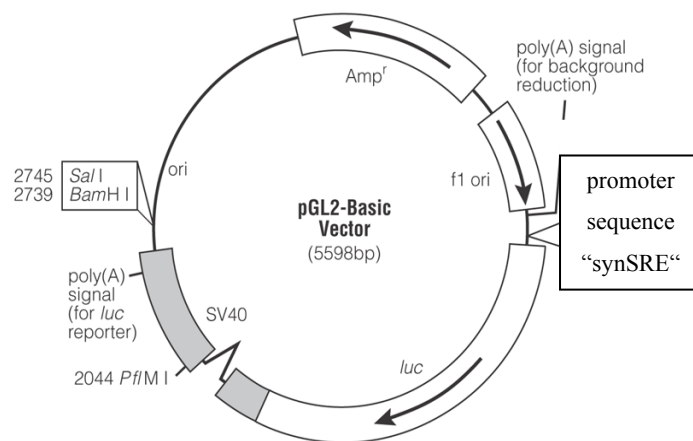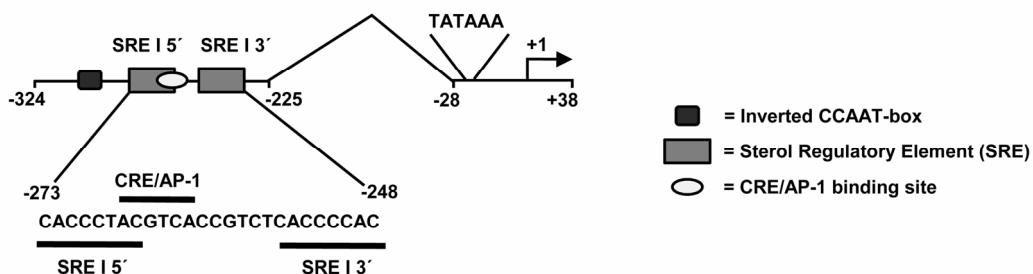
C)
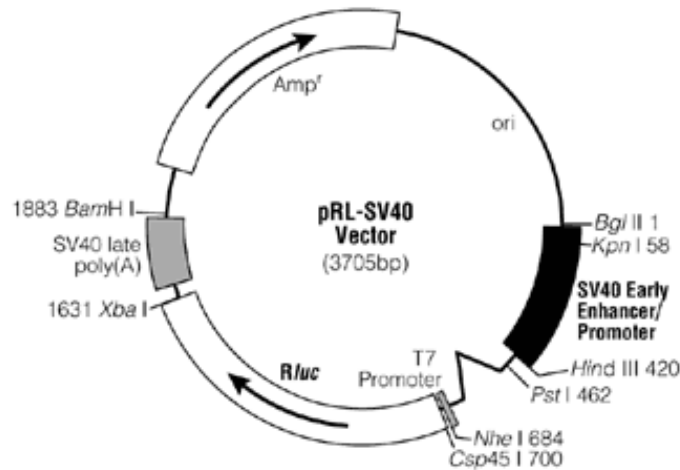
Figure 11 Schematic illustrations of the luciferase reporter gene vectors used: A+B) psynSRE-firefly luciferase plasmid obtained from Dr. Osborne (USA) containing a luciferase open reading frame under the control of an artificial promoter harboring two SRE-motives for selective binding of the transcription factor Srebp2. C) Transfection control plasmid obtained from Promega containing a *Renilla*-luciferase reporter under the control of the constitutive SV40 promoter. (Figures A+C) taken from the Promega website, figure B) taken from (Dooley *et al.* 1998) with modifications)

All Plasmids were amplified in *E. coli* XL-1 Blue (*Sup*E44, *hsd*R17, *end*A1, *ec*A1, *gyr*A46, thi-1, *rel*A1, lac⁻, F'(proABlacl^q, lacZΔM15, Tn10(ter^R); Stratagene, USA)

2.1.8   Instruments

Autoclave V95	Systec, Wettenberg, D
Axiovert 40C microscope	Carl Zeiss Jena GmbH, Göttingen, D
Fuchs-Rosenthal Hemocytometer	Roth GmbH & Co, Karlsruhe, D
CO_2 Incubator	Heraeus GmbH, Hanau, D
Centrifuges:	
Eppendorf 5417C	Eppendorf-Nethaler-Hinz GmbH, Köln, D
Sigma 4K15	Sigma-Aldrich, Schnelldorf, D
Beckmann Avanti	Beckmann Coulter GmbH, Krefeld, D
Beckmann TL-100 ultracentrifuge	Beckmann Coulter GmbH, Krefeld, D
Cryotubes	Corning Inc., USA
Eppendorf tubes (1,5 or 2 ml)	Eppendorf-Nethaler-Hinz GmbH, Köln, D
FACS-polystyrene tubes	Beckton Dickinson, USA
Falcon tubes (15 or 50 ml)	Falcon, Le Pont de Claix, France

Flow cytometer EPICS XL	Beckmann Coulter GmbH, Krefeld, D
GenePix 4000A microarray scanner	Axon Instruments/Molecular Devices Corporation, CA, USA
LightCycler	Roche, Mannheim, D
LSM510 confocal laser microscope	Carl Zeiss Jena GmbH, Göttingen, D
Midi protein gel chamber	Peqlab Biotechnologie GmbH, Erlangen, D
Optimax X-Ray film processor	PROTEC Medizintechnik GmbH & Co-KG, Oberestenfeld, D
Orion Microplate Luminometer	Berthold Detection Systems GmbH; Pforzheim, D
Pipets (0,5-10 µl; 10-100 µl; 100-1000 µl)	Eppendorf-Nethaler-Hinz GmbH, Köln, D
Pipetus	Hirschmann Laborgeräte GmbH & Co-KG, Eberstadt, D
Power Supplies	GE Healthcare, Freiburg, D
Spectrophotometer	GE Healthcare, Freiburg, D
Sunrise ELISA Reader	Tecan, Maennedorf, Switzerland
Tissue culture dishes and plates	Falcon, Le Pont de Claix, France
Trans Blot SD Semi-dry Transfer Cell	Biorad Laboratories GmbH, München, D
Transfer unit Semi dry (TE77)	GE Healthcare, Freiburg, D
Waterbath	GFL, Burgwede, D

2.2   Methods

2.2.1   Biological safety

Guidelines and operation procedures for working with prions were followed. All biologically contaminated materials and solutions were collected separately and inactivated with 1 M NaOH for 24 hours (liquid waste) and by autoclaving. Solid waste was autoclaved for 60 min at 134°C and 2 bar. Genetic engineering of organisms was done according to the German *Gentechnikgesetz* (01.01.2004).

2.2.2 Photodensitometric analysis and statistics

Photodensitometric analysis of Western blots was performed using the ImageQuant TL software (GE Healthcare, Freiburg, D). Quantitative data are shown as mean +/- standard deviation. For evaluation of statistical significance of the data the paired *t* test was used. *p*-values less than 0.05 were considered as significant.

2.2.3 Molecular biological methods

2.2.3.1 Transformation of *E. coli* with plasmid DNA

One ng of plasmid DNA was added to 100 µl of chemically competent *E. coli* XL1 blue, thawed on ice for 10 min. The mixture was gently stirred with a pipette tip and incubated on ice for 15 min. After a heat shock of 60 sec at 42°C in an Eppendorf thermo block the bacteria were chilled for 2 min on ice. 300 µl of SOC medium was added to the bacteria and the transformation mixture was incubated at 37°C for 60 min under constant shaking at 800 rpm. For selection of transformed bacteria the whole mixture was plated on LB agar plates containing the appropriate antibiotic (ampicilline 100 µg/ml or kanamycine 40 µg/ml). The plate was incubated at 37°C for 16 hours.

SOC Medium:	Bacto Tryptone	2 %
	Bacto Yeast extract	0.5 %
	NaCl	10 mM
	KCl	2.5 mM
	$MgCl_2$	10 mM
	$MgSO_4$	10 mM
	Glucose	20 mM in A. dest
LB (Luria-Bertani-) agar:	Bacto Tryptone	10 g/l
	Bacto Yeast extract	5 g/l
	NaCl	10 g/l
	Bacto Agar	15 g/l in A. dest

2.2.3.2 Isolation of plasmid DNA in a preparative scale (Maxi-Prep)

A single colony was transferred to 5 ml LB Medium with antibiotics and incubated over night at 37°C under constant shaking at 180 rpm. 100µl of the mixture was transferred to 100 ml LB medium with antibiotic and incubated for 24 hours at 37°C with constant shaking (180 rpm). After 24 hours bacteria were sedimented by centrifugation for 30 min at 4°C and

12000 rpm in a Beckmann Avanti centrifuge (rotor JA25.50). Plasmid DNA was prepared using the Maxi Plasmid Kit (Qiagen, Hilden, D) based on alkaline lysis according to the manufacturer's protocol. Briefly, after lysis the bacterial components were separated by centrifugation (4°C, 12000 rpm, 30 min, Beckmann Avanti, JA25.50) and the supernatant containing the plasmid DNA was transferred to a column binding plasmid DNA. After several washing steps the plasmid DNA was eluted and precipitated with isopropanol. DNA was pelleted by centrifugation (4°C, 12000 rpm, 30 min, Beckmann Avanti, JA25.50), shortly dried at RT and resuspended in A. dest. The DNA concentration was determined as described in (**2.2.3.4**). The DNA samples were stored at -20°C.

2.2.3.3 Isolation of total cellular RNA

The QIAshredder and RNeasy Mini Kit (both obtained from Qiagen, Hilden, D) were used for isolation of total cellular RNA according to the user's manual. Briefly, cells were grown until confluence on a 6 cm dish, washed once with phosphate buffered saline (PBS) and lysed. During the preparation an on-column DNA digestion was performed, using the RNase-free DNase Kit from Qiagen (Hilden, D). Finally the RNA was eluted with RNase free A. dest and the concentration was determined as described in (**2.2.3.4**). All RNA samples were stored at -80°C. To avoid contamination with RNase or DNA all extraction steps were performed in a laminar flow and only RNase-free material was used (including safe seal tips).

2.2.3.4 Quantification of nucleic acids

To determine the concentration (C) of DNA or cellular RNA the absorbance at a wave length of $\lambda = 260$ nm (A_{260}) was measured. For DNA, an absorbance of 1 at 260 nm corresponds to a concentration of 50 µg DNA/ml, the same absorbance for RNA corresponds to 40 µg RNA/ml, if diluted in A. dest. Samples of RNA and DNA were diluted in Rnase-free A. dest at a ratio of 1:10 for quantification. For estimation of the purity of each preparation the absorbance at 280 nm was also determined. The ration between the absorbance at 260 nm and 280 nm gives an estimation about the purity of each preparation. A ration of 2.0 for RNA and 1.8 for DNA ensures high quality samples.

Calculation of concentrations:
DNA: A_{260} x 50 µg/ml x dilution factor = C_{DNA} µg/ml
RNA: A_{260} x 40 µg/ml x dilution factor = C_{RNA} µg/ml

2.2.3.5   Polymerase chain reaction (PCR) for amplification of DNA fragments

Background:

The *in vitro* technique PCR is used for amplification of DNA fragments, that are flanked by short known sequences and offers the possibility to detect even low copy DNA fragments by amplification to a detectable level. In the first step (denaturation) the double stranded (ds) DNA is separated into single strands by heating. On both DNA strands short oligonucleotides (primers) can bind to their complement sequences (template) on the single stranded (ss) DNA (annealing step). These short dsDNA fragments act as starting points for the amplification. In the last step of a PCR cycle (elongation) both dsDNA fragments are elongated by a thermo stable polymerase, e.g. Taq-polymerase. By repeating all steps each new cycle causes an exponential amplification of the wanted DNA fragment.

Procedure:

For all PCR reactions the mi-*Taq* Mix (Metabion international AG, Martinsried, D) was used according to the manufacturer's manual.

Table 6: standard PCR program

Step	Cycles	Program	Temperature (°C)	Hold Time (sec)
1	1	Start denaturation	95	300
2	30	Denaturation	94	30
		Annealing	--°C*	45
		Elongation	72	30
3	1	Final annealing	72	600
4	1	Cooling	4	∞

*The right annealing temperature of each primer depends on number and nucleotides. The "2+4"-rule can be used for a good estimation:

$$T_M[°C] = \{2 \text{ x } (A + T) + 4 \text{ x } (G + C)\}$$

2.2.3.6   Electrophoretic separation of DNA/RNA (agarose gel electrophoresis)

All nucleic acids were separated by agarose gel electrophoresis by size. For visualisation the DNA/RNA gets stained with ethidium bromide (EtBr), added to the agarose shortly before polymerization. Because of its binding to dsDNA EtBr is a very strong mutagen. As is passes through latex very rapidly special nitrile hand gloves were used to protect the skin.

Separation of DNA

1% agarose (w/v) was dissolved in 1xTAE buffer and a constant power of 100V was applied. As length marker the 2log-standard (Gibco/Invitrogen, New York, USA) was used according to the manufacture's manual.

50xTAE buffer (pH 8.8)	Tris	2 M
	Pure acetic acid	1 M
	EDTA	0.1 M in A. dest

Loading buffer	Ficoll	15 % (w/v)
	EDTA	5 mM
	Bromphenol blue	0.01 % (v/v)
	Xylenxyanol	0.01 % (v/v) in A. dest

Separation of RNA

1% agarose is solved in autoclaved DEPC-water (10% v/v), supplemented with 5 % formaldehyde (v/v). 1-2 µg RNA were mixed with 2.5 µl loading buffer (Sigma-Aldrich Chemie GmbH, Steinheim, D) and a constant power of 100 V was applied. As control RNA from mouse liver (1 µg/µl) was loaded on the gel.

10xMESA (pH 7.0)	3-[N-morpholino]propanesulfonic acid	200 mM
	Sodium acetate	50 mM
	EDTA	10 mM in A. dest

Running buffer	10 x MESA	1 % (v/v)
	Formaldehyde (37%; 12.3 M)	2 % (v/v) in A. dest

2.2.3.7 Mouse genome-wide cDNA microarray

DNA microarray (chip) design

cDNA microarrays, produced at the Institute of Experimental Genetics at the Helmholtz Zentrum München (German Research Center for Environment and Health), contain the fully sequenced 20K cDNA mouse array-TAG library (Lion Bioscience, Heidelberg, Germany) and several hundred additional clones for genes not included in the commercial clone set. A full description of the probes on the microarrays has been submitted to the GEO database

(GPL3697; http://www.ncbi.nlm.nih.gov/projects/geo/). From the mouse array-TAG library, PCR products with 5′ modified-amino groups were amplified and dissolved in threefold SSC buffer (Drobyshev *et al.* 2003). Using a Microgrid TAS II spotter (Biorobotics) the products were spotted with 48 StealthTM SMP3 pins (Telechem) on aldehyde-coated slides (Telechem, USA). The spotted slides were re-hydrated over night in a humid chamber containing 50-70% aqueous solution of glycerol. Rehydrated slides were incubated for five minutes in blocking solution (0.1 M sodium borohydride in 0.75-fold PBS with 25% (v/v) ethanol), boiled in water for 2 minutes, briefly immersed in ethanol (100%) and air-dried. Before use rehydrated slides were pre-hybridized for one hour in pre-hybridization buffer (6xSSC, 1% (w/v) bovine serum albumin, 0.5% (w/v) SDS) at 42°C, rinsed in water, immersed in ethanol and dried.

Reverse transcription and fluorescent labelling

RNA from infected and control cell lines was isolated for the chip experiments by the Trizol method according to the manufacturer's instructions. According to the TIGR protocol (Hegde *et al.* 2000) 20 µg of total RNA of infected and mock infected N2a cells was used for reverse transcription with oligo-dT primer and indirect labelling with the fluorescent dyes Cy3 or Cy5 (Amersham). cDNA of mock infected cells was labelled with Cy3 and cDNA of infected cells with Cy5. For colour flip experiments, RNA from mock infected and prion infected cells was labelled with Cy5 and Cy3, respectively (Geiss *et al.* 2000). Labelled cDNA was resolved in 30 µl hybridization buffer (50% (v/v) formamide, 5x Denhardt's solution, 6x SSC and 0.5% SDS). Differentially labelled and resolved cDNA probes were mixed and placed on a pre-hybridized microarray slide, topped with a cover-slip, placed in a hybridization chamber (Genetix, Hampshire, UK) and placed in a shaded bath at 42°C for 16 hours. Following incubation, slides were washed in 3x, 1x, 0.5x, 0.25x and 0.1x SSC at room temperature. Slides were scanned using the GenePix Microarray scanner and images were analysed with the GenePix Pro3.0 image processing software (Axon Instruments; USA).

Data analysis and analysis of differentially expressed genes

For normalization and identification of significantly differentially regulated genes, the TIGR Microarray Data Analysis System (MIDAS) and Significance Analysis of Microarrays (SAM) was utilized (TM4, (Saeed *et al.* 2003)). Each data set was normalized by transforming the mean $\log_2$ ratio to zero to perform a total intensity normalization (Quackenbush 2002). Several filtering elements were applied to exclusively retrieve high-quality array elements,

including a flip dye consistency assessment, one bad tolerance policy parameter and a background test for both channel with a signal/noise threshold of 2.0 (Quackenbush 2002; Yang *et al.* 2002). For identification of genes with statistically significant changes in expression level we used the SAM Method (Tusher *et al.* 2001; Chu *et al.* 2002). Genes were ranked according to their relative difference value d(i), a score assigned to each gene on the basis of change in gene expression levels relative to the standard deviation. Only genes with d(i) scores greater than a threshold value were determined to be significantly differentially expressed. The percentage of such genes identified by chance is the false discovery rate (FDR). To estimate the FDR, potential nonsense genes were identified by calculating permutations of the measurements. The number of generated permutations was set to 100 and as imputation engine the row average imputer was used. The expression data have been submitted to the GEO database (GSE7119).

Candidate genes were classified based on the relationship of their gene products to one or more functions. Classification was performed using the definitions in the LION and ENSEMBL databases. BiblioSphere PathwayEdition (Genomatix, Munich, Germany; http://www.genomatix.de/) was used to calculate complete networks and rank pathway interactions by z-scoring on basis of Genomatix Knowledge Base Ontology. The over-representation of genes is calculated as a z-score based on the expected number of genes within the filter category (GO). Biological filtering was used to restrict the network to genes which are assigned to the biological function of the respective genes.

2.2.3.8 Quantitative real-time reverse transcription polymerase chain reaction (*Real-Time* PCR)

Background:

The *Real-Time* PCR is based on the detection and quantification of a fluorescent reporter molecule, which signal intensity rises directly proportionally to the produced PCR product (Lee *et al.* 1993; Livak *et al.* 1995). By measuring the fluorescent emission after each PCR cycle, the time-dependent detection of the amount of the PCR product is possible. In all *Real-Time* PCR experiments of this work the fluorescent reporter molecule SYBR-Green was used. This molecule intercalates into double stranded DNA (dsDNA) and emits fluorescent light upon activation. It does not bind to single stranded DNA (ssDNA) and shows only a very weak emission in solution, so the measured emitted fluorescent light correlates with the amount of dsDNA in the PCR sample (Morrison *et al.* 1998).
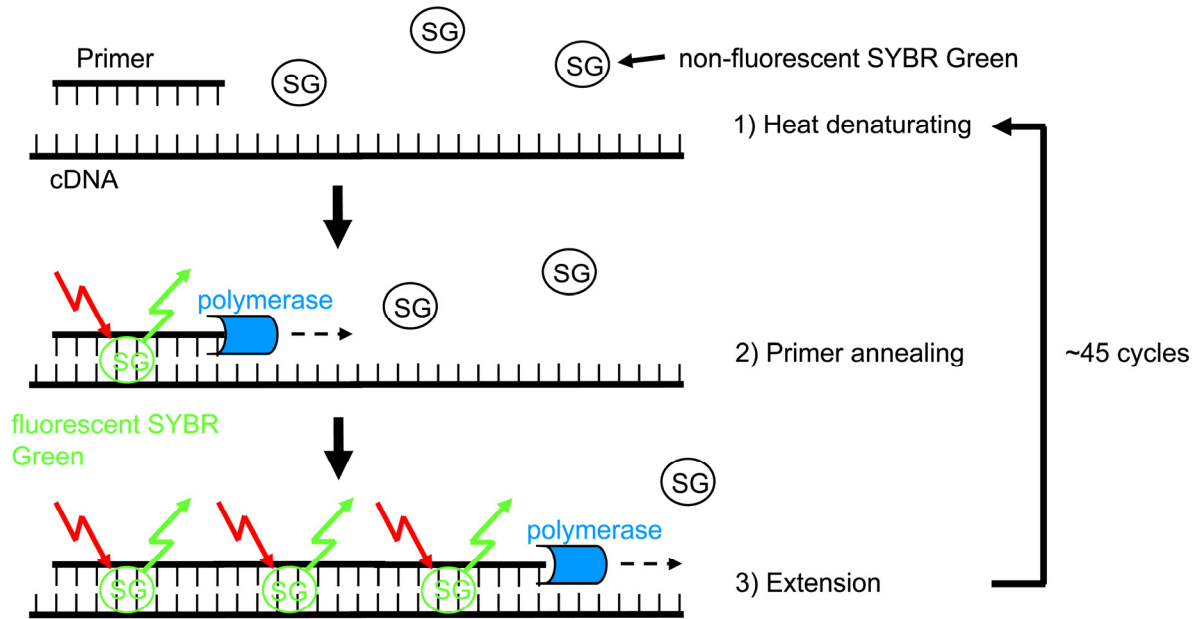
Figure 12: Overview of the mechanism of the *Real-Time* PCR using SYBR-Green as a fluorescent reporter molecule. The graphic shows the important steps during one PCR-cycle. It starts with the heat denaturation with no dsDNA and therefore only fluorescent inactive SYBR-Green molecules, followed by the primer annealing step and the beginning of nucleoside incorporation and intercalation of fluorescent SYBR-Green molecules into the dsDNA. The last step leads to the extension of the dsDNA by polymerase activity and an increase of detectable fluorescent light by more and more incorporation of now activated fluorescent dye molecules into the growing dsDNA strand.

Procedure:

RNA was reverse transcribed using the SuperScript II Reverse Transcription Kit (Gibco/Invitrogen, New York, USA) and random hexamers according to the manufacture's manual. As a negative control, each RNA sample was reverse transcribed without the reverse transcriptase. As control for a successful reverse transcription a normal PCR (**2.2.3.5**) was performed using primers for intracisternal A-particle (IAP) (**2.1.5**) to see if a distinct cDNA band could be detected in an agarose gel electrophoresis (**2.2.3.6**). IAP is a murine retrovirus with approximately 100.000 copies in the genome of a cell. Quantitative *Real-Time* PCR experiments for each gene were performed in triplicate using the LightCycler FastStart DNA Master SYBR Green I Kit according to the user's manual and the LightCycler© One-PCR machine (both Roche, Mannheim, D). Each *Real-Time* PCR run had a length of 45 cycles (**Table 7**) and the sequences of used primers are listed in (**Table 4**).

Reaction mix:

- 2 µl 10x-buffer
- 1.6 µl MgCl$_2$ (25 mM)
- 1 µl forward/reverse primer (20 mM)
- 12.4 µl RNase-free water
- 2 µl template (2.5-5 mM ≈ 50-100 ng cDNA)

Table 7: *Real-Time* PCR program

Program:	Denaturation				Type:	Melting Curves	Cycles:	1
Segment Number	**Temperature Target (°C)**	**Hold Time (sec)**	**Slope (C°/sec)**	**2°Target Temp (°C)**	**Step Size (C°)**	**Step Delay (Cycles)**	**Acquisition Mode**	
1	95	600	20	0	0	0	None	

Program:	Amplification				Type:	Quantification	Cycles:	45
Segment Number	**Temperature Target (°C)**	**Hold Time (sec)**	**Slope (C°/sec)**	**2°Target Temp (°C)**	**Step Size (C°)**	**Step Delay (Cycles)**	**Acquisition Mode**	
1	95	10	20	0	0	0	None	
2	60	5	20	0	0	0	None	
3	72	10	20	0	0	0	Single	

Program:	Melting Curve				Type:	Melting Curves	Cycles:	1
Segment Number	**Temperature Target (°C)**	**Hold Time (sec)**	**Slope (C°/sec)**	**2°Target Temp (°C)**	**Step Size (C°)**	**Step Delay (Cycles)**	**Acquisition Mode**	
1	95	0	20	0	0	0	None	
2	65	15	20	0	0	0	None	
3	95	0	0.1	0	0	0	Continuous	

Program:	Cooling				Type:	None	Cycles:	1
Segment Number	**Temperature Target (°C)**	**Hold Time (sec)**	**Slope (C°/sec)**	**2°Target Temp (°C)**	**Step Size (C°)**	**Step Delay (Cycles)**	**Acquisition Mode**	
1	40	30	20	0	0	0	None	

To confirm that a specific RT-PCR product was amplified 5 µl of each reaction was run on ethidium bromide agarose gels (**2.2.3.6**). The $2^{-\Delta\Delta C_T}$ method (Livak and Schmittgen 2001; Radonic *et al.* 2004) was used to calculate the relative expression levels. With this method the relative expression levels of the gene of interest in prion infected and mock infected cells were calculated normalized to a house-keeping gene (in this study RPII). The threshold cycle (C_T)-value marks the start of the exponential PCR amplification of one gene product and is defined as the PCR cycle number which fluorescence emission of SYBR Green is higher than a cut off emission level defined by the *Real-Time* PCR program (Roche, Mannheim, D). The higher the amount of cDNA in a sample the smaller is the detected C_T-value. To get the

relative expression level of one gene in two samples (prion or mock infected) the evaluation was done following the mathematical scheme of the $2^{-\Delta\Delta C_T}$ method:

1. The ΔC_T-value of the C_T-values of the gene of interest (=target) and the house-keeping gene (=normaliser) was determined:

$$\Delta C_T = C_T \text{ (target) - } C_T \text{ (normaliser)}$$

2. The $\Delta\Delta C_T$-value of one gene was determined out of the ΔC_T-values of this gene in the modified (=sample; here: prion infected) and the control group (=baseline; here: mock infected):

$$\Delta\Delta C_T = \text{sample's } \Delta C_T - \text{baseline's } \Delta C_T$$

3. As the amplification rate of the PCR after n cycles is 2^n, the comparative expression level of the gene of interest was determined as followed:

$$\text{comparative expression level} = 2^{-\Delta\Delta CT}$$

As the minimum detectable change a two-fold expression difference was used (Bubner *et al.* 2004) and only expression differences equal or higher than two-fold were considered as significant.

2.2.3.9   Transient transfection of mammalian cells

<u>Background</u>

The transient transfection method allows the introduction of foreign nucleic acid into eukaryotic cells. Plasmid DNA and siRNA were introduced into mouse cells by lipofection, a special form of transfection. Lipofection is carried out by mixing the plasmid DNA or siRNA with a cationic lipid to form liposomes that fuse with the cell membrane and so free their cargo inside the cell.

Transfection of plasmid DNA for luciferase assay

For transfection of plasmid DNA the transfection reagent Fugene 6 (Roche, Mannheim, D) was used according to the user's manual. Briefly, N2a cells were plated at a density of 1.3×10^5 cells per well in 12 well plates. 6 µl Fugene 6 per 2 µg of plasmid DNA was pre-incubated in 100 µl OptiMem+GlutMAX medium for 10 min at RT. Per reaction 1.6 µg psynSRE-Luc firefly luciferase plasmid and 160 ng of the renilla luciferase plasmid (**2.1.7**) were added to the Fugene 6 mixture and incubated for 20 min at RT. Meanwhile cells were

rinsed two times with the adequate cell medium (without FCS and Pen/Strep) and 900 µl medium was added to the cells. After incubation 100 µl of the transfection mixture was added and cells were incubated for 16 hours in the incubator. Transfection was stopped by a change of medium (including FCS and Pen/Strep).

Transfection with siRNA

The transfection reagent Lipofectamine 2000 (Invitrogen, Karlsruhe, D) was used for all siRNA transfection experiments according to the manufacture's manual. Briefly: 2.2×10^5 22L infected N2a cells were plated in 6 cm dishes for each experiment. 2 µl of siRNA and 2.5 µl of Lipofectamine 2000 were separately incubated in 100 µl OptiMem +GlutaMAX without FCS or Pen/Strep for 5 min at room temperature. Samples were mixed together and further incubated at RT for 30 min. Meanwhile cells were washed twice with the same medium and 1.8 ml medium was added to the cells. 200 µl of transfection mixture was added stepwise to the cells and gently mixed by pivoting the plate. Cells were incubated for seven hours in the incubator at 37°C and the medium was subsequently replaced by fresh medium.

2.2.3.10 Luciferase assay

Background:

The luciferase assay allows the indirect determination of the activity of a given transcription factor in a cell population. For that two plasmids each carrying the sequences for different luciferases are co-transfected into the cells. The luciferase proteins used in this work were isolated from insects and code for enzymes that produce bioluminescence when reacting with their special substrate. The firefly luciferase (*Photinus pyralis*) has a molecular weight of a 61 kDa different to the Renilla luciferase found in *Renilla reniformis* with a size of 36 kDa. Both are monomeric proteins that do not depend on any further post-translational modifications and have, because of their distinct evolutionary origins, different enzyme structures and therefore distinct substrate requirements (Matthews *et al.* 1977; Wood *et al.* 1984; de Wet *et al.* 1985). Because of these differences the respective bioluminescences elicited by reaction of each luciferase can be discriminated from the other (firefly luciferase has an extinction peak at the wavelength of 550-570 nm, whereas the extinction peak of Renilla luciferase lies at 480 nm).
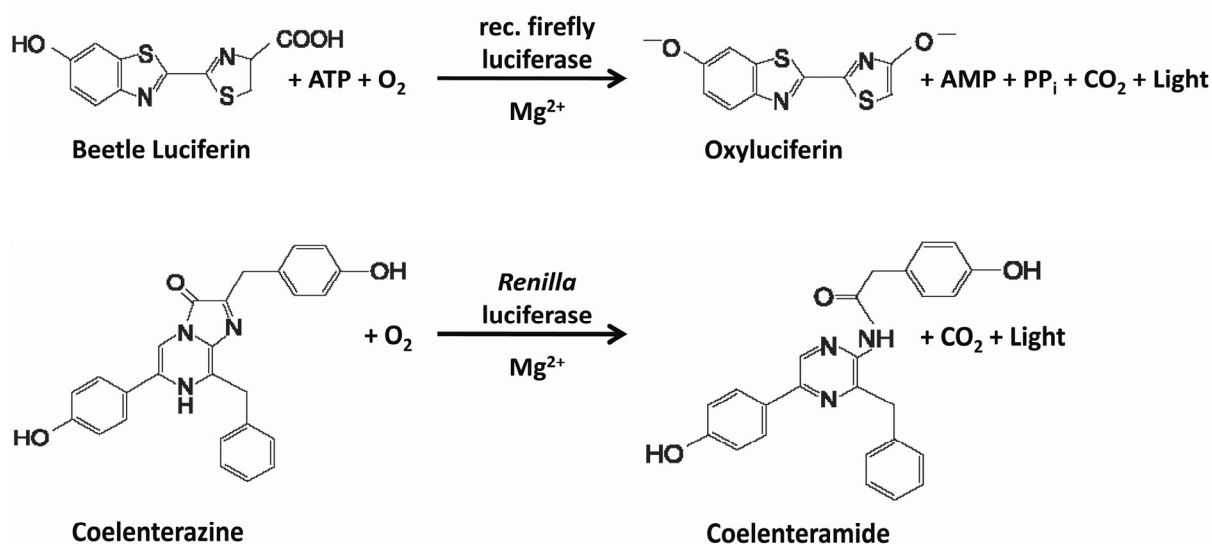
Figure 13: Overview of the chemical reactions resulting in bioluminescence catalyzed by firefly and *Renilla* **luciferase (taken from the Promega technical manual of the dual-luciferase reporter assay system with modifications)**

For the assay the first plasmid codes for the firefly luciferase under the control of a promoter containing transcription factor binding sites especially for the transcription factor of interest. Therefore the amount of produced firefly luciferase correlates directly with the activity of the transcription factor. The second plasmid acts as a internal transfection control, as it codes for *Renilla* luciferase controlled by a constitutive promoter.

Procedure:

N2a cells were plated at a density of 1.3×10^5 cells per well in 12 well plates and co-transfected with the luciferase plasmid psynSRE-Luc (1.6 µg) and as a transfection control with the pGL2 renilla plasmid (160 ng; Promega, Mannheim, D) using FuGene 6 (Roche, Mannheim, D) transfection reagent (**2.2.3.9**). The dual luciferase reporter assay (E1910, Promega, Mannheim, D) was used to measure the bioluminescence 24 hours post transfection. 100 µl of the 1x Passive Lysis Buffer (Promega, Mannheim, D) was used to lyse the cells on ice for 10 minutes. Lysates were cleared of cell debris by centrifugation for 10 minutes (4°C, 14.000 rpm; Eppendorf 5417C centrifuge). Supernatants were analysed for firefly and renilla luciferase activity using the Orion Microplate Luminometer (Berthold detection systems). Relative bioluminescence generated by firefly luciferase was normalized to the bioluminescence generated by the renilla luciferase.

2.2.3.11 Transient knock-down of Srebp2 and Ldlr expression by siRNA

Background:

The transient knock-down of genes with short interference RNA (siRNA) is a powerful tool to diminish one or more proteins in cells without generating a real knock-out cell. The siRNA machinery is a host encoded system activated by dsRNA complexes to protect cells for example against viral dsRNA genomes. For activating this machinery *in vitro* the artificial siRNA normally consists of 21 to 23 nucleotides with a sequence complementary to the mRNA of the protein of interest and must be introduced into the cytoplasm of the cells. In this work the lipofection method was used (**2.2.3.9**). In the cytoplasm the siRNA binds selectively to the complementary mRNA resulting in double stranded (ds) RNA. This dsRNA is recognized by an enzyme called DICER which cleaves the dsRNA and transfers it to RISC (RNA induces silencing complex). One strand of the dsRNA gets degraded while the other one serves as a template for RISC to detect and cleave additional mRNA coding for the same protein. The siRNA machinery of the cell therefore leads to a sequence-specific cleavage of perfectly complementary mRNA resulting in a knock-down of the protein. As siRNA itself gets cleaved by cellular nucleases the effect of the knock-down is time dependent and only transient.

Procedure:

To knock-down Srebp2 expression, two individual siRNAs directed against the murine Srebp2 (SI01433131 and SI01433138; Qiagen, Hilden; D), for Ldlr knock-down one siRNA against the murine Ldl receptor (Sc35803, Santa Cruz Biotechnology, Santa Cruz, USA) and one non-silencing (ns)-siRNA (AllStars Neg. Control siRNA; 1027281; Qiagen, Hilden; D) were utilized. $2.2x10^5$ cells of 22L infected N2a cells were plated in 6 cm dishes for each experiment and transfected with Lipofectamine 2000 (Invitrogen, Karlsruhe, D) and the respective constructs under RNase free conditions for 7 hours (**2.2.3.9**). Cells were subsequently cultured in serum-free OptiMEM medium supplemented with antibiotics and 0.2 µM mevalonate. As controls, un-transfected cells were also cultured. In an additional experiment, cells were transfected with siRNA and subsequently cultured in the presence of 10% FCS. After 48 h, cells were detached from the plate and split into 2 samples. Cells were lysed in two different buffers, allowing detection of PrP^{Sc}, PrP^{C}, Ldlr and GAPDH (**2.2.4.1**) or Srebp2 and GAPDH (**2.2.4.2**). Protein content was determined using the Bradford assay (**2.2.4.4**). After PK treatment of the lysates, the complete PK-treated sample was loaded on a

SDS gel for Western blot analysis. Fifteen µg of total protein present in the samples not treated with PK were loaded as a control.

2.2.4   Protein biochemical methods

2.2.4.1   Preparation of postnuclear lysates for PrP^C/PrP^{Sc} detection

Cells were washed with 5 ml of cold PBS and lysed with 1 ml lysis buffer for 10 min at RT. To remove cell debris the lysate was transferred to a 1.5 ml Eppendorf tube and centrifuged for 1 min and 14000 rpm (Eppendorf 5417C centrifuge) at RT. The supernatant was then subjected to proteinase K digestion (**2.2.4.3**) for PrP^{Sc} detection. For PrP^C detection the supernatants were transferred to a new 15 ml Falcon tube and 0.02 % Pefabloc SC protease inhibitor was added to avoid hydrolization of PrP^C by cellular proteases. Proteins in the supernatant were precipitated with 5 ml (5fold volume) of methanol and the samples were incubated at -20°C over night. Precipitated proteins were sedimented by centrifugation for 25 min at 4°C and 3500 rpm in an Sigma centrifuge (rotor 4K15). Methanol supernatant was discarded, the protein pellets were air-dried for 10-15 min at room temperature and resuspended in 50-100 µl TNE buffer. The samples were stored at -20°C until Western blot analysis (**2.2.4.5**).

Lysis buffer:	NaCl	100 mM
	Tris-HCl (pH 7.5)	10 mM
	EDTA	10 mM
	Triton X-100	0.5 % (w/v)
	DOC	0.5 % (w/v) in A. dest

TNE buffer:	NaCl	150 mM
	Tris-HCl (pH 7.5)	50 mM
	EDTA	5 mM in A. dest

2.2.4.2   Preparation of pre-nuclear lysates for Serbp2 detection

For detection of full length Srebp2 by Western blot, confluent monolayers of mock infected N2a and 22L infected N2a cells were washed twice with 5 ml of cold PBS and incubated in a hypotonic lysis buffer (40 mM Tris-HCl, pH 7.4; 150 mM NaCl; 1 mM EDTA; 0,3% Nonident P40, 1 mM dithiothreitol) on ice for 10 minutes. This buffer at low temperature

disrupts the cell membrane, but leaves the nucleus of the cell intact. Lysates were cleared of cell debris and nuclei (14.000 rpm, Eppendorf 5417C centrifuge, 1 min, RT), the supernatant was transferred to a new 15 ml Falcon tube in and proteins were precipitated with 5 ml (5fold volume) of methanol at -20°C over night. Precipitated proteins were sedimented by a centrifugation step for 25 min at 4°C and 3500 rpm in an Sigma centrifuge (rotor 4K15). Methanol was discarded, the protein pellets were air-dried for 10-15 min at room temperature and resuspended in 50-100 µl TNE buffer. The samples were stored at -20°C until Western blot analysis (**2.2.4.5**).

Hypotonic lysis buffer:	NaCl	150 mM
	Tris-HCl (pH 7.4)	40 mM
	EDTA	1 mM
	Dithiothreitol	1 mM
	Nonident P40	0.3 % in A. dest

2.2.4.3 Proteinase K (PK) digestion of post-nuclear lysates

20 µg/ml of PK was added to aliquots of post-nuclear lysates (**2.2.4.1**) and incubated for 30 min at 37°C. Digestion was stopped with 0.02 % Pefabloc SC proteinase inhibitor and samples were precipitated with methanol (5 x volumes) at -20°C over night. Precipitated proteins were sedimented, resuspended in TNE (both described in **2.2.4.1**) and stored at -20°C for further analysis.

2.2.4.4 Bradford assay for determination of protein concentration

The total protein content in the cell lysates was determined using the Bradford assay with the Coomassie Protein Assay Reagent (Pierce, Rockford, USA) according to the user's manual. The assay depends on the shift of the absorption maximum of the coomassie dye from $\lambda = 465$ nm to $\lambda = 595$ nm upon binding to proteins in an acid solution. This shift can be photometrically detected. A standard curve was established by diluting a 2 mg/ml Albumin Standard (Pierce, Rockford, USA) according to the manufacture's manual into following dilution steps: 0, 50, 75, 150, 250, 500, 1000 and 1500 mg/ml. Before measuring aliquots of the cell lysates were diluted 1:25 with TNE to avoid a sample concentration higher than the maximum standard concentration. 5 µl of all standards and diluted samples were pipetted into a 96 well plate and incubated with 250 µl of coomassie dye. The protein content was

measured using a Sunrise plate reader at $\lambda = 595$ nm and further analysed by the computer software Magellan 2 (both Tecan Austria GmbH, Mainz-Kastel, D).

2.2.4.5 Sodium dodecyl sulfate-polyacrylamide gel electrophoresis (SDS-PAGE)

Two different acrylamide concentrations in the resolving gel were used: 7.5 % for detection of proteins with a molecular weight in a range between appr. 50-200 kDa and 12.5 % for smaller proteins with molecular weight in the range of 12-60 kDa. For all SDS gels glass plates were rinsed with ethanol and spacers were placed on both edges of the plates. Plates were transferred to a plastic bag and placed in a casting chamber. The mixture of the resolving gel (lower gel) was poured between the plates and overlaid with isopropanol to achieve total polymerization. Isopropanol was discarded, the polymerized gel was briefly air dried and then overlaid with the mixture for the stacking gel (upper gel). Combs were immediately inserted before polymerization of the upper gel. After polymerization the combs were removed and the gel with the glass plates was placed in an electrophoresis chamber and covered with 1 x electrophoresis buffer. Samples (max. 50 µl for small slots or max. 100 µl for wide slots) and a molecular weight marker were loaded. Low power (30 mA) was applied until the proteins reached the resolving gel to avoid precipitation of proteins during entering the stacking or resolving gel, respectively. Electrophoresis was performed under a constant power of 45 mA until the tracking dye had reached the bottom of the resolving gel.

4 x Upper gel solution	Tris-HCl (pH 8.8)	1.5 M
	SDS	0.4 % (w/v) in A. dest
4 x Lower gel solution	Tris-HCl (pH 6.8)	0.5 M
	SDS	0.4 % (w/v) in A. dest
APS	10 % (w/v) stock solution in A. dest	
3 x SDS sample buffer	Tris-HCl (pH 6.8)	83 mM
	SDS	6.7 % (w/v)
	Glycerol	33 % (v/v)
	2-mercaptoethanol	16.6 %
	Bromphenol blue	in A. dest

10 x SDS electrophoresis buffer	Tris	250 mM
	Glycine	2.5 mM
	SDS	1 % (w/v) in A. dest

Resolving gel mixture (12.5 % acrylamide)	A. dest	20.3 ml
	Lower gel solution	15.4 ml
	Protogel	28.9 ml
	TEMED	90 μl
	APS	192 μl

(7.5 % acrylamide)	A. dest	30.7 ml
	Lower gel solution	15.4 ml
	Protogel	15.5 ml
	TEMED	90 μl
	APS	192 μl

Stacking gel mixture (5 % acrylamide)	A.dest	12.3 ml
	Lower gel solution	5.3 ml
	Protogel	3.5 ml
	TEMED	38 μl
	APS	210 μl

2.2.4.6   Western blot (Immunoblot)

Per acrylamide gel six blotting papers and one PVDF membrane were cut to the size of the gel. The PVDF membrane was rinsed with methanol and washed with A. dest and the blotting papers were soaked in blotting buffer. On the anode of a semidry blotting chamber three soaked blotting papers were overlaid with the PVDF membrane, followed by the gel and a final layer of three soaked blotting papers. The chamber was closed with the cathode and electrophoresis took place for 30 min at RT and a constant power of 18 V. After transfer of the proteins to the PVDF membrane, the membrane was soaked for 30 min in blocking solution at room temperature. The primary antibody (**Table 5**) was added in an appropriate dilution (in TBST) and incubated under constant horizontal shaking at 4°C over night. After five washing steps in TBST (each longing 5 min) the secondary antibody (**Table 5**) diluted into TBST was added for 60 min at RT. After additional five washing steps (each for 5 min) in TBST the membrane was briefly dried between two blotting papers and then incubated for 3 min with the chemiluminescence substrate (ECL Plus), prepared according to the user's manual. The membranes were exposed to X-ray films for different time periods.

Blotting buffer	Tris	3 g
	Glycine	14.4 g
	Methanol	20 % (v/v)
	A.dest	ad 1000 ml
10 x TBST	Tris-HCl (pH 8.0)	100 mM
	NaCl	100 mM
	Tween-20	0.5 % (v/v) in A. dest
Blocking buffer	skim milk powder	5 %in 1 x TBST

ECL Plus Detection Kit

2.2.4.7 Thin layer chromatography (TLC) for determination of cellular cholesterol level

Cell pellets were suspended in 3 M aqueous solution of guanidine hydrochloride to inactivate prions. Water was added, the samples were sonicated for 30 sec and the protein content was determined (Smith *et al.* 1985; Smith *et al.* 1985). After subsequent addition of 4 ml of methanol and 3 ml of chloroform/methanol/water (10:5:1, v/v/v), lipids were extracted for 24 h at 37°C. The liquid phase was separated by filtration. The solvent was evaporated in a stream of nitrogen and the residues were desalted by reversed phase chromatography on LiChroprep RP18 (Merck, Darmstadt, D) columns (Williams and McCluer 1980). Lipids were applied to high performance thin layer chromatography (HPTLC) Silica Gel 60 plates (Merck, Darmstadt, D), which were pre-washed twice with chloroform/methanol (1:1, v/v) and air-dried for 30 min. Each lane of the TLC plate was loaded with the equivalent of 600 μg protein. For quantification of free cholesterol, the TLC solvent system used was chloroform/methanol/glacial acetic acid (190:9:1, v/v/v). For the quantification of the total cholesterol content, cholesteryl esters were cleaved by alkaline hydrolysis with 2.5 ml of a 100 mM solution of sodium hydroxide in methanol for 2 hours at 37 °C. After neutralization with acetic acid, the mixtures were desalted again on RP18 columns. Lipids were separated into acidic and neutral fractions by anion exchange chromatography on DEAE-cellulose (GE Healthcare, Freiburg, D) columns (Momoi *et al.* 1976) with some modifications. The lipid mixture was solved in 1 ml of chloroform/methanol/water (3:7:1, v/v/v) and applied to the columns. Neutral lipids were eluted with 7 ml of the same solvent, and then acidic lipids were eluted with 8 ml of chloroform/methanol/0.8 M ammonium acetate in water (3:7:1, v/v/v). Neutral lipids were applied to pre-washed HPTLC plates, loading each lane with the equivalent of 400 μg protein. The TLC plates were developed in chloroform/methanol/glacial acetic acid (190:9:1, v/v/v). For quantitative analytical TLC determination, increasing

amounts of standard cholesterol (Sigma-Aldrich Chemie GmbH, Steinheim, D) were applied to the TLC plates in addition to the lipid samples. After development, plates were dried under reduced pressure. For detection of lipid bands, the TLC plates were sprayed with a phosphoric acid/copper sulfate reagent (15.6 g of $CuSO_4(H_2O)_5$ and 9.4 ml of H_3PO_4 (85 %, w/v) in 100 ml of water) and charred at 180 °C for 10 minutes (Yao and Rastetter 1985). Lipid bands were then quantified using a photo-densitometer (Shimadzu, Duisburg, D) at a wavelength of 595 nm.

2.2.4.8 Protein detection with immunofluorescence microscopy

For immunofluorescence analysis cells were seeded on cover slips in a 24 well format. The cover slips were pre-coated with poly-L-lysine for 15 min at RT, washed with PBS, air-dried and sterilized in a UV-crosslinker. All procedure steps were done at room temperature (RT).

Cells were grown for one day in case of murine primary neurons and for 5 days for primary astrocytes. Culture medium was discarded, cover slips with cells transferred to a new 12 well, washed once with PBS and fixed with Roti-Histofix for 30 min. After three washing steps with PBS the cells were quenched for 10 min with quenching solution, washed again three times with PBS and permeabilized for 10 min with Triton-X 100 (0.1 % in A. dest (v/v)). After three rinses with PBS cells were incubated for 7 min in 5 M guanidine hydrochloride solution to denaturate prions and to allow the selective detection of PrP^{Sc} in prion exposed cells. With this step denatured PrP^{C} is almost undetectable with the prion antibody 4H11, whereas detection of aggregated PrP^{Sc} is still possible. After washing the cells with PBS cover slips were blocked with 0.2 % gelatin ((v/v) in A. dest) for 10 min to avoid unspecific binding of the first antibody to the plate surface. The cells were incubated with primary antibody in appropriate dilution (**2.1.6.2**; 0.2% gelatin solution in A. dest (v/v)) in a humid chamber for 30 min, afterwards washed with PBS and then incubated for 30 min in the dark with the secondary antibody (anti-mouse IgG antibody, complexed with fluorescent dye Cy2 or Cy3) in appropriate dilution (**2.1.6.2**) in 0.2 % gelatin solution (v/v) in a humid chamber. To label the nuclei of the cells cover slips were washed with PBS and incubated with Hoechst solution (1:1000 in 0.2 % gelatin (v/v)) for 15 min under the same conditions like before. Cover slips were mounted on glass slides with Roti-Histogel and kept away from light at 4°C in a refrigerator until protein detection with a fluorescent microscope. Cy2 has its absorption and emission maximum at $\lambda = 492$ nm and 510 nm and the Hoechst solution dye at $\lambda = 358$ nm and 461 nm, respectively.

| Quenching solution: | Ammonium chloride | 50 mM |
| | Glycine | 20 mM in A. dest |

2.2.4.9 Fluorescent-activated cell sorting (FACS) analysis

Cells were detached from the plate as described (**2.2.5.1**), 10^6 cells were transferred to FACS tubes and centrifuged for 3 min at 1200 rpm (Sigma 4K15 centrifuge) and 4°C. The supernatant was discarded, the cell pellet resuspended in 500 µl FACS buffer and blocked on ice for 10 min. Cells were again pelleted by centrifugation as described before and supernatant was discarded. Then primary antibody diluted in FACS buffer (**2.1.6.2**) was given to the cells for 30 min on ice, followed by three washing steps. Cells were afterwards incubated with secondary antibodies, conjugated to fluorescent dyes and appropriate diluted in FACS buffer (**2.1.6.2**). Cells were treated for 5 min on ice with 7-AAD diluted in FACS buffer shortly before measurement to exclude permeabilised dead cells from the analysis. For gating of the cell population cells without any staining and as a control for background fluorescence through unspecific binding cells only incubated with the secondary antibody were used. Samples were analysed in a Coulter EPICS XL apparatus.

| FACS buffer | FCS | 2.5 % (v/v) |
| | NaN$_3$ | 0.05 % (v/v) in PBS |

2.2.5 Culturing and passaging of eukaryotic cell lines

The experiments with mammalian cells were performed in a biosafety level 2 laminar flow. Cell cultures were regularly screened by PCR to ensure the absence of *Mycoplasma sp.* and disposable plastic pipets and gloves were used to avoid any contamination of the cells with microbes. Appropriate safety protection shields and suitable gloves were worn for handling of liquid nitrogen.

2.2.5.1 Cultivation and passaging of mammalian cell lines

All cells were cultured on cell culture dishes in a humidified atmosphere containing 5 % CO_2 at 37°C. Different culture media were used for different cell lines as listed below:

| N2a: | OptiMEM + GlutaMAX + 10 % FCS + Pen/Strep |
| GT1: | OptiMEM + GlutaMAX + 10 % FCS + Pen/Strep |

L929: DMEM + GlutaMAX + 10 % FCS + Pen/Strep

BV-2: RPMI1680 + 7.5 % FCS + 50 mM Et-SH + Pen/Strep

Culture medium was exchanged every two days. After reaching confluence the cells were once rinsed with PBS and detached from the culture dish by incubation with 1 ml Trypsin/EDTA solution. Cells were resuspended in an appropriate volume of culture medium and diluted 1:10 unless otherwise stated to a new plate. 10 ml of culture medium were added for further cultivation.

2.2.5.2 Subcloning of N2a cells

For obtaining N2a cells highly susceptible to prion infection, the N2a population was subcloned by limiting dilution in a 96 well plate. 180 µl culture medium was added to each well. Starting with row A 20 µl of a cell suspension were mixed with the medium and the same volume was transferred to row B. This step was repeated until the last row. After the cells settled down to the bottom each well was monitored using a microscope looking for wells with single cells. Clones were expanded and further on tested for susceptibility to infection with 22L prion infected brain homogenate (**2.2.5.7**).

2.2.5.3 Preparation of primary neurons and astrocytes

All cell culture wells were pre-coated with poly-L-lysine (5 µg/ml in $H_20_{bidest.}$) for one hour at RT, then washed three times with PBS and air-dried. Primary neurons from hippocampi and astrocytes of C57BL/6 embryonic mice (gestation day 16) were prepared as described elsewhere (Lopes *et al.* 2005) with some modifications. Briefly, embryonic brains were extracted and kept in Hanks' balanced salt solution (HBSS) with 10% PS. Hippocampi were excised, transferred to a 1.5 ml reaction tube, washed with HBSS and incubated in 1 ml trypsin at 900 rpm and 37°C for 20min in a thermo mixer. Next the trypsin was discarded, the hippocampi were rinsed in HBSS complemented with 10% fetal calf serum to inactivate the trypsin and cells were collected by centrifugation at 2000 rpm (Eppendorf 5417C centrifuge) for 3 minutes at RT. The supernatant was discarded, the cells washed twice with HBSS (+PS) and incubated with DNase I (2U/ml) in 1 ml neurobasal medium for 2 minutes at RT. Single cell suspensions were obtained by carefully pipetting the cells approx. 10-20 times. Trypane Blue was added to an aliquot of the cell suspension to identify dead cells and to determine the number of viable cells using a Fuchs-Rosenthal cell counter chamber. Approx. $1x10^6$ viable

cells were plated in neurobasal medium supplemented with B-27 and antibiotics in 6 wells for infection studies or 5×10^3 viable cells on cover slips in 24 wells for immunofluorescence analysis. 10 µM of antimitotics uridine and fluorodeoxiuridine were added (Cronier *et al.* 2007) to avoid growing of any dividing cell type (e.g. astrocytes). Weekly, one third of the medium was replaced with fresh medium. For isolation of primary astrocytes, meninges were removed, hemispheres were rinsed with HBSS and transferred to a 15 ml Falcon tube with 10 ml DMEM (+PS and 10% FCS). For dissection of the cells the complete solution was passed twice through a syringe needle with a diameter of 0.9 mm. Complete cell solution of two hemispheres was plated per 10 cm cell plate for infection or 500 µl per 24 well for immunofluorescence studies. Of note: astrocytes were not counted before plating as most of them die and so no exact cell number can be seeded. Cells were grown in DMEM with Pen/Strep and 10% FCS and rinsed every other day thoroughly with PBS for one week to prevent any other cell type from growing on the plate. The medium was exchanged every three days. Cells were cultured for up to 3-4 weeks.

2.2.5.4   Cryoconservation of cells

Confluent cell monolayers were detached from the plate as described in (**2.2.5.1**), transferred to a 15 ml Falcon tube and cells were pelleted by centrifugation at 21°C and 1000 rpm for 10 min (Sigma 4K15 centrifuge). Cells were resuspended in freshly prepared cryo-medium (90 % culture medium and 10 % DMSO). Aliquots of 1 ml were transferred to cryoconservation tubes, placed at -80°C over night and than transferred to a liquid nitrogen tank for long-term storage.

2.2.5.5   Determination of cell number

Cells were detached from (**2.2.5.1**) and resuspended in 10 ml culture medium. An aliquot was diluted 1:10 in culture medium and transferred to a Fuchs-Rosenthal hemocytometer for counting. The number of cells per ml was determined according to the following equation:

Cell number/ml = (counted cells : number of counted squares) x dilution factor x 5000

2.2.5.6   Preparation of prion containing and normal brain homogenates

The mouse-adapted scrapie strain 22L was propagated in C57BL/6 mice and 22L infected mouse brains were kindly provided by Prof. Dr. M. Groschup, Friedrich-Löffler-Institut,

Bundesforschungsinstitut für Tiergesundheit, Isle of Riems. Normal brains were obtained from healthy C57BL/6 mice. The brains were weighed and a 10 % (w/v) homogenate was prepared in PBS using a glass douncer. Aliquots of the homogenate were stored in cryoconservation tube at -80°C.

2.2.5.7 Infection of cells with prions

All cell lines:

Cells were plated in 24 well plates and were infected at a density of 20-25%. The final concentration in each well was 1.0% brain homogenate (v/v). After 24 hour incubation the medium was discarded, the cells were washed 3-4 times with PBS to remove residual brain homogenate and cells were further cultured in normal cell culture medium until analysis.

Primary cells:

Primary neurons were exposed to 0.1% brain homogenates (final concentration; mock and 22L) one day post plating and astrocytes shortly before reaching confluence. The next day the medium of the neuronal populations was sterile filtered and returned to the primary neurons, as these cells do not survive any washing procedure. The medium of the primary astrocytes was discarded, the cells washed three times thoroughly with PBS to remove homogenate debris and fresh medium was added to the cells. Cells were cultured as described in **2.2.5.1.**

3. Results

3.1 Isolation of a N2a cell clone highly susceptible to prion infection

An essential step for obtaining reliable microarray results of prion infected cells is a high prion infection rate within a given cell population. As already mentioned in the introduction a microarray experiment with prion infected N2a cells had already been performed by our group (Greenwood *et al.* 2005). The infection rate of an un-cloned N2a cell population is usually around 5 % (Race *et al.* 1987a). A method for getting a higher rate of infection is isolation of susceptible cell clones out of the normal population (Bosque and Prusiner 2000). Using this method a N2a cell clone highly susceptible to prion infection was established and used for the cDNA microarray experiment. An overview of the isolation process is shown in **Figure 14A**. The normal N2a cell population was single cell cloned and infected by Sabine Gilch. The resulting clones were either infected with the mouse-adapted prion strain 22L or mock infected and then tested by Western blot analysis for susceptibility to prion infection. The most susceptible cell clone number 5 that displayed a strong scrapie signal by Western blot was sub-cloned 18 passages post infection and 13 sub-clone populations were tested for PrP^{Sc} signal in Western blot analysis to estimate the final infection rate. 9 out of 13 sub-clones were tested positive for PrP^{Sc}, so the prion infection rate within the N2a clone 5 population was estimated to be approx. 70 % (**Figure 14B**). The lack of a PrP^{Sc} signal after PK treatment of the mock cell lysate was also tested and confirmed by Western blot analysis. These two cell populations (22L and mock) of N2a clone 5 were both cultured until passage 18, tested for PrP^{Sc} and PrP^{C} (**Figure 14C**) and used for the cDNA microarray experiment.
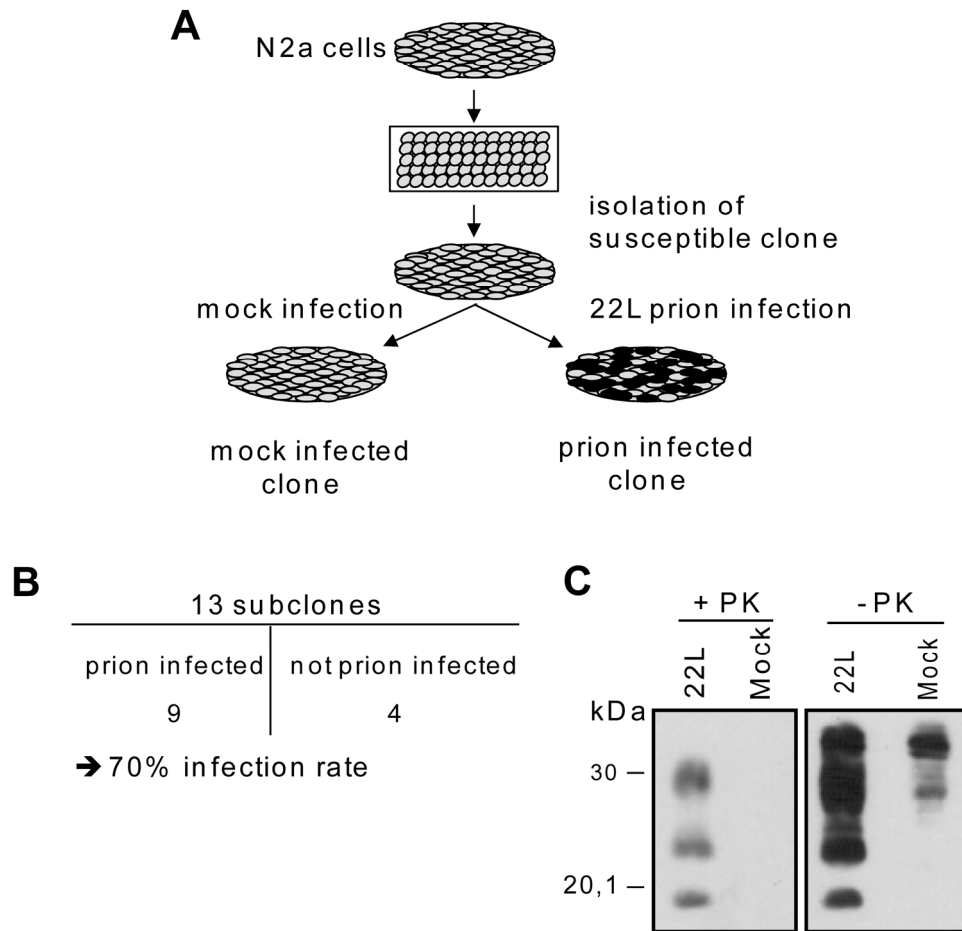
Figure 14: Isolation of a N2a clone highly susceptible to 22L prions. (A) N2a cells were cloned by limiting dilution and single cell clones were tested for 22L prion susceptibility. Cells were exposed to 1 % brain homogenate from a mouse terminally ill with 22L scrapie or to brain homogenate from an uninfected mouse as a mock control. Clones were subsequently passaged and tested for PrP^{Sc} formation. Black dots represent prion infected cells within the total population. (B) Clone 5 persistently infected with scrapie strain 22L was subcloned 18 passages post infection and single cell clones were tested for PrP^{Sc} content. The number of PrP^{Sc} positive cell clones per clones tested is given. (C) Western blot analysis of N2a clone 5 exposed to normal brain homogenate (mock) or 22L brain homogenate. Cells were lysed 18 passages post exposure to brain homogenates and lysates were left untreated (PK-) or subjected to proteinase K treatment (PK+). Western blots were developed using the mouse monoclonal antibody 4H11.

3.2   RNA isolation of 22L and mock infected cells for gene expression experiments

The N2a cell clone 5 was prion and mock infected. Prion infected and uninfected cells of passage 18 were expanded to several 10 cm cell dishes. One was used for detection of PrP^{Sc} by Western blot. As expected the prion infected cells showed a clear PrP^{Sc} banding pattern whereas in the mock infected cells no signal was detectable after PK digestion of post nuclear lysates (**Figure 14C**). RNA of all other 22L and mock infected N2a cells was isolated using

the Qiagen RNeasy Kit according to the user's manual (**Figure 15**). The RNA was tested for DNA contamination by PCR using primers for the intracisternal A-particle (IAP) to see if a distinct cDNA band could be detected in an agarose gel electrophoresis. IAP is a murine retrovirus with approximately 100.000 copies in the genome of a cell, therefore a positive PCR signal indicates genomic DNA contamination. Only RNA samples lacking any PCR band were pooled and used for further experiments.
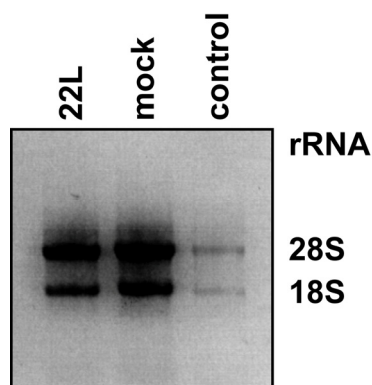
Figure 15: Extracted RNA of N2a clone 5 (22L and mock infected). Undigested RNA was detected after extraction and analysed by formamide gel separation. Two distinct bands are visible indicating the 28S and 18S rRNA. RNA extracted of mouse liver (1µg/µl) was loaded as a positive control.

3.3 Gene expression profile of the 22L infected N2a cell clone

Knowledge of altered gene expression caused by prion infection could provide new insights into the host reaction to the pathogen. The gene expression profile experiment was performed in collaboration with the group of PD Dr. Johannes Beckers from the Institute of Experimental Genetics (Helmholtz Zentrum München - German Research Center for Environment and Health). With the cDNA microarray established by this group the expression level of over 20.000 murine genes can be detected, so an almost mouse genome wide microarray study was accomplished. Both RNA samples of 22L and mock infected N2a cells were reverse transcribed and differentially labeled with the fluorescent dyes Cy3 and Cy5. The pooled cDNA probes were hybridized on the microarray and the resultant expression levels for each gene in each sample were detected by a scanning process, in which the fluorescent intensity of each color was measured separately for each gene. An overlay of both intensities was performed automatically by the scanning program and the results were displayed in a false color image (**Figure 16**). Each spot on the slide represents one gene, with yellow spots indicating an equal gene expression level in both cell groups, whereas red spots

represent a higher and green spots a lower gene expression level in the prion infected cells compared to the mock control.
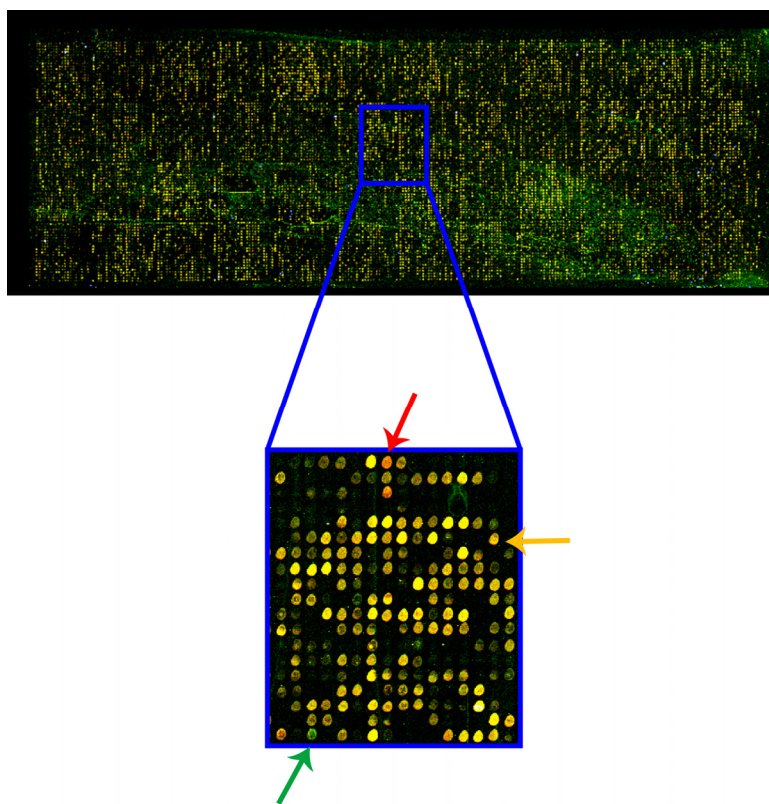
Figure 16: False color image of a representative cDNA microarray (upper part) and a higher magnification (lower part). Fluorescent intensities of a cDNA microarray hybridized with Cy3 and Cy5 labeled cDNA from 22L infected and mock infected N2a clone 5 cells are given as false colors. For better visualization of the hybridization area, one part of the chip is shown at higher magnification. Red dots indicate over-expressed and green dots down-regulated genes in prion infected cells. Equally expressed genes are displayed in yellow.

In total, eight microarrays were hybridized. Statistical analysis revealed that out of 3309 detected genes, 203 were significantly differentially regulated with a $d(i) > 4$, a score assigned to each gene on the basis of change in gene expression levels relative to the standard deviation, and a reproducible differential expression was found for all microarray experiments (**Table 8**). The number of false positives per 100 permutations was estimated as a false discovery rate (FDR) of 0% for each data set. For 37 genes increased expression levels were identified while 166 genes were down-regulated. Differentially transcribed genes were classified according to the biological function of their gene products based on definitions in the LION and ENSEMBL databases. Functional information was limited or absent for some of the candidate genes. For 27 up- and 94 down-regulated genes, a putative function is known or has been suggested.

Table 8: Genes with putative known function differentially expressed in prion infected N2a *vers*. N2a mock infected cells

Superscript letter used in this table: [a] The putative gene function; [b] The microarray clone ID; [c] Gene name; [d] In the microarray experiment determined average fold gene expression

Putative function[a]	Clone ID[b]	Gene[c]	Avg fold[d]
1) Up-regulated			
Catalytic activity	MG-15-252a12	**Blvrb**: Biliverdin reductase B	4.62
Cell cycle	MG-3-76n3	**Ddit3**: DNA-damage inducible transcript 3 (**Synonyms:** C/EBP homoologous protein 10, chop, CHOP-10, CHOP10, Gadd153)	4.53
Cholesterol metabolism	MG-3-37f4	**Idi1:** Isopentenyl-diphosphate delta-isomerase 1 (**Synonym:** Ipp)	3.22
	MG-6-57e23	**Hmgcs1**: 3-hydroxy-3-methylglutaryl-Coenzyme A synthase 1	7.46
	MG-8-94d7	**Hmgcr**: 3-hydroxy-3-methylglutaryl-Coenzyme A reductase (**Synonyms:** HMG-CoAR, Red)	3.32
	MG-8-50j2	**Dhcr7**: 7-dehydrocholesterol reductase	3.53
	MG-8-117d11	**Glul**: Glutamine synthetase (**Synonyms:** Glns, GS)	6.17
	MG-14-106l5	**Sc4mol**: C-4 methyl sterol oxidase	10.91
	MG-3-12a15	**Fdft1**: farnesyl diphosphate farnesyl transferase 1 (**Synonyms:** SQS, squalene synthase)	5.58
	MG-6-12i22	**Srebf2**: sterol regulatory element binding factor 2 (**Synonym:** SREBP-2)	3.25
Cholesterol/Lipid metabolism	MG-15-189g14	**Scd2**: stearoyl-Coenzyme A desaturase 2 (**Synonym:** Scd-2)	4.31
	MG-15-90m19	**Ldlr:** Low-density lipoprotein receptor precursor	3.82
DNA binding; DNA integration	MG-3-49p12	**Ppfibp2**: protein tyrosine phosphatase, receptor-type, F interacting protein, binding protein 2 (**Synonyms:** Cclp1, liprin beta 2)	3.56
Energy metabolism	MG-13-1a23	**Eno2**: enolase 2, gamma neuronal (**Synonyms:** Eno-2, NSE)	3.16
GTPase Regulator	MG-6-13l7	**Gdi1**: guanosine diphosphate (GDP) dissociation inhibitor 1 (**Synonyms:** GDIA, GDIalpha, MGC:21593, Rab GDIalpha)	3.32

Table 8 (*continued*)

Putative function[a]	Clone ID[b]	Gene[c]	Avg fold[d]
Intracellular signaling cascade	MG-13-117j9	**Ahnak**: AHNAK nucleoprotein (desmoyokin) (**Synonym:** DY6)	8.17
Iron ion binding	MG-14-106n17	**Trf:** Transferrin (**Synonyms:** Cd176, HP, Tfn)	5.16
MAP kinase; Hydrolase activity	MG-3-150c14	**Dusp4**: Dual specificity phosphatase 4	3.46
Proteolysis; metal ion binding	MG-3-5f9	**X83328**: EST X83328 (**Synonym:** ESTM12)	3.19
Transcription elongation factor	MG-16-5b5	**Supt6h**: suppressor of Ty 6 homolog (S. cerevisiae) (**Synonym:** SPT6)	3.49
Transferase activity	MG-3-81d5	**Gstm1**: glutathione S-transferase, mu 1 (**Synonyms:** Gstb-1, Gstb1)	3.60
Translation	MG-8-22p22	**Rps10**: ribosomal protein S10	3.22
Translocation elongation factor	MG-12-267k10	**Gtpbp2:** GTP binding protein 2	3.53
Transport and binding protein	MG-3-68i14	**Ucp2**: uncoupling protein 2 (mitochondrial, proton carrier) (**Synonyms:** Slc25a8)	3.29
	MG-6-74c18	**IER3**: immediate early response 3 (**Synonyms:** cAMP inducible gene 3, cI-3, gly96, IEX-1)	4.90
	MG-8-79a16	**Snag1**: Sorting nexin associated golgi protein 1	3.06
Unknown function	MG-3-28i9	PREDICTED: similar to putative retrovirus-related gag protein	11.47

2) Downregulated

Aminoacyl-tRNA ligase	MG-6-1c9	**Nars**: asparaginyl-tRNA synthetase (**Synonym:** ASNRS)	-2.83
Apoptosis	MG-6-19l12	**Eif5a**: eukaryotic translation initiation factor 5A (**Synonym:** D19Wsu54e)	-3.16
ATP binding	MG-14-80g20	**Ddx3x**: DEAD/H (Asp-Glu-Ala-Asp/His) box polypeptide 3, X-linked (**Synonyms:** embryonic RNA helicase, Fin14)	-4.22
	MG-6-43d8	**Ak2**: Adenylate kinase 2 (mitochondrial)	-3.10
	MG-15-86p19	**Rrm1**: ribonucleotide reductase M1 (**Synonym:** RnrM1)	-4.66
ATP binding, DNA-binding	MG-15-98p23	**Top2a**: topoisomerase (DNA) II alpha (**Synonyms:** DNA Topoisomerase II alpha, Top-2)	-5.31

Table 8 (*continued*)

Putative function[a]	Clone ID[b]	Gene[c]	Avg fold[d]
ATP binding, kinase activity	MG-6-1a13	**Nme1**: Nucleoside diphosphate kinase A	-3.86
ATP binding, nucleotide binding	MG-3-141m24	**Cct3**: chaperonin subunit 3 (gamma) (**Synonyms**: Cctg, Tcp1-rs3, TriC-P5)	-3.78
ATP metabolism	MG-6-11e3	**Ak1**: adenylate kinase 1	-2.77
Cell cycle	MG-16-9b23	**Cdc2a**: cell division cycle 2 homolog A (**Synonyms:** Cdc2, CDK1, p34)	-4.57
	MG-13-57h1	**Cks1b**: CDC28 protein kinase 1b (**Synonym:** Cks1)	-7.39
	MG-8-12n3	**Mcm2**: minichromosome maintenance deficient 5; DNA replication licensing factor Mcm2 (**Synonyms:** Cdcl1, Mcmd2)	-4.11
	MG-15-222i11	**Mcm4:** minichromosome maintenance deficient 4 homolog (S. cerevisiae) (**Synonyms:** 19G, Cdc21, mcdc21, Mcmd4)	-3.03
Cell proliferation	MG-15-195c13	**Mki67:** antigen identified by monoclonal antibody Ki 67 (**Synonym:** Ki-67)	-3.90
	MG-15-206n21	**Cse1l:** chromosome segregation 1-like (**Synonyms:** Capts, Cas, Xpo2)	-3.49
Chromatin binding, histone methylation	MG-8-46e20	**Enx-1**: Enhancer of zeste homolog 2 (**Synonyms:** Enx1h, Ezh2)	-3.35
Cytoskeleton	MG-14-72k10	**Pfn1**: profilin 1 (**Synonyms:** actin binding protein, Pfn)	-5.42
	MG-6-15l1	**Mylc2b**: myosin light chain, regulatory B (**Synonym:** RLC-B)	-2.56
	MG-3-137j23	**Tuba2**: Tubulin alpha 2	-2.69
	MG-3-18m8	**Tubb2c:** tubulin, beta 2c	-3.56
	MG-8-15n24	**Tubb6**: tubulin, beta 6	-3.86
	MG-8-100j17	**Flna**: filamin, alpha	-2.61
	MG-6-3c22	**Tmsb4x** : thymosin, beta 4, X chromosome (**Synonym:** Ptmb4)	-4.26

Table 8 (*continued*)

Putative function[a]	Clone ID[b]	Gene[c]	Avg fold[d]
DNA binding	MG-13-1g21	**Ncl**: nucleolin (**Synonym:** Nucl)	-2.53
	MG-13-54a15	**Pole4**: polymerase (DNA-directed), epsilon 4 (p12 subunit)	-3.13
	MG-3-91d6	**Dek**: DEK oncogene	-4.57
	MG-14-25l9	**Hmgn2:** high mobility group nucleosomal binding domain 2 (**Synonyms:** HMG-17, Hmg17)	-12.55
DNA binding, DNA packaging	MG-10-1m3	**Ard1**: N-acetyltransferase Ard1 homolog (**Synonym:** Te2)	-3.39
DNA binding, DNA replication	MG-16-6l1	**Ris2**: etroviral integration site 2 (**Synonym:** Cdt1)	-3.22
DNA binding; nucleosome assembly	MG-3-24h23	**H3f3b**: H3 histone, family 3B (**Synonym:** H3.3B)	-2.59
DNA binding; protein binding	MG-3-33o2	**Bclaf1**: BCL2-associated transcription factor 1	-2.64
DNA repair; mRNA processing	MG-8-93b10	**Sfpq**: splicing factor proline/glutamine rich (polypyrimidine tract binding protein associated)	-3.13
Electron transport	MG-6-1a15	**Txn1**: Thioredoxin 1	-3.03
	MG-6-1a17	**Cycs**: Cytochrome c, somatic	-4.76
Energy metabolism	MG-6-1k17	**Ctbp1**: C-terminal binding protein 1 (**Synonym:** BARS)	-2.66
GTP binding	MG-3-8a7	**Ran:** RAN, member RAS oncogene family	-3.71
GTPase activation	MG-3-76d11	**Rangap1:** RAN GTPase activating protein 1 (**Synonym:** Fug1)	-2.64
Heparin binding	MG-4-86a20	**Hdgf**: hepatoma-derived growth factor	-2.64
Iron ion binding	MG-14-36k20	**Plod3**: procollagen-lysine, 2-oxoglutarate 5-dioxygenase 3 (**Synonyms:** LH3, lysyl hydroxylase 3)	-2.59
Lipid metabolism	MG-3-58f20	**Prdx6**: peroxiredoxin 6 (**Synonyms:** 1-Cys Prx, Brp-12, CP-3, GPx, Ltw-4)	-2.64
Malate metabolism; electron carrier	MG-8-77i22	**Me2**: malic enzyme 2, NAD(+)-dependent, mitochondrial	-2.51
Metal ion binding	MG-15-203l12	**Lyar**: Ly1 antibody reactive clone	-3.10
Metal ion binding, zinc ion binding	MG-3-17g16	**Crip2**: cysteine rich protein 2 (**Synonyms:** Crp, ESP1, Hlp)	-2.86
Methyltransferase activity	MG-4-145m17	**Srm**: Spermidine synthase	-3.82

Table 8 (*continued*)

Putative function[a]	Clone ID[b]	Gene[c]	Avg fold[d]
mRNA processing	MG-12-188i10	**Pm14**: Pre-mRNA branch site protein p14	-2.89
	MG-16-170m19	**Sfrs3**: splicing factor, arginine/serine-rich 3 (SRp20) (**Synonym:** X16)	-6.30
	MG-3-43d7	**Snrpg**: small nuclear ribonucleoprotein polypeptide G (**Synonym:** SMG)	-2.97
	MG-6-1a19	**Ptbp1**: polypyrimidine tract binding protein 1 (**Synonyms:** hnRNP I, pPTB, Ptb, PTB-1, PTB2, PTB3, PTB4)	-3.90
	MG-6-41o6	**Pabpn1**: poly(A) binding protein, nuclear 1 (**Synonyms:** PAB2, Pabp3, poly(A) binding protein II)	-2.75
Protein binding	MG-12-233n24	**Sla2**: Src-like-adapter 2 (**Synonyms:** SLAP-2, SLAP2)	-3.10
	MG-3-5g6	**Rasa1**: RAS p21 protein activator 1 (**Synonym:** Gap)	-3.53
	MG-3-70b18	**Maged1**: melanoma antigen, family D, 1 (**Synonyms:** Dlxin-1, DXBwg1492e)	-3.35
	MG-3-3k20	**Stmn1**: Stathmin (**Synonyms:** 19K, Lag, Lap18, leukemia associated phosphoprotein p18, metablastin, oncoprotein18, op18, p18, p19, pig, PP17, PP18, PR22, prosolin, SMN)	-4.85
	MG-3-4i4	**Tipin** (Interim): timeless interacting protein	-2.53
Protein binding, histone binding	MG-3-31o18	**Nasp:** Nuclear autoantigenic sperm protein (**Synonym**: Epcs32)	-6.11
Protein binding; metal ion binding	MG-3-10a14	**Trim28**: tripartite motif protein 28 (**Synonyms:** KAP-1, KRIP-1, Tif1b)	-3.03
Protein binding; protein folding	MG-6-22p24	**Ppia:** peptidylprolyl isomerase A (**Synonyms:** Cphn, cyclophilin A, CyP-18, CypA)	-3.39
Protein binding; protein inport into nucleus	MG-13-144a3	**Kpnb1:** karyopherin (importin) beta 1 (**Synonym:** Impnb)	-3.06
Protein biosynthesis	MG-14-83c21	**Cars**: cysteinyl-tRNA synthetase (**Synonym:** CA3)	-2.75
	MG-14-68e19	**Gfm1**: G elongation factor, mitochondrial 1	-2.75
	MG-3-37k5	**Mrpl12**: mitochondrial ribosomal protein L12 (**Synonyms:** MRP-L12, Rpml12)	-6.11
	MG-8-89h3	**Gspt1**: G1 to S phase transition 1 (**Synonyms:** G1st, Gst-1)	-2.72

Table 8 (*continued*)

Putative function[a]	Clone ID[b]	Gene[c]	Avg fold[d]
Protein folding	MG-8-1e3	**Fkbp4**: FK506 binding protein 4 (**Synonyms:** FKBP-52, FKPB52, p59)	-3.03
	MG-3-71m8	**Dnajb4**: DnaJ (Hsp40) homolog, subfamily B, member 4	-2.59
	MG-4-2h1	**Hsp110**: heat shock protein 110 (**Synonyms:** 105kDa, hsp-E7I, Hsp105, HSP105 42 C-HSP, HSP1)	-4.85
Protein transporter	MG-14-110m7	**Xpo5**: exprotin 5 (**Synonym:** Exp5)	-4.53
Ribosome biogenesis	MG-15-188a15	**Nol5a**: Nucleolar protein 5a (**Synonym:** Nop56)	-4.85
RNA binding; RNA processing	MG-3-10k3	**Hnrpc**: heterogeneous nuclear ribonucleoprotein C (**Synonyms:** hnRNP C1, hnRNP C2, hnRNPC1, hnRNPC2, snoRNA MBI-122)	-2.56
RNA binding; RNA processing	MG-12-228l7	**Hnrpa2b1**: Heterogeneous nuclear ribonucleoproteins A2/B1 (**Synonyms:** hnrnp-A, Hnrpa2)	-4.22
	MG-15-95e6	**Hnrpab**: Heterogeneous nuclear ribonucleoprotein A/B (**Synonyms:** CBF-A, Cgbfa)	-3.53
	MG-8-31a6	**Hnrpu**: Heterogenous nuclear ribonucleoprotein U (**Synonym:** Sp120)	-4.53
RNA processing; DNA binding	MG-6-19g10	**Pcbp2**: poly(rC) binding protein 2 (**Synonyms:** alphaCP-2, Hnrpx)	-2.97
RNA binding	MG-3-76o9	**Nhp2l1**: NHP2-like protein 1 (High mobility group-like nuclear protein 2 homolog 1) (**Synonyms:** FA-1, Fertilization antigen-1, Fta1, Ssfa1)	-2.83
	MG-6-42b15	Splicing factor U2AF 65 kDa subunit	-3.03
Succinyl-CoA metabolism	MG-6-65c15	**Oxct1**: 3-oxoacid CoA transferase 1 (**Synonym:** Scot-s)	-2.61
Transcription regulation	MG-14-81j6	**Id1**: inhibitor of DNA binding 1 (**Synonym:** Idb1)	-3.03
Translation	MG-8-32a23	**Eif1:** eukaryotic translation initiation factor 1 (**Synonym:** Sui1-rs1)	-3.03
	MG-16-5j12	**Itgb4bp:** integrin beta 4 binding protein (**Synonym:** Eif6)	-2.53

Table 8 (*continued*)

Putative function[a]	Clone ID[b]	Gene[c]	Avg fold[d]
Transport and binding protein	MG-15-66g15	**Ranbp1**: Ran binding protein 1 (**Synonym:** Htf9a)	-4.90
	MG-6-3h11	**Cplx1**: complexin 1	-3.00
	MG-8-42j10	**Cd24**: Signal transducer CD24 precursor	-2.80
tRNA processing	MG-3-49o10	**Rpp21**: ribonuclease P 21 subunit (human)	-3.39
Unknown function	MG-14-56o5	**Slc38a2**: solute carrier family 38, member 2	-2.83
	MG-14-91g24	**Rbm13**: RNA binding motif protein 13	-3.74
	MG-16-179o20	**Lsm2**: U6 snRNA-associated Sm-like protein Lsm2	-3.71
	MG-16-3e3	**NM_024096**: XTP3-transactivated protein A	-5.37
	MG-3-103a23	**NP_109610**: stress-associated endoplasmic reticulum protein 1	-2.77
	MG-3-106g16	**Erh**: Enhancer of rudimentary homolog (**Synonyms:** Mer, Prei1)	-4.66
	MG-3-22j13	**Gpiap1**: GPI-anchored membrane protein 1	-2.72
	MG-6-10a10	**Cdk2ap1**: Cyclin-dependent kinase 2-associated protein 1	-2.92
	MG-6-41h1	**SET**: SET protein	-7.46
	MG-8-40d18	**Anp32b**: acidic nuclear phosphoprotein 32 family, member B (**Synonyms:** PAL31, PHAPI2a)	-5.00

3.4 Clustering of genes into biological pathways validated by Gene Ontology annotation

The Bibliosphere (Genomatix, Munich, Germany) software was used to analyse and filter for Gene Ontology (GO) categories to integrate differentially regulated genes into pathways. These GOFilters consist of a hierarchy of terms and the corresponding annotations for the BiblioSphere analysis. Bibliosphere generated a list of biological process terms ranked by their probability of over- or under-representation in a specific gene list. Z scores indicate how the results deviate from the distribution mean. Thus, it ranks the probability that the genes in this category are over- or under-represented in the gene list. **Table 9** lists biological processes over-represented within the group of down-regulated genes

Table 9: Classification of significantly down-regulated genes in prion infected cells by molecular functions and biological processes

Gene Ontology terms		
Biological processes overrepresented within the group of differentially **down-regulated genes**.		
Term	**Z-Score**	**Genes**
Biopolymer metabolic process	4,41	*Ard1, Bclaf1, Cars, Ccnb1, Cdc2a, Cdt1, Ezh2, Gspt1, H3f3b, Hmgn2, Hnrpa2b1, Hnrpab, Hnrpc, Id1, Lsm2, Maged1, Mcm2, Mcm4, Nars, Nasp, Nhp2ll, Pabpn1, Pcbp2, Pfn1, Plod3, Ptbp1, Rasa1, Rrm1, Set, Sfpq, Sfrs3, Sla2, Top2a, Trim28*
↳ DNA metabolic process	5,72	
↳ DNA replication	5,29	
↳ DNA replication initiation	9,89	
↳ DNA packaging	5,48	
↳ DNA genometric change	7,83	
↳ RNA metabolic process	4,89	
↳ RNA processing	7,46	
↳ mRNA metabolic process	7,77	
Macromolecule complex assembly	8,02	*Cse1l, Eif1, Eif5a, Fkbp4, H3f3b, Itgb4bp, Kpnb1, Lsm2, Mcm2, Set, Sfrs3*
↳ Protein-RNA complex assembly	7,59	
↳ assembly of spliceosomal tri-snRNP	7,96	
↳ Ribosome assembly	6,1	
nucleobase, nucleoside, nucleotide and nucleic acid metabolic process	6,38	*Ak2, Ard1, Bclaf1, Cars, Cdt1, Erh, Ezh2, Gspt1, H3f3b, Hmgn2, Hnrpa2b1, Hnrpab, Hnrpc, Id1, Lsm2, Maged1, Mcm2, Mcm4, Nars, Nasp, Nhp2ll, Nme1, Pabpn1, Pcbp2, Pfn1, Ptbp1, Rasa1, Rrm1, Set, Sfrs3, Sla2, Top2a, Trim28*
Mitotic cell cycle	5,85	*Anp32b, Ccnb1, Cdc2a, Cdt1, Gspt1, Incenp, Stmn1*
Cell cycle process	5,15	*Anp32b, Ranbp1, Cdc2a, Ccnb1, Cdk2ap1, Cdt1, Erh, Gspt1, Incenp, Mki67, Stmn1*
Ribonucleoprotein complex biogenesis and assembly	5,88	*Eif5a, Eif1, Itgb4bp, LSM2, Nhp2ll, Sfrs3*

Cell cycle phase	5,36	*Anp32b, Ccnb1, Cdc2a, Cdt1, Gspt1, Incenp, Mki67*
Regulation of centrosome cycle	13,92	*Ranbp1*

No single clear defined pathway could be found within the down-regulated genes but most affected pathways belong to the RNA/DNA metabolism.

The identical GO filtering method was used for the up-regulated genes and resulted in the identification of the most overrepresented prion affected pathway, the lipid biosynthetic process (**Table 10**). Genes of this biological process group mainly belonged to the cholesterol biosynthetic pathway. Notably, transcripts for the sterol regulatory element-binding protein 2 (Srebp2) (*Srebf2*: 3.25) were increased. Furthermore, *Ldlr* transcripts were increased almost 4-fold in prion infected N2a cells.

Table 10: Classification of up-regulated genes in the prion infected cell by biological processes

Gene Ontology terms		
Biological processes overrepresented within the group of differentially **up-regulated genes**.		
Term	**Z-Score**	**Genes**
Lipid biosynthetic process	12.53	*Dhcr7, Fdft1, Hmgcr, Hmgcs1, Idi1, Sc4mol, Srebf2*
↳ Steroid biosynthetic process	20.47	
↳ Sterol biosynthetic process	31.40	
Alcohol metabolic process	15.62	*Dhcr7, Eno2, Fdft1, Hmgcr, Hmgcs1, Idi1, Ldlr, Sc4mol, Srebf2*
↳ Sterol metabolic process	26.26	
↳ Cholesterol metabolic process	23.72	

In contrast to the annotation results of the down-regulated genes, each GO term found within the over-expressed genes displayed a much higher Z-Score (from 12.53 up to 31.40). Additionally the ranked genes belong to similar metabolic pathways, the sterol and cholesterol pathways, indicating that these pathways are the most affected one in the prion infected N2a cell.

3.5 Chip data and up-regulation of the cholesterol metabolic pathway confirmed by *Real-Time* PCR

The next step after clustering and ranking of the differentially expressed genes in prion infected N2a cells was the confirmation of the microarray data by *Real-Time* PCR analysis, as microarray analysis is expected to underestimate the changes in expression of genes relative to *Real-Time* PCR. The technique is based on the detection and quantification of a fluorescent reporter molecule, here SYBR-Green, which signal intensity rises directly proportionally to the produced PCR product. The $2^{-\Delta\Delta C_T}$ method (Livak and Schmittgen 2001; Radonic *et al.* 2004) was used to calculate the relative expression levels of the genes of interest in prion infected and mock infected cells normalized to the *RPII* house-keeping gene.

Altogether six genes were chosen for *Real-Time* PCR analysis, all of them belonging to the cholesterol pathway. Four genes were already detected by the microarray experiment (*Srebf2, Fdft1, Ldlr* and *Sc4mol*) and two additional genes were chosen from the cholesterol metabolic pathway (*Mvk* and *Cyp51*). Thus with this experiment the microarray results and the detected up-regulation of the cholesterol pathway in prion infected N2a cells should be confirmed. The results of the *Real-Time* PCR experiment are given in **Figure 17A** and demonstrate a significant up-regulation of all analysed genes in prion infected N2a cells. These data confirmed the microarray data set and significant up-regulation almost of the whole cholesterol pathway, as all nine tested genes out of 18 genes were found up-regulated throughout the pathway (**Figure 17B**). These genes include the two major regulators of the cholesterol synthesis, the HMGCoA-reductase and importantly also the gene for the regulatory transcription factor Srebp2 (sterol regulatory element binding protein 2) that regulates transcription of all genes within this pathway.

A

	Srebf2	Mvk	Fdft1	Cyp51	Ldlr	Sc4mol
Chip	3,25	not detected	5,58	not detected	3,81	10,91
RealTime-PCR	3,74	2,33	6,98	4,63	5,46	8,94

B

Acteyl CoA

(3,74 ↑) Srebf2*   Acetoacteyl-CoA thiolase

Acetoacteyl CoA

HMG-CoA synthase (7,46 ↑)

HMG-CoA

HMG-CoA reductase (3,32 ↑)

Mevalonate

Mevalonate kinase* (2,33 ↑)

Phosphomevalonate kinase

Mevalonate PP decarboxylase

GPP synthase

IPP isomerase = Idi1 (3,22 ↑)

FPP synthase

Squalene synthase = Fdft1* (6,98 ↑)

Squalene

Squalene epoxidase

Lanosterol synthase

CYP51* (4,63 ↑)

Sc4mol* (8,94 ↑)

Lathosterol oxidase

DHCR

Cholesterol   ◄────   LDL receptor* (5,46 ↑)

Figure 17: 22L prion infection of N2a cells induces increased transcription of genes regulated by Srebp2. Differential gene expression of genes involved in cholesterol synthesis. (A) Up-regulation of *Srebf2* (sterol regulatory element binding factor 2), *Mvk* (mevalonate kinase), *Fdft1* (farnesyl diphosphate farnesyl

transferase 1), *Cyp51* (cytochrome P450, family 51), *Ldlr* (low density lipoprotein receptor) and *Sc4mol* (C4-sterol methyl oxidase) was determined by *Real-Time* PCR in the 22L infected clone 5 (passage 18) compared to mock infected clone 5 (passage 18). All results were normalized to the *RPII* (RNA polymerase 2) expression levels. For triplicate experiments the standard deviation is shown for each gene. The Y-axis denotes the comparative gene expression levels. (B) Overview of important genes in the cholesterol pathway activated by Srbp2 (Horton and Shimomura 1999). Genes in bold were found up-regulated in prion infected N2a cells compared to mock infected N2a cells either in the chip experiment (underlined) or as detected by *Real-Time* PCR (marked with asterisks). Srebp2 is the limiting transcription factor of cholesterol synthesis.

3.6 Significantly higher amount and activity of transcription factor Srebp2 detected in prion infected neuronal cells

The chip experiment and the *Real-Time* PCR revealed a significant up-regulation of the cholesterol metabolic pathway in prion infected N2a cells at least on gene expression level, including the genes for the regulatory proteins HMGCoA-reductase and Srebp2. Srebp2 acts as a transcription factor regulating the cholesterogenic gene expression and is synthesized as an inactive precursor protein that is incorporated into the endoplasmic reticulum membrane. To study if increased *Srebf2* transcript levels also result in elevated Srebp2 protein levels, the amount of Srebp2 precursor protein in whole lysates of 22L infected and mock infected N2a cells was assessed by Western blot analysis (**Figure 18A, left side**). In total, six individual experiments were performed per N2a group (22L and mock) and Srebp2 signals, normalized to GAPDH as an internal loading control, were analysed on the same blot. Relative Srebp2 protein levels in mock infected cells were set to 100 % and the paired *t* test was used for *p*-value calculation. The experiment revealed a significant increase of the amount of full-length Srebp2 in prion infected cells compared to mock infected N2a cells ($p < 0.05$) (**Figure 18A, right side**).
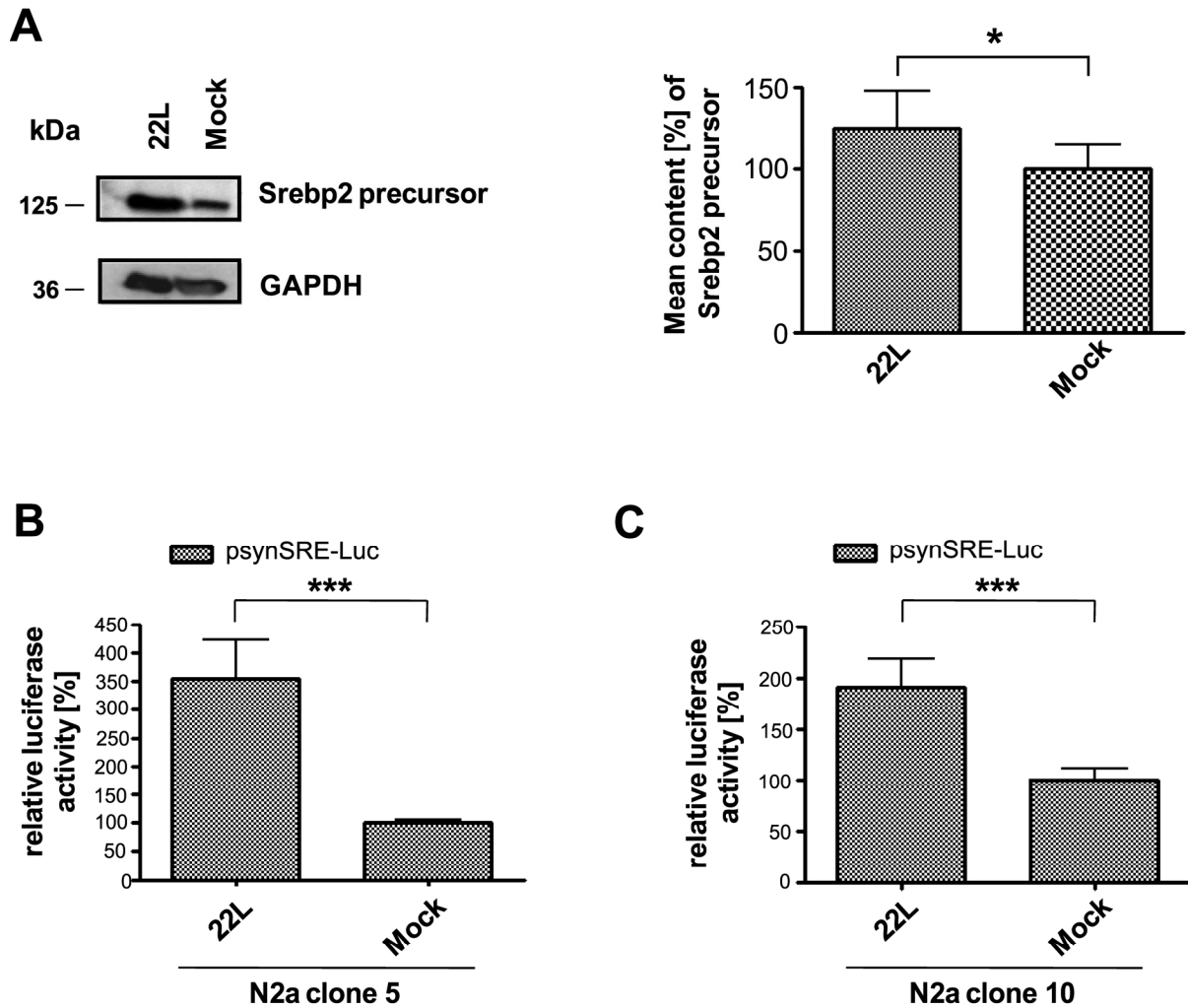
Figure 18: Increased Srebp2 transcriptional activity and cholesterol levels in prion infected cells. (A) Western blot analysis of full-length Srebp2 in cell lysates using rabbit polyclonal antibody ab28482. For photodensitometric analysis of the data, for each group (22L or mock) n=6 samples were analysed and normalized to the GAPDH signals detected on the same Western blot. Relative Srebp2 protein levels in mock infected cells were set to 100%. *p*-values were determined using a paired *t* test and significant differences are indicated by asterisks. **(B)** and **(C).** The activity of Srebp2 in two independent N2a clones (clones 5 and 10) was determined by a luciferase reporter gene assay, using the psynSRE-firefly luciferase construct and the pGL3-Renilla luciferase plasmid as a transfection control. The activity of Srebp2 was assessed by measuring the bioluminescence generated by the firefly luciferase normalized to the bioluminescence of Renilla luciferase in the same samples (n=8). Relative firefly luciferase activities in the prion and mock infected cells clone 5 (B) and clone 10 (C). The activity in the mock infected cells was set to 100%. *p*-values were determined by the paired *t* test (* = p<0.05; *** = p≤0.0005).

Upon cholesterol depletion, full-length Srebp2 is cleaved and translocates to the nucleus, where it binds to target genes harbouring sterol regulatory elements (SRE). Activation (and thus cleavage) of Srebp2 can best be studied by reporter gene assays. To determine the Srebp2 transcriptional activity in prion infected and uninfected cells a plasmid vector coding for

luciferase under the control of a synthetic promoter harboring two SRE motifs (Dooley *et al.* 1998) was used. Prion infected and mock infected N2a cells were co-transfected with psynSRE-firefly luciferase plasmid (reporter gene) and the pGL3-renilla luciferase plasmid as a transfection efficiency control. A significantly higher luciferase activity ($p \leq 0.0005$) was observed measuring bioluminescence in infected cells compared to mock infected cells (**Figure 18B**).

The use of cloned cell populations for the experiments could possibly lead to clonal artifacts. To ensure cholesterogenic pathway up-regulation is independent from the N2a cell clone 5 the luciferase reporter gene assay was repeated with another N2a cell clone (clone 10). Significantly increased luciferase activity ($p \leq 0.0005$) was again detected in 22L prion infected cells (**Figure 18C**), arguing that clonal artifacts did not account for the observed differences in cholesterol metabolism between prion infected and uninfected cells.

3.7 Enhanced levels of total and free cholesterol found in prion infected cells

The confirmed up-regulation of the cholesterol pathway and the higher activity of the important transcription factor Srebp2 in prion infected N2a cells should consequently lead to a higher amount of total or free cholesterol in these cells compared to mock controls. In collaboration with Prof. Konrad Sandhoff and Dr. Susanne Brodesser (both from the University of Bonn) the amount of total (including free and esterified) and free cholesterol (**Figure 19**) per total protein in 22L infected N2a cells compared to a mock control group was determined using high performance thin layer chromatography (HPTLC). Due to time limitation only one experiment was performed for total and two for free cholesterol level detection, therefore no standard deviation can be given. Both total and free cholesterol levels were found elevated in prion infected cells. Thus, prion infection of neuronal cells induces up-regulation of cholesterol biosynthesis and leads to elevated total and free cholesterol levels.
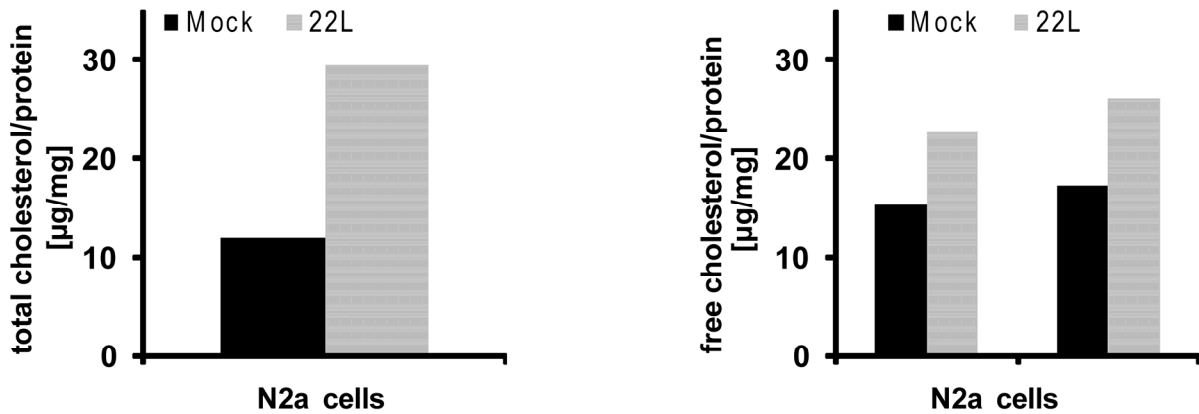
Figure 19: Increased cholesterol levels in prion infected cells. Lipids from prion infected and uninfected N2a cells were extracted and applied to high performance thin layer chromatography (HPTLC) Silica Gel 60 plates. Free cholesterol (right side) and total cholesterol (left side) levels were determined as described in the material and methods section. For quantitative analytical TLC determination, lipid samples were compared to cholesterol standards. The amounts of total and free cholesterol per mg protein are given. For free cholesterol, results of independent samples are shown.

3.8 Up-regulation of cholesterol synthesis in another prion infected neuronal cell line but not in prion exposed microglia cells

To study if prion infection leads to elevated expression of cholesterogenic genes in another neuronal cell line, the relative expression levels of *Srebf2*, *Sc4mol* and *Ldlr* in RML prion strain infected or uninfected GT-1 cells were compared by *Real-Time* PCR. Cells of the murine hippocampal cell line GT-1 do undergo apoptosis upon prion infection, in contrast to N2a cells (Schatzl *et al.* 1997). Western blot analysis of RML infected GT-1 cells prior to RNA isolation demonstrated that cells accumulated substantial amounts of PrP[Sc] (published in Greenwood 2005). Transcript levels of all three genes were found increased in infected GT-1 cells compared to uninfected cells (**Figure 20A**). Thus, these results strongly suggest that up-regulation of cholesterol metabolism related genes is a general neuronal response to prion infection that might be independent of the prion strain.

A

B
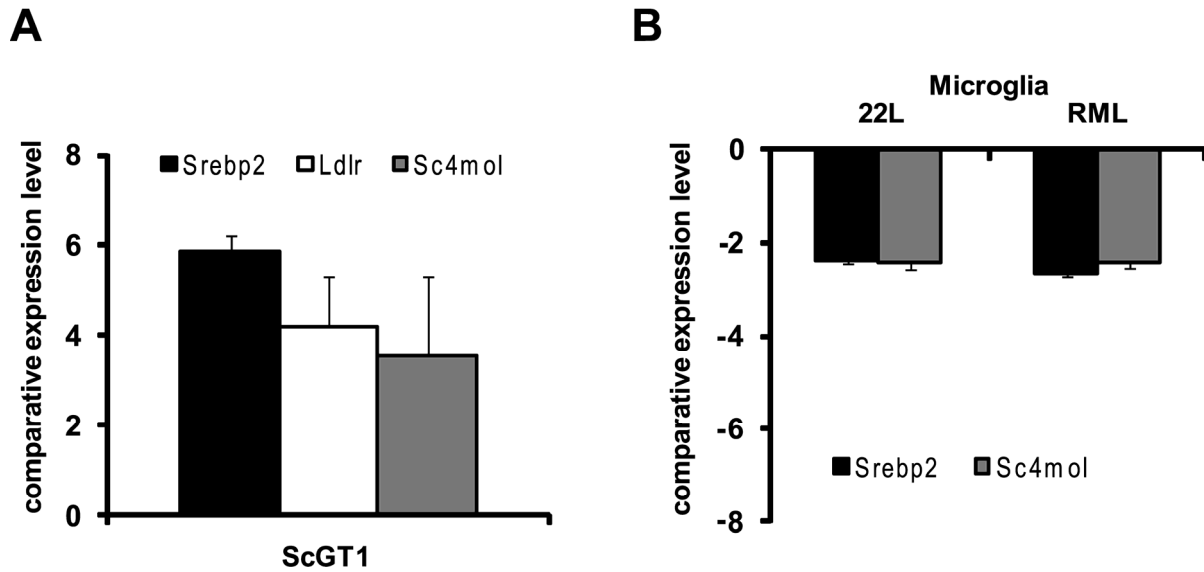
Figure 20: Up-regulation of cholesterol biosynthesis transcripts in neuronal cell lines. (A) *Srebf2*, *Ldlr* and *Sc4mol* **expression levels in RML infected and un-infected GT1 cells determined by** *Real-Time* **PCR, normalized to the housekeeping gene** *RPII*. **(B) Microglia cells were exposed to 22L and RML prions (Gilch** *et al.* **2007). One day post exposure, total RNA was extracted from cells and relative mRNA concentrations were determined by** *Real-Time* **PCR as above. Bars represent mean values ± S.D. (n=3).**

Microarray analysis of brains from prion infected mice (Xiang *et al.* 2007) revealed down-regulation of cholesterogenic genes, in conflict with our data of neuronal cells. However, in the brain microarray study a strong inflammatory reaction was evident, suggesting that the observed changes in gene expression reflect a profound microglial activation that could obscure potential transcriptional changes in neurons. Interestingly, microglial cells do not appear to become infected with prions *in vivo* (Priller *et al.* 2006). To test if prion exposure could impact cholesterol biosynthesis in microglial cells, relative transcript levels of *Srebf2* and *Sc4mol* in murine BV-2 cells that had been exposed to 22L or RML prion strains or normal brain homogenate for 1 day (Gilch *et al.* 2007) were analysed by *Real-Time* PCR (**Figure 20B**). Immunofluorescence as well as Western blot analysis of BV-2 cells exposed to RML and 22L have previously shown that cells stained positive for PrP^{Sc} one day post exposure (Gilch *et al.* 2007). Surprisingly, both cholesterogenic genes were significantly down-regulated in the microglia cell line BV-2 exposed to prions, suggesting that prions modulate cholesterol biosynthesis dependent on the cell type.

3.9 Analysis of prion exposed primary hippocampal neurons and astrocytes revealed up-regulation of the cholesterol metabolic pathway as a neuronal response to prion infection

It has recently been reported that primary neurons and astrocytes are permissive to prions *in vitro* (Cronier et al., 2004). To test if also primary neuronal cultures respond to prions by up-regulation of the cholesterol biosynthetic pathway, cultures of hippocampal neurons of C57BL/6 fetal mice gestation day 16 were prepared. As controls, primary astrocytes of these mice were also isolated (**Figure 21**).
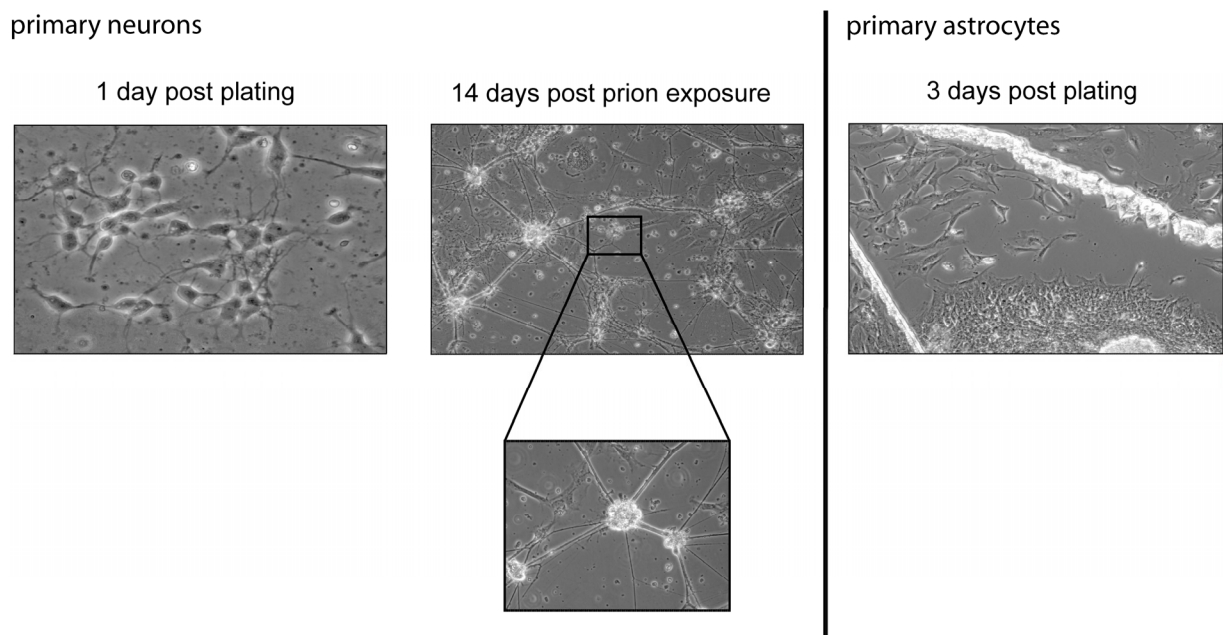
Figure 21: Microscopic images of primary murine hippocampal neurons and astrocytes. Primary neurons are shown 1 day post plating (left part) and 14 days after exposure to 22L brain homogenate (middle section). A higher magnitude of these neurons is given below for better visualization of neuronal cell bodies and growing dendrites. Primary astrocytes 3 days post plating are shown on the right. White lines in the right picture originate from scratches in the bottom of the cell plate.

Cells were exposed to 0.1% brain homogenate from an uninfected mouse or to 22L brain homogenate. Cells were tested for PrP^{Sc} content 3-22 days post exposure. Western blot analysis of astrocytic and neuronal cell lysates revealed that PrP^{Sc} was detectable in all lysates of cells exposed to 22L brain homogenate but not in lysates of cells exposed to mock brain homogenate (**Figure 22A** and **B**, left part). Interestingly, in astrocytes the amount of PK resistant PrP increased over time, suggesting that cells might generate PrP^{Sc}. In primary neurons the PrP^{Sc} signal was stable over time. Primary neurons could not be rinsed with PBS

after treatment with brain homogenate, due to their loose attachment to the culture dish. These cells also essentially needed their primary medium and did not survive any change of culture medium. Therefore, the medium was sterile filtered after treatment with brain homogenate to get rid of most of the floating debris but not exchanged. A strong inoculum signal that might have masked the weaker signal of newly formed PrP^{Sc} could be an explanation for the stable scrapie signal. In contrast, primary astrocytes were extensively rinsed to clear the cells of any PrP^{Sc} originating from the inoculum. Although it cannot be excluded that detected PrP^{Sc} in both cell cultures might originate from the inoculum, the data clearly demonstrate that PrP^{Sc} was present throughout the course of the experiment. Transcript levels for cholesterogenic genes were assessed at different time points post exposure. In neurons cholesterogenic transcript levels were significantly increased (**Figure 22A** and **B**, right panels) while in astrocytes, transcript levels remained largely unaltered. In summary, the results presented in this study strongly argue that neurons up-regulate cholesterol biosynthesis in response to prions.
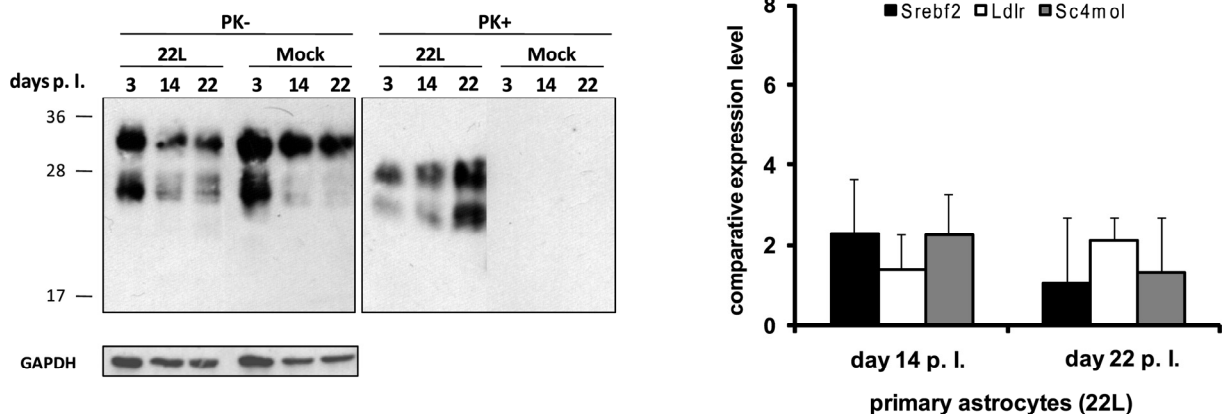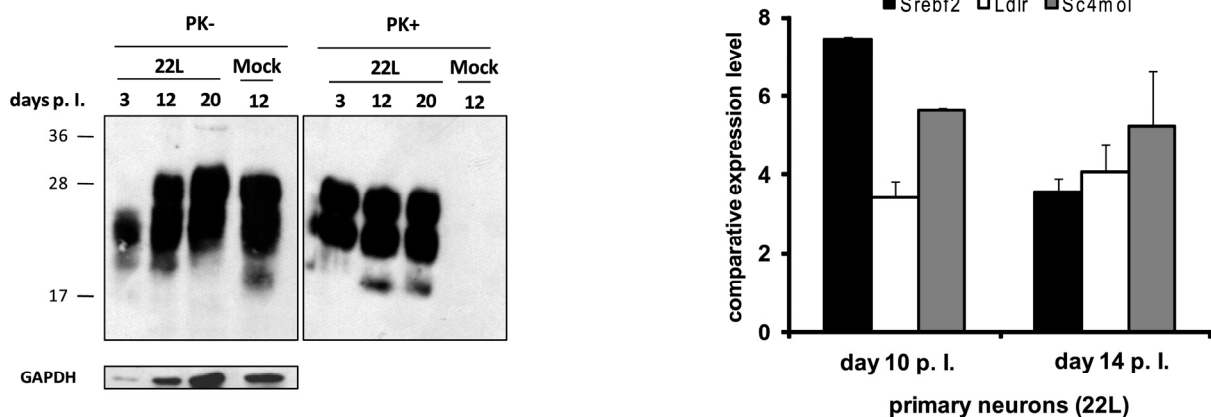

Figure 22: Up-regulation of cholesterogenic genes in prion exposed primary hippocampal neurons. Left panels: Primary astrocytes (A) and neurons (B) were lysed at three different time points following inoculation with 0.1% 22L or normal brain homogenate and cells were analysed for total PrP (PK-) and

PrP^{Sc} upon digestion with proteinase K (PK+). GAPDH levels in each lane are shown. Additional lanes were excised for presentation purposes. Right panels: After RNA extraction at two different time points per cell type *Srebf2*, *Ldlr* and *Sc4mol* expression levels were determined in prion exposed cells compared to mock treated cells by *Real-Time* PCR. The experiments were performed in triplicates and results were normalized to the housekeeping gene *RPII*. Bars represent mean values ± S.D.

Additionally to Western blot analysis immunoflourescent experiments were performed with primary astrocytes and neurons to analyse where PrP^{Sc} is found after prion exposure. The cells were fixed on glass slides, permeabilized and stained for PrP/PrP^{Sc} and also for either the astrocytic marker glial fibrillary acidic protein (GFAP) or the neuronal marker neurofilament N. The PrP antibody 4H11 can only differentiate between PrP^{C} and PrP^{Sc} after treatment of the fixed cells with 6 M guanidine hydrochloride (GndHCl). A normal PrP staining in unexposed primary astrocytes can be detected without GndHCl treatment (**Figure 23A**). The lack of PrP signal in primary astrocytes exposed to mock brain homogenate after treatment with GndHCl demonstrates the successful blocking of PrP^{C} detection using GndHCl and the 4H11 antibody. After exposure to 22L brain homogenate and denaturation of PrP^{C} using GndHCl PrP^{Sc} was detected as clear red dots on the cell surface and also intra-cellular in the cytoplasm, supporting the suggestion that PrP^{Sc} was internalized into the cells. Upon prion exposed primary hippocampal neurons PrP^{Sc} could also be visualized, at least, on the cell surface (**Figure 23B**). Due to smaller neuronal cell bodies a clear internal staining of PrP^{Sc} could not be detected but there is great evidence that attached PrP^{Sc} was internalized into the neurons like it occurs during infection of normal cell culture systems. The limited number of primary neurons was the reason for the missing PrP^{C} staining of unexposed cells, as most of the neurons were used for testing the expression of cholesterogenic genes in prion and mock exposed neurons as described before. The rest of the primary neuron population was exposed for PrP^{Sc} detection using IF microscopy, as this was considered of more importance than the visualization of PrP^{C}.
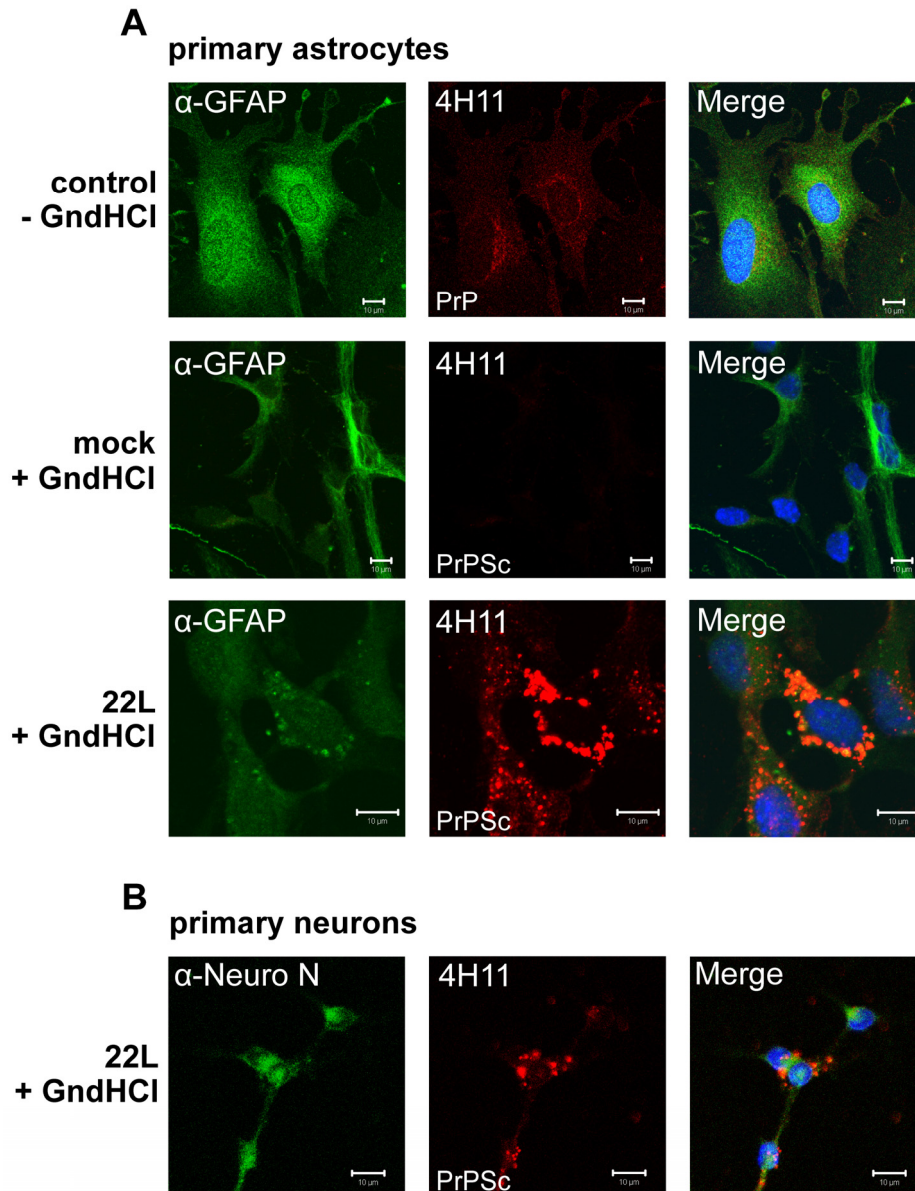
Figure 23: Up-take (primary astrocytes) and uptake/binding (primary neurons) of PrP^{Sc} to primary cells after exposure to 22L brain homogenate as detected by immunofluorescence microscopy. Primary astrocytes and neurons were exposed to 0.1% of 22L brain homogenate and astrocytes additionally to 0.1% mock brain homogenate. Cells were analysed after three days. **(A)** Non-exposed and mock treated primary astrocytes were stained for PrP^{C} (4H11) without (first lane) and after (second lane) treatment with GndHCl, respectively. PrP^{C} was undetectable after GndHCl treatment (second lane) resulting in a possible differentiation between PrP^{C} and PrP^{Sc} by the antibody 4H11. PrP^{Sc} (third lane) was therefore detectable after treatment of prion exposed astrocytes with GndHCl indicated by bright red fluorescent aggregates. **(B)** Identical PrP^{Sc} aggregates were detected around the cell surface of prion exposed primary neurons after treatment of the cells with GndHCl. In astrocytes the glial fibrillary acidic protein (α-GFAP) and in neurons the neuronal marker neurofilament N (α-Neuro N) as cell type specific marker proteins were stained in green. Nuclei were stained with Hoechst dye (blue). Scale bars: 10 µm.

3.10 Transient down-regulation of Srebp2 by siRNA negatively influences PrP^{Sc} formation in N2a cells in the absence of exogenous cholesterol sources

To determine if a reduced cholesterol biosynthesis due to a transient down-regulation of Srebp2 has an effect on PrP^{Sc} accumulation, mock infected and 22L prion infected N2a cells (clone 5) were transfected either with siRNA targeting *Srebf2* transcripts or with non-silencing siRNA. Cells were kept in serum free medium supplemented with 0.2 µM mevalonate for the course of the experiment. Cells transfected with siRNA targeting *Srebf2* mRNA grew slightly slower than non-silencing siRNA transfected cells. Samples were adjusted to comparable protein contents and analysed for total PrP and PrP^{Sc} (**Figure 24A**). Interestingly, in N2a cells the silencing of *Srebf2* did not lead to a decrease in total PrP content but led to reduced levels of PrP^{Sc}, while PrP^{Sc} levels in cells treated with non-silencing siRNA remained largely unaffected. Similar results were obtained when cells were transfected with an alternative siRNA targeting *Srebf2* transcripts (**Figure 25**). In both cases the reduction of PrP^{Sc} could not be explained with a reduction of PrP^{C} and therefore limited PrP^{Sc} substrate, as the level of total PrP was not altered by the knock-down. We next tested if down-regulation of cholesterol biosynthesis affects PrP^{Sc} accumulation when cells are capable of replenishing their cholesterol from the medium. Silencing of *Srebf2* expression in the presence of 10% FCS did not significantly influence PrP^{Sc} levels (**Figure 24B**) demonstrating that neuronal cholesterol biosynthesis is not required for PrP^{Sc} accumulation if an external cholesterol source exists. In conclusion, up-regulation of cholesterol biosynthesis is a direct response to prion infection, even in the presence of external cholesterol.
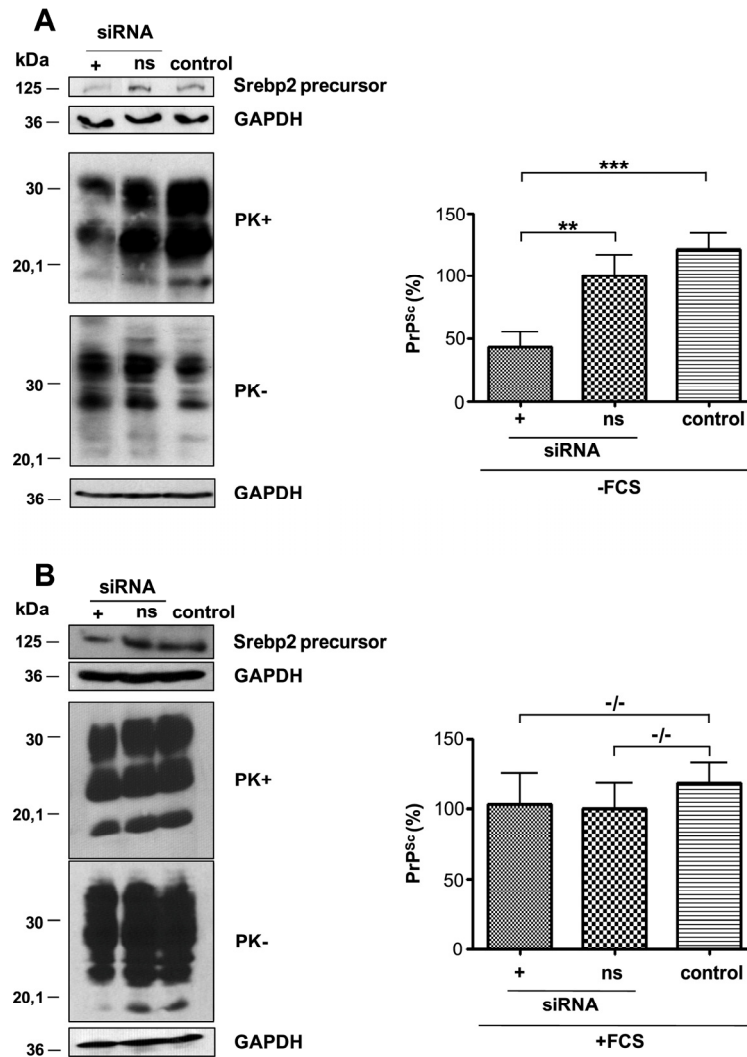
Figure 24: Knock-down of Srebp2 only interferes with PrP^{Sc} accumulation in the absence of exogenous cholesterol. 22L infected N2a cells (clone 5) were transfected with siRNAs against Srebp2, non-silencing siRNA (ns), or left un-transfected either in the absence (A) or presence (B) of FCS as an external source of cholesterol. Cells were lysed 48h post transfection and analysed for total PrP (PK-) and PrP^{Sc} contents following proteinase K treatment (PK+). GAPDH levels were determined for the PK- samples. Successful knock-down of Srebp2 was determined by using ab28482. Antibody 4H11 was used for PrP detection. Experiments were repeated four times and results were normalized to GAPDH levels. PrP^{Sc} levels in Srebp2 siRNA transfected cells were compared to PrP^{Sc} levels in non-silencing siRNA transfected cells (A and B, right panels). Significant changes are indicated by asterisks (** = p≤0.005;*** = p≤0.0005; paired t test). -/- denotes no significant differences.
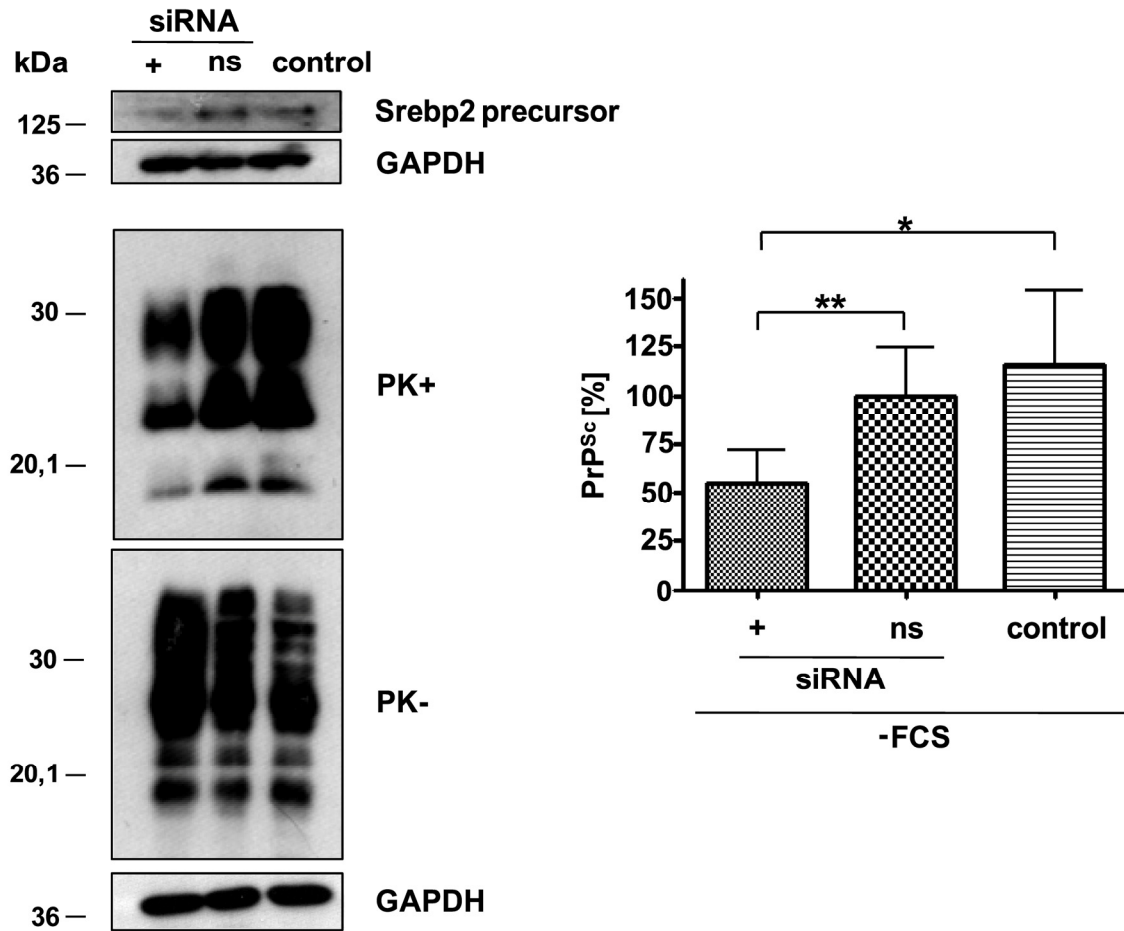
Figure 25: Knock-down of Srebp2 with an alternative siRNA also interferes with PrP^{Sc} accumulation in the absence of exogenous cholesterol. 22L infected N2a cell clone 5 were transfected with an alternative siRNA directed against *Srebf2* and passaged in the absence of FCS for 48 hours. Cells lysates were analysed for PrP^{Sc} and total PrP by Western blot using 4H11 (left panel). Srebp2 knock-down is given and GAPDH protein levels demonstrate equal sample loading. Densitometric and statistical analysis of five independent transfections revealed a significant reduction of PrP^{Sc} in prion infected cells transfected with siRNA against *Srebf2* compared to non-silencing siRNA (right panel) (* = p<0.05;** = p≤0.005).

To ensure that specifically the up-take of cholesterol counteracts the negative effect of Srebf2 down-regulation on prion propagation upon presence of FCS and not any other compound in FCS the effect of a reduced up-take of cholesterol via siRNA-mediated down-regulation of the Ldl receptor was investigated. Therefore, 22L infected N2a cells were transfected with siRNA against Ldl receptor and cultured in medium supplemented with 10% FCS. After 48h the cells were lysed and analysed for PrP^{Sc} and total PrP as described before. As expected the transiently knock-down of the Ldl receptor led to a significant reduction of the PrP^{Sc} level compared to cells transfected with non-silencing siRNA as control (**Figure 26**).
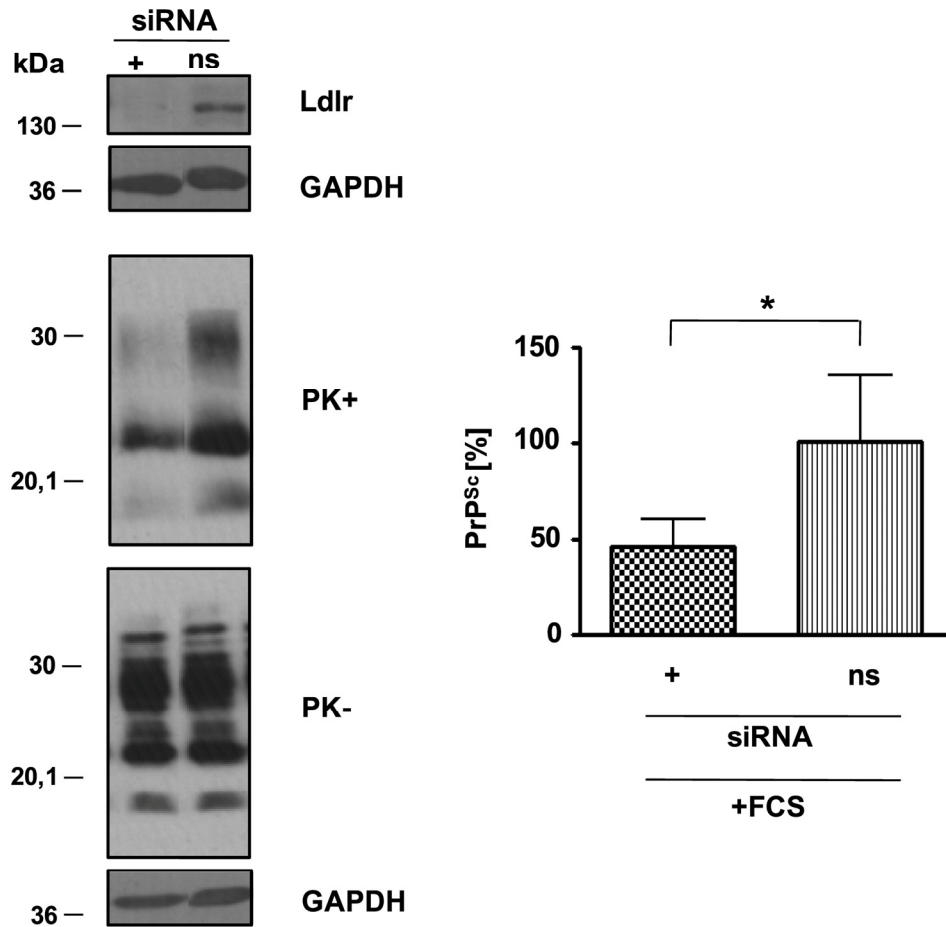
Figure 26: Decreased cholesterol up-take through siRNA-mediated knock-down of the Ldl receptor reduces PrP^{Sc} in 22L infected N2a cells. Ldl receptor expression was transiently down-regulated in 22L infected N2a clone 5 cells using siRNA. Cells were cultured for 48 hours in medium supplemented with FCS as an external cholesterol source. Cell lysates were analysed for PrP^{Sc} and total PrP by Western Blot analysis using antibody 4H11 (left panel). GAPDH protein levels demonstrate equal sample loading and the Ldlr knock-down is given. Densitometric and statistical analysis of three independent transfections revealed a significant reduction of PrP^{Sc} in prion infected cells transfected with siRNA against *Ldlr* compared to non-silencing siRNA (right panel) (* = p<0.05). For presentation purpose additional bands were excised.

This finding supports the suggestion that only cholesterol is needed to abolish the effect of transient *Srebf2* down-regulation upon prion propagation.

3.11 *Srebf2* knock-down does not alter cell surface expression of PrP

It has already been published that cholesterol is needed for a normal PrP^{C} cell surface expression (Gilch *et al.* 2006). To analyse if the reduction of PrP^{Sc} under cholesterol depletion conditions depends on a reduction of PrP expression on the cell surface, 22L and mock

infected N2a cells were transfected with siRNA against *Srebf2* or with ns siRNA and cultured in the absence of FCS but medium was supplemented with 0.2 μM mevalonate for the course of the experiment. After 48 hours the PrP expression on the cell surface was determined via cell surface fluorescence-activated cell sorting (FACS) analysis in three independent experiments. **Figure 27** shows one representative graph of three independent FACS analysis for each group (22L (**Figure 27A**) and mock (**Figure 27B**))
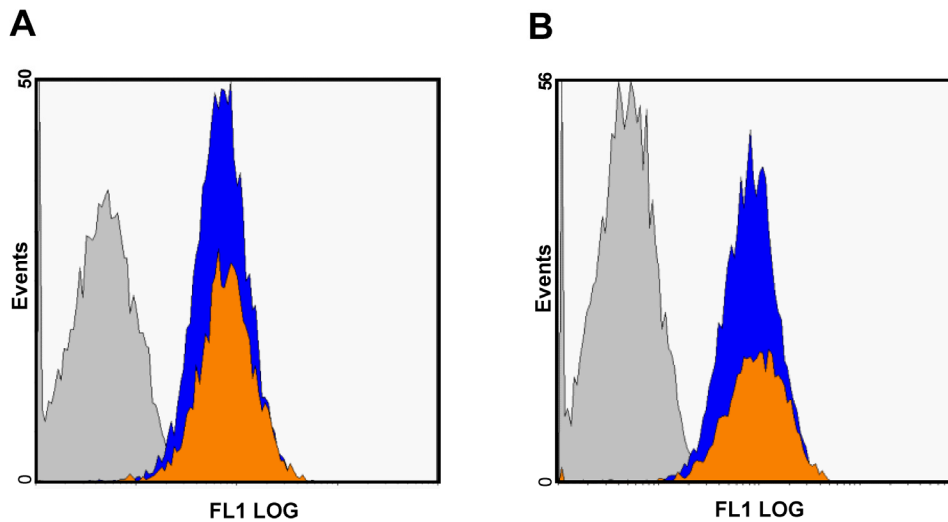

Figure 27: Flow cytometry analysis revealed unaltered total PrP cell surface expression after transient *Srebf2* knockdown in the absence of an external cholesterol source. N2a cells clone 5 (A) 22L infected or (B) mock control were transfected with siRNA directed against Srebf2 transcripts or non-silencing siRNA and tested for cell surface PrP^C 48 h post transfection. FACS analysis was performed using primary anti-PrP antibody 4H11 and Cy2-labelled secondary antibody anti-mouse IgG. Blue graphs denote cells transfected with ns siRNA, the orange graphs indicate cells transfected with Srebf2 siRNA. The grey graph represents N2a cells incubated only with Cy2-labelled secondary antibody as a background control. One representative graph is given for each cell group (22L or mock).

No shift of fluorescent peaks could be detected between the fluorescence on cells transfected with siRNA against Srebp2 (orange graph) and the ns siRNA control group (blue graph), either in the 22L infected nor in the mock infected N2a cells. This indicates an unaltered PrP cell surface expression upon transient Srebp2 knockdown under cholesterol depletion conditions. Due to a missing Srebp2 knockdown confirmation this data has to be considered as preliminary.

3.12 Murine fibroblast L929 cells show no effect on PrP^{Sc} propagation upon transient knock-down of cholesterol metabolism

To analyse if the reduction of PrP^{Sc} upon transient knock-down of *Srebf2* detected in prion infected neuronal N2a cells is a cell type specific effect the murine fibroblast cell line L929, prion infected with the adapted prion strains 22L and RML, was investigated for the identical effect. L929 cells were transfected identically like previous described for the N2a cells. Cells were cultured without exogenous cholesterol and 72 hours post transfection the amount of total PrP and PrP^{Sc} (22L and RML) was determined by Western blot analysis (**Figure 28**). Samples were adjusted to GAPDH for equal protein load.
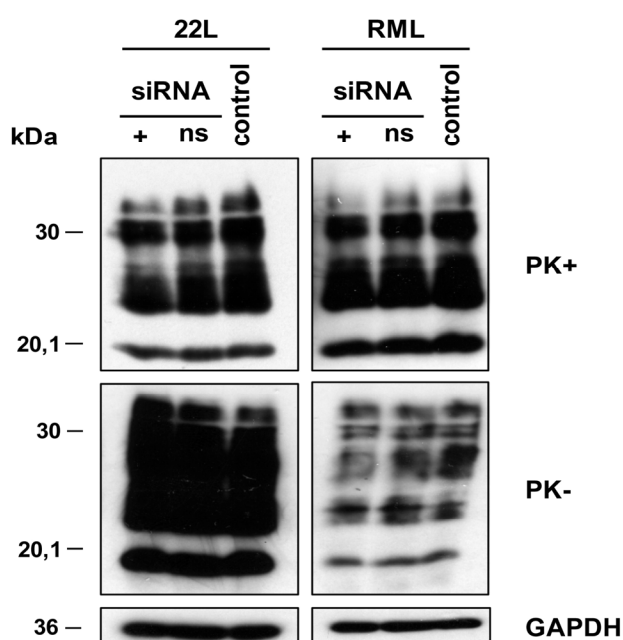

Figure 28: No effect of *Srebf2* knock-down on PrP^{Sc} accumulation in prion infected fibroblastoma cells in the absence of an external cholesterol source. 22L and RML infected L929 cells were transfected with siRNAs against Srebp2, non-silencing siRNA (ns), or left un-transfected. 72 hours after transfection the cell lysates were tested for PrP^{Sc} (PK+) or total PrP (PK-) by Western blot analysis using the antibody 4H11. Equal loading amounts are indicated by GAPDH protein levels.

No reduction in PrP^{Sc} accumulation could be determined for the 22L and RML infected L929 cells after transfection with siRNA against *Srebf2* in the absence of external cholesterol. Cell type specificity could be an explanation for the different reaction of both cell lines upon the transient knock-down of *Srebf2* under cholesterol depletion conditions but further experiments are needed to confirm the data. This result must be interpreted as preliminary data due to a lack of successful Srebp2 knockdown analysis and the limited number of experiments.

4. Discussion

Despite the fact that many groups are focusing on the pathology of prion diseases in the central nervous system (Budka 2003), the response of the neuronal host cell to prion infection and potential alterations in metabolic pathways caused by prions still remain unclear. Aim of this study was the detection of a host reaction towards prions in mammalian neuronal cells. In the first part of this project an almost genome wide cDNA microarray study was performed using a N2a cell clone highly susceptible to prion infection in a paired fashion. We detected over 100 differentially expressed genes in prion infected compared to mock infected cells with the cholesterol metabolism as a major functional group within the up-regulated genes. Further investigations on protein levels revealed a significantly higher amount and increased transcriptional activity of Srebp2, the regulatory transcription factor of the cholesterol synthesis. Additionally, thin-layer chromatography showed increased levels of free and total cholesterol in prion infected cells. Up-regulation of cholesterogenic genes, including the gene for Srebp2, was also found in scrapie infected GT1 cells, a murine hypothalamic cell line and prion exposed primary hippocampal neurons. Interestingly, these genes were down-regulated in prion exposed BV2 murine microglia cells and expression was un-altered in prion exposed primary astrocytes, suggesting that the up-regulation of the cholesterol metabolism is a neuronal specific reaction to prion infection. Further siRNA experiments against the Srebp2 precursor and the Ldl receptor revealed that, although prion infection triggers an up-regulation of cholesterol synthesis, *de novo* synthesis of cholesterol is not required for prion propagation in the presence of an external cholesterol source.

4.1 Identification of differentially expressed genes and their possible role in other neurological diseases

In the microarray analysis performed in this study 203 genes were detected as significantly differentially regulated upon prion infection with over 100 genes (27 up- and 94 down-regulated) of which a putative function is known or has been suggested. Within the group of down-regulated genes, genes belonging to diverse functional groups (with more than one gene) were identified. Most hits belonged to ATP binding, cell cycle, cytoskeleton, DNA binding, mRNA processing and protein binding. Genes that were down-regulated the most in each group are shown in **Table 11:**

Table 11: List of genes that were drastically down-regulated upon prion infection (as assessed by microarray analysis)

Gene	Putative function	Average fold
Top2a (topoisomerase (DNA) II alpha	ATP binding	-5.31
Cks1b (CDC28 protein kinase 1b)	Cell cycle	-7.39
Pfn1 (profilin 1)	Cytoskeleton	-5.42
Hmgn2 (high mobility group nucleosomal binding domain 2	DNA binding	-12.55
Sfrs3 (splicing factor, arginine/serine-rich 3)	mRNA processing	-6.30
Stmn1 (stathmin)	Protein binding	-4.85

For the genes *Top2a*, *Hmgn2* and *Sfrs3* no link to neurodegenerative diseases has been reported so far. For the other genes a certain role in neurological diseases was published:

- The protein CDC28 is an essential sub-unit for proper function of the cyclin-dependent kinase (CDK) that is important for the regulation of the cell cycle. Alterations in cell cycle regulation have been reported for neurons undergoing apoptosis in Alzheimer's disease (Vincent *et al.* 2001).

- Profilin appears to play a role in actin regulation during neuronal differentiation and for plasticity (Neuhoff *et al.* 2005). It has been linked to spinal muscular atrophy, an autosomal recessive disease characterized by the loss of alpha-motoneurons in the spinal cord, resulting in the atrophy of skeletal muscles (Sharma *et al.* 2005).

- The stathmin protein regulates microtubule dynamics by promoting depolymerisation of microtubules and by preventing polymerization of tubulin heterodimers during mitosis and cell cycle (Rubin and Atweh 2004). Interestingly, a decreased expression of stathmin has also been found in patients suffering from other neurological diseases like Down-syndrome and Alzheimer's disease (Cheon *et al.* 2001).

In contrast to the high number of functional groups within the down-regulated genes, the up-regulated genes only fall into two main functional groups, the smaller cluster of transport and binding proteins and the most prominent group belonging to the cholesterol metabolism. The gene with the highest expression level for each group is given in **Table 12**.

Table 12: Highly up-regulated genes in prion infected N2a cells detected by cDNA microarray

Gene	Putative function	Average fold
IER3 (immediate early response 3)	Transport and binding	+4.90
Sc4mol (C-4 methyl sterol oxidase;)	Cholesterol metabolism	+10.91

- IER3, also known as IEX-1, is a stress-inducible gene that plays a role in regulation of cell death and oncogenesis. The promoter of this gene harbours a variety of transcription factor binding motifs, e.g. for p53, TNF-α and IL-β1 and also the SRE-motive for Srebp2 (Wu 2003). The SRE motif in the promoter region may explain the up-regulation of IER3 in prion infected N2a cells, as this is the specific binding site for the transcription factor Srebp2, showing an increased activity upon prion infection. Recently, a study suggested increased *IER3* transcript levels as a potential marker for Huntington disease (Runne *et al.* 2007).

- Sc4mol takes part in the cellular cholesterol metabolic pathway. A direct link between this protein and neurodegenerative diseases has not been reported so far, but an increased gene expression was published for macrophages during cardiovascular diseases like arteriosclerosis (Svensson *et al.* 2003).

The fact that most of the up-regulated genes in the microarray screen (7 out of 23) play a role in cholesterol synthesis and uptake led us to further analysis of this metabolic pathway.

4.2 Prion infection alters cholesterol biosynthesis in neuronal cells

Our study now provides strong evidence that cholesterol homeostasis is directly altered upon prion infection of neuronal cells. Microarray analysis revealed that the predominant change observed in 22L prion infected N2a cells was in the cholesterol biosynthetic pathway. The findings of this work are in line with microarray experiments of other groups that also showed a differential expression pattern of some genes belonging to the lipid or cholesterol pathway (**Table 13**). However, it was recently reported that infection of N2a cells with RML scrapie prions did not lead to significant transcriptional changes (Julius *et al.* 2008), contrasting with microarray data on RML prion infected GT1 and N2a cells (Greenwood *et al.* 2005) and data from this study. While differences in experimental design, prion strains, and the use of different microarray platforms can certainly account for these results, the lack of differential gene expression of N2a cells reported by Julius *et al.* could also be due to the specific cell clone PK1 that was used for the experiment. As this clone had been retrieved by several

rounds of subcloning (as opposed to one round in this study) for drastically increased prion susceptibility (Klohn *et al.* 2003), it is possible that this procedure led to the selection of a clone in which prion replication minimally interferes with normal cellular metabolism. Another microarray study done by Fasano *et al.* revealed no altered gene expression in the cholesterol metabolism of a quinacrine-cured GT1 cell clone population compared to the prion infected cell clone population (Fasano *et al.* 2008). The group used a microarray platform comprising 15.000 EST clones including sequences for genes involved in cellular energy metabolism. Quinacrine is a compound that is known to clear cells from PrP^{Sc} by a redistribution of cholesterol from the plasma membrane to intra-cellular compartments (Klingenstein *et al.* 2006). The lack of detection of altered cholesterogenic gene expression could be due to side effects caused by quinacrine. Possibly, the re-distribution of cholesterol could have led to an increase in the *de novo* cholesterol synthesis. This increase could be at similar levels as the synthesis rate caused by prion infection, resulting in a masking of effects in the microarray analysis.

Table 13: Overview of differentially expressed genes belonging to the lipid or cholesterol metabolism detected in already published microarray studies

Study/reference	Differentially regulated genes of the lipid/cholesterol metabolism	Prion strain(s)	Analysed mouse material	Microarray system
(Booth *et al.* 2004)	•*Apolipoprotein D* •*Apolipoprotein E* •*Diacepam binding inhibitor (Dbi)* •*Granulin* •*Sphingosine-1-phosphate phosphatase 1* •*Phospholipid transfer protein*	•ME7 •79a	whole brain	non-commercial
(Riemer *et al.* 2004)	•*Protein lipase* •*ABCA-1* •*Apolipoprotein D*	•139A	cortex, medulla and pons	Mouse Genome U74Av2 array (Affimetrix)
(Xiang *et al.* 2004)	•*Lipoprotein lipase*	•ME7 •RML	whole brain	Mouse expression array 430A (Affimetrix)

(Brown *et al.* 2005)	•*Fatty acid binding protein 7* •*Sc4mol* •*Acetyl-CoA-acetyltransferase 1* •*Sortilin-related receptor (Ldlr family)* •*Sterol-C5-desaturase*	•ME7	hippocampus	Mouse Genome U74Av2 array (Affimetrix)
(Skinner *et al.* 2006)	•*Apolipoprotein D* •*Apolipoprotein E* •*Dbi*	•ME7 •22L •RML	whole brain	non-commercial
(Xiang *et al.* 2007)	•*Very low-density lipoprotein receptor* •*Sc4mol* •*Ldlr* •*3-hydroxy-3-methylglutaryl-CoA reductase* •*Sortilin-related receptor (Ldlr family)* •*Isopentenly-diphosphate delta isomerase (Idi1)*	•ME7	whole brain	Mouse expression array 430A (Affimetrix)
(Hwang *et al.* 2009)	•*Dbi* •*3-hydroxy-3-methylglutaryl-Coenzyme A synthase 1* •*NAD(P) dependent steroid dehydrogenase-like* •*cytochrome P450, family 51* •*Sc4mol* •*Idi1* •*sterol-C5-desaturase* •*squalene epoxidase*	•RML •301V	whole brain	Mouse expression array 430A (Affimetrix)

Nevertheless, also between the other microarray analyses conflicting results exist as to whether prion infection leads to up-regulation (Riemer *et al.* 2004; Brown *et al.* 2005) or

down-regulation (Xiang *et al.* 2007; Hwang *et al.* 2009) of cholesterol biosynthesis genes. Interestingly, up- or down-regulation appeared to be at least partially dependent on the time point of sampling during the infection process. In one study, the pre-clinical stage of prion infection had only marginal influence on cholesterogenic gene expression, while at terminal stages of disease, cholesterogenic transcripts decreased (Xiang *et al.* 2007). In another study, pre-clinical animals infected with mouse adapted ME7 scrapie prion strain displayed increased cholesterol biosynthesis gene expression in the CNS that decreased at terminal stages of the disease (Brown *et al.* 2005). Thus, cholesterol metabolism in the brain following prion infection appears to underlie dynamic changes that correlate with the disease state. Therefore, the detected changes in cholesterol biosynthesis genes upon prion infection *in vivo* might either reflect a.) cell-type dependent differential expression, b.) disease progression dependent differential expression, c.) neuronal cell loss dependent differential expression or d.) any combination thereof. Since microglial activation, mainly during clinical stages of disease, prominently influences transcript levels in mouse models of prion diseases (Baker and Manuelidis 2003; Xiang *et al.* 2004; Booth *et al.* 2004; Xiang *et al.* 2007), it is possible that down-regulation of cholesterol biosynthesis during clinical prion disease reflects a glial response to prion disease that masks neuronal up-regulation. This hypothesis is in agreement with our finding that exposure of microglia cells and primary astrocytes to prions *in vitro* either caused down-regulation of genes involved in cholesterol biosynthesis (**3.8**), e.g. S*c4mol* and S*rebf2,* or left transcript levels relatively unaffected (**3.9**). Alternatively, neuronal cells *in vivo* might respond to prion infection dependent on the disease progression. Recent evidence shows that neuronal down-regulation of cholesterol biosynthesis can correlate with apoptosis (Koh *et al.* 2007). Neuronal loss is a hallmark of prion diseases and several lines of evidence suggest that neurons infected with prions undergo programmed cell death (Schatzl *et al.* 1997). In agreement with this the human neuroblastoma cell line SH-SY5Y treated with the neurotoxic prion peptide 106-126 showed a down-regulation of several cholesterogenic genes like 3-Hydroxy-3-methylglutaryl-coenzyme A synthase 1 (*HMGCS1*), 3-Hydroxy-3-methylglutaryl-coenzyme A reductase (*HMGCR*), *IDI1, SC4MOL* and *LDLR* (Martinez and Pascual 2007). This down-regulation could very likely be due to ongoing cell death caused by the PrP peptides.

Interestingly, recent studies on neuronal cultures demonstrate that de-regulation of intracellular cholesterol transport induces apoptotic cell-death and leads to decreased cholesterol biosynthesis transcripts. Notably, at earlier time points when no apoptosis was apparent, most cholesterol transcripts were increased, suggesting that damaged neurons might

initially up-regulate cholesterol biosynthesis, potentially to compensate for cholesterol imbalances (Koh *et al.* 2007). Importantly, N2a cells can be persistently infected with prions and do not appear to undergo apoptosis, which could explain why N2a cells do not demonstrate decreased cholesterol biosynthesis transcripts upon prion infection. Similarly, primary hippocampal neurons exposed to 22L scrapie brain homogenate did not show decreased viability compared to primary neurons exposed to normal brain homogenate, at least not during the course of the experiment (data not shown).

Interestingly, several genes that are involved in cholesterol biosynthesis (*Sc4mol*, *Cyp51*) or harbour the sterol responsive element SRE in their promoter region (e.g. Diazepam-binding inhibitor *Dbi*, Stearoyl-coenzyme A desaturase 2 *Scd2*) were also found up-regulated in previous gene expression studies done in our group utilizing N2a cells persistently infected with RML/Chandler mouse adapted scrapie (Greenwood *et al.* 2005). Analysis of GT-1 cells persistently infected with RML scrapie prions confirmed increased levels of S*rebf2* and S*c4mol* transcripts. Thus, up-regulation of cholesterogenic genes might be a general neuronal event following prion challenge.

4.3 Cholesterol in the central nervous system

For the proper function of neuronal cells a tight balance between up-take and *de novo* synthesis of cholesterol is essential. In general, the human brain is the cholesterol richest organ of the human body. It contains approx. 25 % of the total cholesterol but accounts for only ~2 % of the body mass. In the brain cholesterol is mainly located in the myelin sheath and the membranes of astrocytes and neurons. There it plays an important role in normal brain development, gene transcription and regulation of cell signaling pathways to maintain proper function of neuronal cells and the availability of bioactive steroids (Pfrieger 2003; Dietschy and Turley 2004; Vaya and Schipper 2007; Canevari and Clark 2007). Brain cholesterol is almost exclusively synthesized locally, as the blood-brain barrier restricts import of plasma lipoproteins from peripheral circulation (Turley *et al.* 1996; Turley *et al.* 1998). Cholesterol synthesis is mainly accomplished by astroglia, but neuronal cells also synthesize cholesterol at basal levels. The up-take of cholesterol from the environment occurs by receptor-mediated endocytosis via the Ldl receptor (Ldlr). This receptor binds particles such as low density lipoprotein (Ldl) containing apolipoprotein B or E (apoB or E) (Brown and Goldstein 1986). Ldl loaded Ldlr is internalized into clathrin-coated vesicles and enters the clathrin-mediated endocytic pathway by fusion with early endosomes and further transport to acidic endocytotic compartments. To provide free cholesterol for cellular needs the cholesteryl esters are

hydrolysed by acid lipase in these compartments. The release is mediated by two transporting proteins, NPC1 and NPC2, named after the rare Niemann-Pick type C disease (Chang *et al.* 2005). An overview of the influx of cholesterol is given in **Figure 29**.
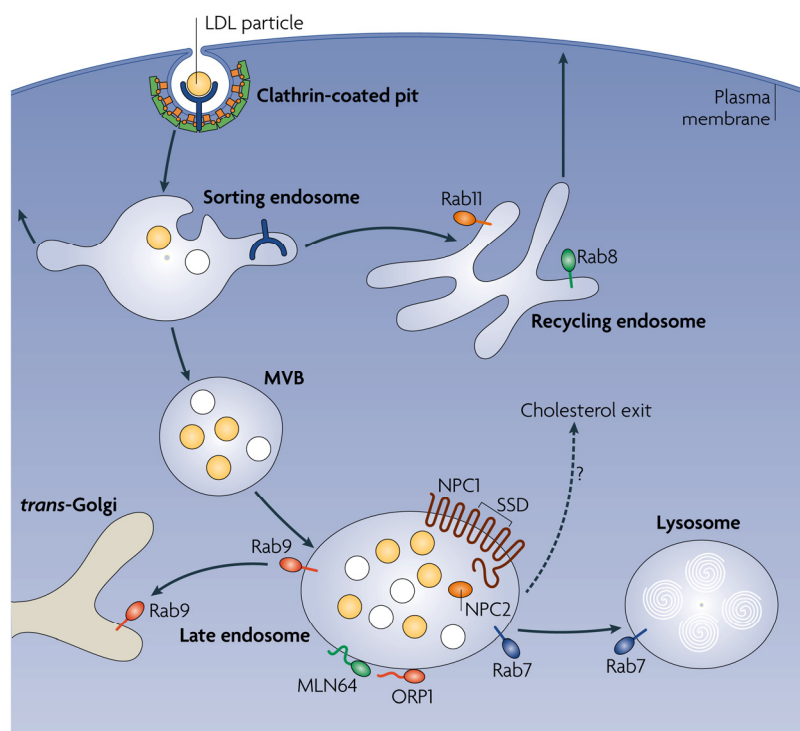

Figure 29: Schematic overview of up-take and endosomal trafficking of cholesterol. Low density lipoprotein (Ldl; yellow) binds to the Ldl receptor (blue), is internalized by clathrin-coated pits and is transported to early sorting endosomes. The Ldl receptor recycles back to the plasma membrane and Ldl is delivered to later endocytic compartments for hydrolysis. Hydrolysed cholesteryl esters can exit as free cholesterol for delivery to other compartments like the plasma membrane and the endoplasmatic reticulum. Niemann-Pick C1 (NPC1) with its sterol sensing domain (SSD) is essential for the efflux of cholesterol from late endosomal compartments. Additional proteins involved in cholesterol trafficking are MLN64, ORP1 and several members of the Rab protein family. The efflux of cholesterol takes place before cargo delivery to lysosomes, as it is enriched in the internal membrane of multivesicular bodies (MVB) but not in lysosomes (taken with modifications from (Ikonen 2008)).

Besides the up-take of cholesterol via Ldl the cell can also synthesize cholesterol *de novo* from acetyl CoA through the mevalonate pathway. The sterol regulatory element binding protein 2 (Srebp2) plays an important role in the regulation of the cholesterol biosynthesis in a sterol dependent manner (Espenshade 2006). It is synthesized as a large inactive precursor protein, encompassing two membrane-spanning domains with which it is incorporated into the membrane of the endoplasmatic reticulum (ER). In the ER the carboxy-terminus of Srebp interacts with a sterol sensitive protein called Scap (Srebp-cleavage-activating protein) (Edwards *et al.* 2000; Goldstein *et al.* 2006). Scap functions in sterol-depleted cells as a guide

for Srebps from the ER to the Golgi where two membrane-associated proteases, site 1 (S1P) and site 2 (S2P), process the Srebp precursors to the mature forms. The transcriptionally active mature Srebps translocate to the nucleus where they bind as dimers to a sterol regulatory element (SRE) in the promoters of Srebp target genes (including the *Srebf2* gene) and activate transcription in a sterol-regulated manner (Hua *et al.* 1993; Yokoyama *et al.* 1993; Wang *et al.* 1994; Brown and Goldstein 1997). A key mechanism in this sterol-dependent regulation of Srebp activity is the binding of another protein located in the ER, Insig-1 (insulin induced gene). At high sterol levels Insig-1 binds to Scap resulting in blockage of the transfer of the Srebp2/Scap complex from the ER to the Golgi. Additionally, the regulation of the Scap protease through its sterol-sensing domain located in the transmembrane domain also influences the activation of Srebp2 as binding of cholesterol to Scap induces a conformational change in the protein (Feramisco *et al.* 2005). As a consequence, Srebp is not transported to the Golgi and is not activated by S1P and S2P. In the absence of cholesterol Insig-1 is ubiquitinated by the E3 ubiquitin ligase gp78/ATPase VCP complex and degraded by the proteasome, resulting in the translocation of Srebp2/Scap to the Golgi and further activation of Srebp2. An overview of the regulation in cells with high and low levels of cholesterol is illustrated in **Figure 30**.
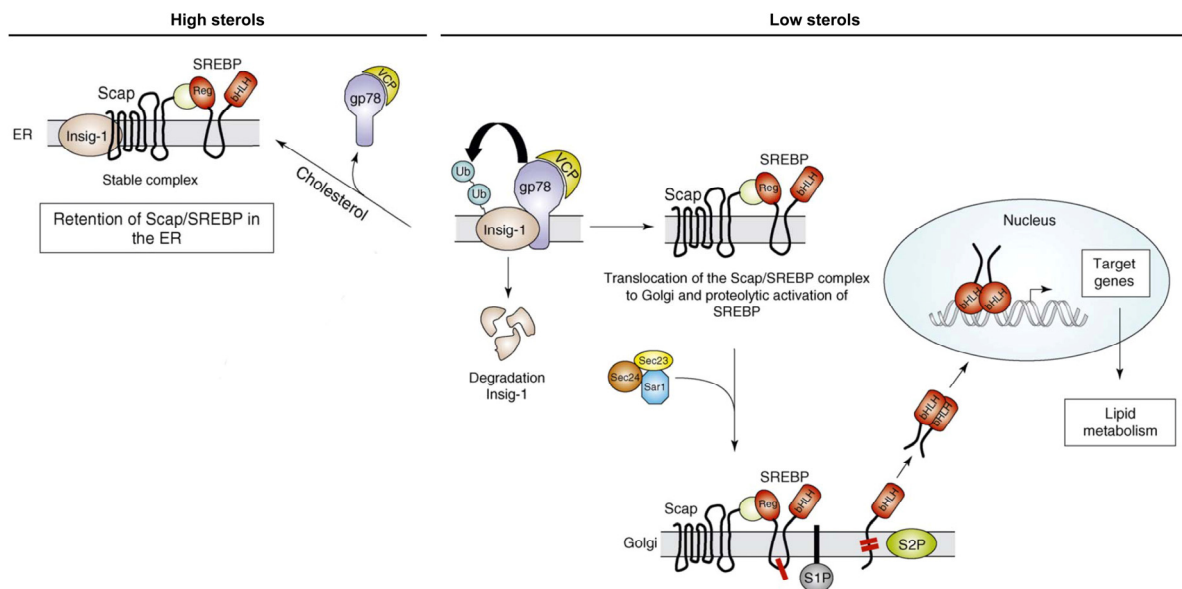

Figure 30: Overview of the cholesterol-dependent regulation of Srebp. (A) High sterol levels prevent the ubiquitination of Insig-1 through the E3 ubiquitin ligase gp78/ATPase VCP complex by mediating a stable complex of Insig-1, Scap and Srebp. Srebp activation is blocked and the Scap/Srebp complex is retained in the ER (B) A lack of cholesterol leads to ubiquitination and degradation of Insig-1 resulting in the translocation of the Scap/Srebp complex from the ER to the Golgi and activation of Srebp through

proteolytic cleavage by the proteases S1P and S2P. Activated Srebps translocate into the nucleus and bind as dimers to the SRE motive in the promoter of Srebp target genes. Subsequently, this leads to transcriptional activation of the lipid metabolism (taken from (Bengoechea-Alonso and Ericsson 2007) with modifications).

4.4   Cholesterol and PrP metabolism

How prion infection activates cholesterogenic genes is unclear. Interestingly, conversion of PrP^C to PrP^{Sc} is believed to occur on the cell surface or along the endocytic pathway, compartments also involved in cholesterol trafficking (Caughey and Baron 2006). Cholesterol might also play a role in proper PrP^C trafficking within the cell. After translation PrP^C is modified and glycosylated in the ER, mature PrP^C is transported to the cell surface via the Golgi network and incorporated into the plasma membrane by its GPI-anchor (Stahl *et al.* 1987). PrP^C on cell surface resides in lipid rafts by interaction of its GPI-anchor with saturated sphingolipids (Brown and London 2000). Lipid rafts are special areas within the plasma membrane rich in cholesterol and sphingolipids (Simons and Ikonen 1997). Not only mature PrP^C has been found associated with rafts, but recently an immature diglycosylated PrP^C species was detected associated with cholesterol-rich rafts in the endoplasmatic reticulum (ER), indicating that this association may be important for PrP^C maturation (Sarnataro *et al.* 2004). Additionally, Gilch *et al.* described an un-proper PrP^C cell surface expression mediated through the inhibition of cholesterol synthesis by treatment of cells with the HMGCoA reductase blocker mevinolin (Gilch *et al.* 2006). Moreover, cholesterol depletion leads to PrP^C accumulation in the secretory pathway of the cells. Furthermore, an effect of cholesterol on PrP^C location was reported by the study of Marella *et al.*, showing an increased release of PrP^C from the plasma membrane into the culture medium of cells treated with the polyene antibiotic filipin, a compound that sequesters cholesterol (Marella *et al.* 2002). Similar to PrP^C, also PrP^{Sc} is believed to be present in rafts in cultured cells (Vey *et al.* 1996; Naslavsky *et al.* 1997). The exact cellular location of prion conversion is unknown but appears to depend on localisation of PrP^C to rafts (Taraboulos *et al.* 1995; Vey *et al.* 1996; Kaneko *et al.* 1997) that can be found in the membrane of cells or endosomal vesicles.

A link between cholesterol and prion disease has been reported by several studies, using pharmacological substances like e.g. cylodextrin to affect cholesterol in the plasma membrane leading to decreased prion propagation in treated cells (Rothblat *et al.* 1999). Other groups used drugs known to re-distribute cellular cholesterol (Mange *et al.* 2000; Klingenstein *et al.* 2006) or treated prion infected cells (Taraboulos *et al.* 1995; Bate *et al.* 2004; Bate *et al.*

2007) or mice (Mok *et al.* 2006; Kempster *et al.* 2007) with different statins to specifically inhibit the activity of HMGCoA reductase and therefore block *de novo* cholesterol biosynthesis. These attempts resulted in the clearance of prion infection in the cell culture system and a prolonged survival time in simvastatin treated mice, although progression of the disease could not be stopped or reversed. Controversially, another study using simvastatin in a mouse model (Haviv *et al.* 2008) reported a neuroprotective effect of this drug without altering the cholesterol content in the brain of treated mice, suggesting that the prolonged incubation time reported in the study by Mok *et al.* could be due to a cholesterol independent effect of simvastatin. In conclusion, results from pharmacological inhibition of cholesterol synthesis or cholesterol homeostasis argue that reduction of cellular cholesterol levels decreases PrP^{Sc} formation. In all these studies cholesterol metabolism or membrane and lipid raft composition was altered by pharmalogically decreasing of the cholesterol content in the neuronal cell, suggesting that prion biogenesis is highly sensitive to changes in cholesterol homeostasis.

4.5 How might prion infection mediate the up-regulation of cholesterol metabolism?

Several possible explanations might account for the up-regulation of the cholesterol metabolism in the prion infected cell. First of all, the cell could have an impaired Ldlr-mediated up-take of cholesterol from the outer environment. This could lead to insufficient intracellular cholesterol levels and therefore to an increase of cholesterol synthesis to replenish the cholesterol pool within the cell. However, the experimental finding in this work that the negative effect of the transient knock-down of cholesterol biosynthesis on prion propagation could be compensated in the presence of an external cholesterol source makes this explanation unlikely (**3.10**). This indicates that prion infected N2a cells are still capable of taking up exogenous cholesterol.

Alternatively, the appearance and accumulation of PrP^{Sc} in neuronal cells could limit the cycling of cholesterol from the membranes of endosomes and lysosomes to other cellular compartments. PrP^{Sc} located within rafts or along the endocytic pathway might also change membrane fluidity and/or turn-over. PrP^{Sc} has a much longer half-life time (Borchelt *et al.* 1990) compared to PrP^{C}, thereby possibly prolonging cholesterol association with lipid rafts. As cholesterol deficiency is sensed in the ER, a change in the distribution of cellular cholesterol upon prion infection, might lead to a decrease in ER cholesterol levels and thus to an activation of cholesterol biosynthesis. Prion infection might increase the necessity for membrane biogenesis, as PrP^{Sc} appears to be associated with membranes (Taylor and Hooper

2006; Avrahami *et al.* 2008). Castoreno *et al.* reported that the synthesis of cholesterol is the main way for replenishing membrane material used for phagocytosis (Castoreno *et al.* 2005). In their study the proteolytic activity of Srebp1a and Srebp2 in human embryonic kidney 293 cells was triggered by phagocytosis of latex beads. This led to the appearance of transcriptionally active mature Srebps in the nucleus and a 3-fold activation of a Srebp-specific reporter gene. Castoreno *et al.* concluded that Srebps are essential regulators of membrane biogenesis. Interestingly, a recent study on neuronal cells now suggests an imbalance between free cholesterol and cholesterol esters in prion infected cells (Bate *et al.* 2008).

Alternatively, sensing in the ER might be impaired upon prion infection due to pathologic changes in the ER. PrP^{Sc} infection can cause ER stress in the cell, possibly due to an accumulation of misfolded PrP protein. This might lead to a vicious cycle in which the induced ER stress could promote the conformational changes of PrP^C to an intermediate state more susceptible to conversion into PrP^{Sc} (Hetz *et al.* 2007). A direct link between ER stress and cholesterol biosynthesis has recently been described (Colgan *et al.* 2007). Treatment of the human cervix carcinoma cell line HeLa with different ER stress-inducing compounds like thapsigargin (Tg), A23187, tunicamycin and homocysteine led to a significantly increased activation of Srebp2 compared to untreated cells. The cleavage of the Srebp2 precursor was not mediated by caspases, that can also activate the transcription factor in a sterol-dependant manner (Pai *et al.* 1996; Higgins and Ioannou 2001), as caspase inhibition did not reduce the Srebp2 activity in Tg-treated cells. In contrast to this, the serine protease inhibitor Pefabloc, a known inhibitor of the cellular Srebp2 activating protease S1P, blocked Tg-induced Srebp2 cleavage. Thus, ER stress can induce Srebp2 activation through the normal pathway that regulates the activity of Srebp2 according to intracellular sterol concentrations. Interestingly, ER stress is associated with up-regulation of several ER stress-response genes like *Ddit3* (also termed *Chop* or *Gadd153*) (Rao *et al.* 2004) which was also significantly up-regulated in the microarray analysis performed in this work. Therefore it is possible that ER stress in prion infected N2a cells results in an up-regulation of the cholesterol biosynthesis.

4.6 The role of cholesterol in other neurological diseases

Neuronal integrity is critically dependent on cholesterol. The detected imbalance and role of cholesterol homeostasis in prion infected neuronal cells is in line with the pivotal role of cholesterol in other neurodegenerative diseases, including Huntington's disease (HD)

(Valenza *et al.* 2005; Valenza and Cattaneo 2006), Niemann Pick disease type C (NPC) (Ohm *et al.* 2003) and Alzheimer's disease (AD) (Burns and Duff 2002).

HD is a rare inherited neurological disease with typical symptoms like abnormal body movements, a lack of coordination and an altered cognition. The disease is caused by an expansion of trinucleotide repeats in the huntingtin gene (*Htt*). Healthy individuals harbour a gene with less than 36 repeats of the nucleotide triplet CAG, whereas the gene of patients suffering from HD contains more than 40 repeats. Data from patients with HD or HD mouse models suggest that this disease may be associated with an impaired cholesterol homeostasis. A transcriptional regulation of cholesterogenic genes harbouring the SRE motive by the huntingtin protein has been described. Furthermore, the presence of the mutated *Htt* is associated with a down-regulation of these genes in HD patience and mouse models (Valenza and Cattaneo 2006).

The autosomal recessive genetic disorder Nieman-Pick disease type C leads to a mutation in the *NPC1* (95 % of all cases) or *NPC2* gene causing a failure in intra-cellular cholesterol trafficking from the late endosomes to other cellular compartments (Maxfield and Tabas 2005). The processes in NPC that cause neurodegeneration are only incompletely understood. Studies suggest an altered neurotrophin signalling, stabilization of microtubules and cholesterol supply to neuronal processes due to cholesterol accumulation in the endosomal-lysosomal pathway (Patterson 2003; Sevin *et al.* 2007). During disease cholesterol accumulation is detected in all tissues except the brain, where cholesterol decreased with age (Vance 2006). Since most of cholesterol in the brain is contained in myelin and a strong demyelinisation occurs in NPC, it is possible, that the loss of cholesterol (due to the loss of myelin) might mask the accumulation of cholesterol in neurons and astrocytes. Additionally, a significant accumulation of cholesterol was reported in a mouse model of NPC 9 days after birth, when only mild neurodegeneration signs were detectable (Reid *et al.* 2004). Despite of the accumulation of cholesterol neither cholesterol lowering drugs nor dietary measures slowed the progression of the disease (Garcia-Calvo *et al.* 2005; Temel *et al.* 2007) suggesting that the disturbed transport of cholesterol within the cell might contribute to the pathogenesis of NPC and not the cholesterol accumulation *per se*.

Interestingly, several publications report a connection between cholesterol and the development and progression of AD, providing growing evidence for a role of cholesterol in AD. Hallmarks of AD are the accumulation of the amyloid β-peptide (Aβ) with plaque formation and the hyperphosphorylation of tau protein, leading to formation of neurofibrillary tangles. Aβ is produced by cleavage of amyloid precursor protein (APP) by the cellular

enzymes β- and γ-secretase into Aβ (Mandavilli 2006). A mutation in the gene for the cholesterol carrier ApoE, the APOE ε4 allele, was identified as a significant risk factor for AD (Puglielli 2008). In cell culture and animal models elevated cholesterol levels were found to increase Aβ formation and inhibition of cholesterol synthesis using drugs like statins resulted in lowered Aβ levels (Whitfield 2006; Hartmann *et al.* 2007; Puglielli 2008). However, prospective trials in AD patients evaluating statin therapy could not show any improvement in the cognitive function in comparison to an untreated control group (Caballero and Nahata 2004). Cholesterol is also the precursor for biosynthesis of neurosteroids and many neurosteroids are known to have neuroprotective function. Therefore, lower cholesterol levels might contribute to Aβ neurotoxicity, although it is unclear whether these low levels contribute to or result from AD pathology (Wang *et al.* 2008).

Thus, many neurological diseases are associated with an imbalance in cholesterol homeostasis indicating the importance of normal cholesterol levels for proper neuronal function. The detection of an up-regulated cholesterol metabolism in prion infected cells in this work is in line with that, suggesting that this imbalance caused by the prion disease may also be associated with neurodegeneration. Furthermore, up-regulation of cholesterol and lipid metabolism have been shown to cause neurological disease (Ntambi and Miyazaki 2004). In summary, our results show that prions have the potential to alter the cholesterol homeostasis of cells in a cell-type specific manner. These data provide new insights into the cellular and molecular biology and pathology of prion infection and might delineate new targets which can be used for selective interference with cellular prion propagation.

5. References

Aguzzi, A., Glatzel, M., Montrasio, F., Prinz, M., and Heppner, F. L. (2001) Interventional strategies against prion diseases. *Nat Rev Neurosci* **2,** 745-749.

Aguzzi, A. and Heppner, F. L. (2000) Pathogenesis of prion diseases: a progress report. *Cell Death Differ* **7,** 889-902.

Aguzzi, A., Sigurdson, C., and Heikenwaelder, M. (2008) Molecular mechanisms of prion pathogenesis. *Annu Rev Pathol* **3,** 11-40.

Aguzzi, A. and Sigurdson, C. J. (2004) Antiprion immunotherapy: To suppress or to stimulate? *Nature Reviews Immunology* **4,** 725-736.

Alper, T., Cramp, W. A., Haig, D. A., and Clarke, M. C. (1967) Does the agent of scrapie replicate without nucleic acid? *Nature* **214,** 764-766.

Alper, T., Haig, D. A., and Clarke, M. C. (1966) The exceptionally small size of the scrapie agent. *Biochem Biophys Res Commun* **22,** 278-284.

Angers, R. C., Browning, S. R., Seward, T. S., Sigurdson, C. J., Miller, M. W., Hoover, E. A., and Telling, G. C. (2006) Prions in skeletal muscles of deer with chronic wasting disease. *Science* **311,** 1117.

Arjona, A., Simarro, L., Islinger, F., Nishida, N., and Manuelidis, L. (2004) Two Creutzfeldt-Jakob disease agents reproduce prion protein-independent identities in cell cultures. *Proc Natl Acad Sci U S A* **101,** 8768-8773.

Avrahami, D., Dayan-Amouyal, Y., Tal, S., Mincberg, M., Davis, C., Abramsky, O., and Gabizon, R. (2008) Virus-induced alterations of membrane lipids affect the incorporation of PrP Sc into cells. *J Neurosci Res* **86,** 2753-2762.

Azzalin, A., Ferrara, V., Arias, A., Cerri, S., Avella, D., Pisu, M. B., Nano, R., Bernocchi, G., Ferretti, L., and Comincini, S. (2006) Interaction between the cellular prion (PrPC) and the 2P domain K+ channel TREK-1 protein. *Biochem Biophys Res Commun* **346,** 108-115.

Baker, C. A. and Manuelidis, L. (2003) Unique inflammatory RNA profiles of microglia in Creutzfeldt-Jakob disease. *Proc Natl Acad Sci U S A* **100,** 675-679.

Baron, G. S., Magalhaes, A. C., Prado, M. A., and Caughey, B. (2006) Mouse-adapted scrapie infection of SN56 cells: greater efficiency with microsome-associated versus purified PrP-res. *J Virol* **80,** 2106-2117.

Basler, K., Oesch, B., Scott, M., Westaway, D., Walchli, M., Groth, D. F., McKinley, M. P., Prusiner, S. B., and Weissmann, C. (1986) Scrapie and cellular PrP isoforms are encoded by the same chromosomal gene. *Cell* **46,** 417-428.

Bate, C., Rumbold, L., and Williams, A. (2007) Cholesterol synthesis inhibitors protect against platelet-activating factor-induced neuronal damage. *J Neuroinflammation* **4,** 5.

Bate, C., Salmona, M., Diomede, L., and Williams, A. (2004) Squalestatin cures prion-infected neurons and protects against prion neurotoxicity. *J Biol Chem* **279,** 14983-14990.

Bate, C., Tayebi, M., and Williams, A. (2008) Sequestration of free cholesterol in cell membranes by prions correlates with cytoplasmic phospholipase A2 activation. *BMC Biol* **6,** 8.

Belay, E. D. (1999) Transmissible spongiform encephalopathies in humans. *Annu Rev Microbiol* **53,** 283-314.

Belay, E. D., Maddox, R. A., Williams, E. S., Miller, M. W., Gambetti, P., and Schonberger, L. B. (2004) Chronic wasting disease and potential transmission to humans. *Emerg Infect Dis* **10,** 977-984.

Bendheim, P. E., Brown, H. R., Rudelli, R. D., Scala, L. J., Goller, N. L., Wen, G. Y., Kascsak, R. J., Cashman, N. R., and Bolton, D. C. (1992) Nearly ubiquitous tissue distribution of the scrapie agent precursor protein. *Neurology* **42,** 149-156.

Bengoechea-Alonso, M. T. and Ericsson, J. (2007) SREBP in signal transduction: cholesterol metabolism and beyond. *Curr Opin Cell Biol* **19,** 215-222.

Bessen, R. A. and Marsh, R. F. (1992) Biochemical and physical properties of the prion protein from two strains of the transmissible mink encephalopathy agent. *J Virol* **66,** 2096-2101.

Bessen, R. A. and Marsh, R. F. (1994) Distinct PrP properties suggest the molecular basis of strain variation in transmissible mink encephalopathy. *J Virol* **68,** 7859-7868.

Blasi, E., Barluzzi, R., Bocchini, V., Mazzolla, R., and Bistoni, F. (1990) Immortalization of Murine Microglial Cells by A V-Raf/V-Myc Carrying Retrovirus. *Journal of Neuroimmunology* **27,** 229-237.

Bolton, D. C., McKinley, M. P., and Prusiner, S. B. (1982) Identification of a protein that purifies with the scrapie prion. *Science* **218,** 1309-1311.

Booth, S., Bowman, C., Baumgartner, R., Sorensen, G., Robertson, C., Coulthart, M., Phillipson, C., and Somorjai, R. L. (2004) Identification of central nervous system genes involved in the host response to the scrapie agent during preclinical and clinical infection. *J Gen Virol* **85,** 3459-3471.

Borchelt, D. R., Scott, M., Taraboulos, A., Stahl, N., and Prusiner, S. B. (1990) Scrapie and cellular prion proteins differ in their kinetics of synthesis and topology in cultured cells. *J Cell Biol* **110,** 743-752.

Borchelt, D. R., Taraboulos, A., and Prusiner, S. B. (1992) Evidence for synthesis of scrapie prion proteins in the endocytic pathway. *J Biol Chem* **267,** 16188-16199.

Bosque, P. J. and Prusiner, S. B. (2000) Cultured cell sublines highly susceptible to prion infection. *J Virol* **74,** 4377-4386.

Bounhar, Y., Zhang, Y., Goodyer, C. G., and LeBlanc, A. (2001) Prion protein protects human neurons against Bax-mediated apoptosis. *J Biol Chem* **276,** 39145-39149.

Bragason, B. T. and Palsdottir, A. (2005) Interaction of PrP with NRAGE, a protein involved in neuronal apoptosis. *Mol Cell Neurosci* **29,** 232-244.

Brockes, J. P. (1999) Topics in prion cell biology. *Curr Opin Neurobiol* **9,** 571-577.

Brotherston, J. G., Renwick, C. C., Stamp, J. T., Zlotnik, I., and Pattison, I. H. (1968) Spread and scrapie by contact to goats and sheep. *J Comp Pathol* **78,** 9-17.

Brown, A. R., Rebus, S., McKimmie, C. S., Robertson, K., Williams, A., and Fazakerley, J. K. (2005) Gene expression profiling of the preclinical scrapie-infected hippocampus. *Biochem Biophys Res Commun* **334,** 86-95.

Brown, D. A. and London, E. (2000) Structure and function of sphingolipid- and cholesterol-rich membrane rafts. *J Biol Chem* **275,** 17221-17224.

Brown, D. R., Qin, K., Herms, J. W., Madlung, A., Manson, J., Strome, R., Fraser, P. E., Kruck, T., von Bohlen, A., Schulz-Schaeffer, W., Giese, A., Westaway, D., and Kretzschmar, H. (1997a) The cellular prion protein binds copper in vivo. *Nature* **390,** 684-687.

Brown, D. R., Schulz-Schaeffer, W. J., Schmidt, B., and Kretzschmar, H. A. (1997b) Prion protein-deficient cells show altered response to oxidative stress due to decreased SOD-1 activity. *Exp Neurol* **146,** 104-112.

Brown, M. S. and Goldstein, J. L. (1986) A receptor-mediated pathway for cholesterol homeostasis. *Science* **232,** 34-47.

Brown, M. S. and Goldstein, J. L. (1997) The SREBP pathway: regulation of cholesterol metabolism by proteolysis of a membrane-bound transcription factor. *Cell* **89,** 331-340.

Brown, P., Preece, M. A., and Will, R. G. (1992) "Friendly fire" in medicine: hormones, homografts, and Creutzfeldt-Jakob disease. *Lancet* **340,** 24-27.

Bruce, M., Chree, A., McConnell, I., Foster, J., Pearson, G., and Fraser, H. (1994) Transmission of bovine spongiform encephalopathy and scrapie to mice: strain variation and the species barrier. *Philos Trans R Soc Lond B Biol Sci* **343,** 405-411.

Bubner, B., Gase, K., and Baldwin, I. T. (2004) Two-fold differences are the detection limit for determining transgene copy numbers in plants by real-time PCR. *BMC Biotechnol* **4,** 14.

Budka, H. (2003) Neuropathology of prion diseases. *Br Med Bull* **66,** 121-130.

Bueler, H., Aguzzi, A., Sailer, A., Greiner, R. A., Autenried, P., Aguet, M., and Weissmann, C. (1993) Mice devoid of PrP are resistant to scrapie. *Cell* **73,** 1339-1347.

Burger, D. and Hartsough, G. R. (1965) Encephalopathy of mink. II. Experimental and natural transmission. *J Infect Dis* **115,** 393-399.

Burns, C. S., Aronoff-Spencer, E., Legname, G., Prusiner, S. B., Antholine, W. E., Gerfen, G. J., Peisach, J., and Millhauser, G. L. (2003) Copper coordination in the full-length, recombinant prion protein. *Biochemistry* **42,** 6794-6803.

Burns, M. and Duff, K. (2002) Cholesterol in Alzheimer's disease and tauopathy. *Ann N Y Acad Sci* **977,** 367-375.

Butler, D. A., Scott, M. R., Bockman, J. M., Borchelt, D. R., Taraboulos, A., Hsiao, K. K., Kingsbury, D. T., and Prusiner, S. B. (1988) Scrapie-infected murine neuroblastoma cells produce protease-resistant prion proteins. *J Virol* **62,** 1558-1564.

Caballero, J. and Nahata, M. (2004) Do statins slow down Alzheimer's disease? A review. *J Clin Pharm Ther* **29,** 209-213.

Canevari, L. and Clark, J. B. (2007) Alzheimer's disease and cholesterol: the fat connection. *Neurochem Res* **32,** 739-750.

Castilla, J., Saa, P., Hetz, C., and Soto, C. (2005) In vitro generation of infectious scrapie prions. *Cell* **121,** 195-206.

Castoreno, A. B., Wang, Y., Stockinger, W., Jarzylo, L. A., Du, H., Pagnon, J. C., Shieh, E. C., and Nohturfft, A. (2005) Transcriptional regulation of phagocytosis-induced membrane biogenesis by sterol regulatory element binding proteins. *Proc Natl Acad Sci U S A* **102,** 13129-13134.

Caughey, B. and Baron, G. S. (2006) Prions and their partners in crime. *Nature* **443,** 803-810.

Caughey, B., Kocisko, D. A., Raymond, G. J., and Lansbury, P. T., Jr. (1995) Aggregates of scrapie-associated prion protein induce the cell-free conversion of protease-sensitive prion protein to the protease-resistant state. *Chem Biol* **2,** 807-817.

Chang, T. Y., Reid, P. C., Sugii, S., Ohgami, N., Cruz, J. C., and Chang, C. C. (2005) Niemann-Pick type C disease and intracellular cholesterol trafficking. *J Biol Chem* **280,** 20917-20920.

Cheon, M. S., Fountoulakis, M., Cairns, N. J., Dierssen, M., Herkner, K., and Lubec, G. (2001) Decreased protein levels of stathmin in adult brains with Down syndrome and Alzheimer's disease. *J Neural Transm Suppl* 281-288.

Chu, G., Narasimhan, B., Tibshirani, R., and Tusher, V. G. SAM "Signigicance Analysis of Microarrays". Users Guide and Technical Document: http://www.stat.standford.edu/~tibs/SAM/ . 2002.
Ref Type: Electronic Citation

Clarke, M. C. and Haig, D. A. (1970) Evidence for the multiplication of scrapie agent in cell culture. *Nature* **225,** 100-101.

Clarke, M. C. and Millson, G. C. (1976) Infection of a cell line of mouse L fibroblasts with scrapie agent. *Nature* **261,** 144-145.

Cohen, F. E., Pan, K. M., Huang, Z., Baldwin, M., Fletterick, R. J., and Prusiner, S. B. (1994) Structural clues to prion replication. *Science* **264,** 530-531.

Coitinho, A. S., Dietrich, M. O., Hoffmann, A., Dall'Igna, O. P., Souza, D. O., Martins, V. R., Brentani, R. R., Izquierdo, I., and Lara, D. R. (2002) Decreased hyperlocomotion induced by MK-801, but not amphetamine and caffeine in mice lacking cellular prion protein (PrP(C)). *Brain Res Mol Brain Res* **107,** 190-194.

Colgan, S. M., Tang, D., Werstuck, G. H., and Austin, R. C. (2007) Endoplasmic reticulum stress causes the activation of sterol regulatory element binding protein-2. *Int J Biochem Cell Biol* **39,** 1843-1851.

Collinge, J. (1997) Human prion diseases and bovine spongiform encephalopathy (BSE). *Hum Mol Genet* **6,** 1699-1705.

Collinge, J. (2001) Prion diseases of humans and animals: their causes and molecular basis. *Annu Rev Neurosci* **24,** 519-550.

Collinge, J., Beck, J., Campbell, T., Estibeiro, K., and Will, R. G. (1996a) Prion protein gene analysis in new variant cases of Creutzfeldt-Jakob disease. *Lancet* **348,** 56.

Collinge, J. and Clarke, A. R. (2007) A general model of prion strains and their pathogenicity. *Science* **318,** 930-936.

Collinge, J., Harding, A. E., Owen, F., Poulter, M., Lofthouse, R., Boughey, A. M., Shah, T., and Crow, T. J. (1989) Diagnosis of Gerstmann-Straussler syndrome in familial dementia with prion protein gene analysis. *Lancet* **2,** 15-17.

Collinge, J., Palmer, M. S., Sidle, K. C., Hill, A. F., Gowland, I., Meads, J., Asante, E., Bradley, R., Doey, L. J., and Lantos, P. L. (1995) Unaltered susceptibility to BSE in transgenic mice expressing human prion protein. *Nature* **378,** 779-783.

Collinge, J. and Rossor, M. (1996) A new variant of prion disease. *Lancet* **347,** 916-917.

Collinge, J., Sidle, K. C., Meads, J., Ironside, J., and Hill, A. F. (1996b) Molecular analysis of prion strain variation and the aetiology of 'new variant' CJD. *Nature* **383,** 685-690.

Creutzfeldt, H. G. (1920) Über eine eigenartige herdförmige Erkrankung des zentralen Nervensystems. *I Ges Neuro Prychiatr* **57,** 1-18.

Cronier, S., Beringue, V., Bellon, A., Peyrin, J. M., and Laude, H. (2007) Prion strain- and species-dependent effects of antiprion molecules in primary neuronal cultures. *J Virol* **81,** 13794-13800.

Davanipour, Z., Alter, M., Sobel, E., Asher, D., and Gajdusek, D. C. (1985) Creutzfeldt-Jakob disease: possible medical risk factors. *Neurology* **35,** 1483-1486.

de Almeida, C. J., Chiarini, L. B., da Silva, J. P., PM, E. S., Martins, M. A., and Linden, R. (2005) The cellular prion protein modulates phagocytosis and inflammatory response. *J Leukoc Biol* **77,** 238-246.

de Wet, J. R., Wood, K. V., Helinski, D. R., and DeLuca, M. (1985) Cloning of firefly luciferase cDNA and the expression of active luciferase in Escherichia coli. *Proc Natl Acad Sci U S A* **82,** 7870-7873.

Dickinson, A. G., Stamp, J. T., and Renwick, C. C. (1974) Maternal and lateral transmission of scrapie in sheep. *J Comp Pathol* **84,** 19-25.

Dietschy, J. M. and Turley, S. D. (2004) Thematic review series: brain Lipids. Cholesterol metabolism in the central nervous system during early development and in the mature animal. *J Lipid Res* **45,** 1375-1397.

Dlakic, W. M., Grigg, E., and Bessen, R. A. (2007) Prion infection of muscle cells in vitro. *J Virol* **81,** 4615-4624.

Dodelet, V. C. and Cashman, N. R. (1998) Prion protein expression in human leukocyte differentiation. *Blood* **91,** 1556-1561.

Doh-Ura, K., Perryman, S., Race, R., and Chesebro, B. (1995) Identification of differentially expressed genes in scrapie-infected mouse neuroblastoma cells. *Microb Pathog* **18,** 1-9.

Dooley, K. A., Millinder, S., and Osborne, T. F. (1998) Sterol regulation of 3-hydroxy-3-methylglutaryl-coenzyme A synthase gene through a direct interaction between sterol regulatory element binding protein and the trimeric CCAAT-binding factor/nuclear factor Y. *J Biol Chem* **273,** 1349-1356.

Drobyshev, A., Machka, C., Horsch, M., Seltmann, M., Liebscher, V., Hrabe de Angelis, M., and Beckers, J. (2003) Specificity assessment from fractionation experiments (SAFE): a novel method to evaluate microarray probe specificity based on hybridisation stringencies. *Nucleic Acids Res* **31,** E1-1.

Edenhofer, F., Rieger, R., Famulok, M., Wendler, W., Weiss, S., and Winnacker, E. L. (1996) Prion protein PrPc interacts with molecular chaperones of the Hsp60 family. *J Virol* **70,** 4724-4728.

Edwards, P. A., Tabor, D., Kast, H. R., and Venkateswaran, A. (2000) Regulation of gene expression by SREBP and SCAP. *Biochim Biophys Acta* **1529,** 103-113.

Ertmer, A., Gilch, S., Yun, S. W., Flechsig, E., Klebl, B., Stein-Gerlach, M., Klein, M. A., and Schatzl, H. M. (2004) The tyrosine kinase inhibitor STI571 induces cellular clearance of PrPSc in prion-infected cells. *Journal of Biological Chemistry* **279,** 41918-41927.

Espenshade, P. J. (2006) SREBPs: sterol-regulated transcription factors. *J Cell Sci* **119,** 973-976.

Fasano, C., Campana, V., Griffiths, B., Kelly, G., Schiavo, G., and Zurzolo, C. (2008) Gene expression profile of quinacrine-cured prion-infected mouse neuronal cells. *J Neurochem* **105,** 239-250.

Feramisco, J. D., Radhakrishnan, A., Ikeda, Y., Reitz, J., Brown, M. S., and Goldstein, J. L. (2005) Intramembrane aspartic acid in SCAP protein governs cholesterol-induced conformational change. *Proc Natl Acad Sci U S A* **102,** 3242-3247.

Gajdusek, D. C. (1977) Unconventional viruses and the origin and disappearance of kuru. *Science* **197,** 943-960.

Gajdusek, D. C. and ZIGAS, V. (1957) Degenerative disease of the central nervous system in New Guinea; the endemic occurrence of kuru in the native population. *N Engl J Med* **257,** 974-978.

Garcia-Calvo, M., Lisnock, J., Bull, H. G., Hawes, B. E., Burnett, D. A., Braun, M. P., Crona, J. H., Davis, H. R., Jr., Dean, D. C., Detmers, P. A., Graziano, M. P., Hughes, M., Macintyre, D. E., Ogawa, A., O'neill, K. A., Iyer, S. P., Shevell, D. E., Smith, M. M., Tang, Y. S., Makarewicz, A. M., Ujjainwalla, F., Altmann, S. W., Chapman, K. T., and Thornberry, N. A.

(2005) The target of ezetimibe is Niemann-Pick C1-Like 1 (NPC1L1). *Proc Natl Acad Sci U S A* **102,** 8132-8137.

Gasset, M., Baldwin, M. A., Fletterick, R. J., and Prusiner, S. B. (1993) Perturbation of the secondary structure of the scrapie prion protein under conditions that alter infectivity. *Proc Natl Acad Sci U S A* **90,** 1-5.

Gauczynski, S., Peyrin, J. M., Haik, S., Leucht, C., Hundt, C., Rieger, R., Krasemann, S., Deslys, J. P., Dormont, D., Lasmezas, C. I., and Weiss, S. (2001) The 37-kDa/67-kDa laminin receptor acts as the cell-surface receptor for the cellular prion protein. *EMBO J* **20,** 5863-5875.

Geiss, G. K., Bumgarner, R. E., An, M. C., Agy, M. B., 't Wout, A. B., Hammersmark, E., Carter, V. S., Upchurch, D., Mullins, J. I., and Katze, M. G. (2000) Large-scale monitoring of host cell gene expression during HIV-1 infection using cDNA microarrays. *Virology* **266,** 8-16.

Gerstmann, J., Sträussler, E., and Scheinker, I. (1936) Über eine eigenartige hereditär-familiäre Erkrankung des Zentralnervensystems. Zugleich ein Beitrag des vorzeitigen lokalen Alterns. *Z Neur Psychiat* **154,** 736-762.

Gilch, S., Kehler, C., and Schatzl, H. M. (2006) The prion protein requires cholesterol for cell surface localization. *Mol Cell Neurosci* **31,** 346-353.

Gilch, S., Schmitz, F., Aguib, Y., Kehler, C., Bulow, S., Bauer, S., Kremmer, E., and Schatzl, H. M. (2007) CpG and LPS can interfere negatively with prion clearance in macrophage and microglial cells. *FEBS J* **274,** 5834-5844.

Goldstein, J. L., DeBose-Boyd, R. A., and Brown, M. S. (2006) Protein sensors for membrane sterols. *Cell* **124,** 35-46.

Govaerts, C., Wille, H., Prusiner, S. B., and Cohen, F. E. (2004) Evidence for assembly of prions with left-handed beta-helices into trimers. *Proc Natl Acad Sci U S A* **101,** 8342-8347.

Greenwood, A. D., Horsch, M., Stengel, A., Vorberg, I., Lutzny, G., Maas, E., Schadler, S., Erfle, V., Beckers, J., Schatzl, H., and Leib-Mosch, C. (2005) Cell line dependent RNA expression profiles of prion-infected mouse neuronal cells. *J Mol Biol* **349,** 487-500.

Griffith, J. S. (1967) Self-replication and scrapie. *Nature* **215,** 1043-1044.

Hartmann, T., Kuchenbecker, J., and Grimm, M. O. (2007) Alzheimer's disease: the lipid connection. *J Neurochem* **103 Suppl 1,** 159-170.

Haviv, Y., Avrahami, D., Ovadia, H., Ben Hur, T., Gabizon, R., and Sharon, R. (2008) Induced neuroprotection independently from PrPSc accumulation in a mouse model for prion disease treated with simvastatin. *Arch Neurol* **65,** 762-775.

Head, M. W., Northcott, V., Rennison, K., Ritchie, D., McCardle, L., Bunn, T. J., McLennan, N. F., Ironside, J. W., Tullo, A. B., and Bonshek, R. E. (2003) Prion protein accumulation in eyes of patients with sporadic and variant Creutzfeldt-Jakob disease. *Invest Ophthalmol Vis Sci* **44,** 342-346.

Hegde, P., Qi, R., Abernathy, K., Gay, C., Dharap, S., Gaspard, R., Hughes, J. E., Snesrud, E., Lee, N., and Quackenbush, J. (2000) A concise guide to cDNA microarray analysis. *Biotechniques* **29,** 548-4, 556.

Herms, J., Tings, T., Gall, S., Madlung, A., Giese, A., Siebert, H., Schurmann, P., Windl, O., Brose, N., and Kretzschmar, H. (1999) Evidence of presynaptic location and function of the prion protein. *J Neurosci* **19,** 8866-8875.

Hetz, C., Castilla, J., and Soto, C. (2007) Perturbation of endoplasmic reticulum homeostasis facilitates prion replication. *J Biol Chem* **282,** 12725-12733.

Higgins, M. E. and Ioannou, Y. A. (2001) Apoptosis-induced release of mature sterol regulatory element-binding proteins activates sterol-responsive genes. *J Lipid Res* **42,** 1939-1946.

Hill, A. F., Butterworth, R. J., Joiner, S., Jackson, G., Rossor, M. N., Thomas, D. J., Frosh, A., Tolley, N., Bell, J. E., Spencer, M., King, A., Al Sarraj, S., Ironside, J. W., Lantos, P. L., and Collinge, J. (1999) Investigation of variant Creutzfeldt-Jakob disease and other human prion diseases with tonsil biopsy samples. *Lancet* **353,** 183-189.

Hill, A. F., Desbruslais, M., Joiner, S., Sidle, K. C., Gowland, I., Collinge, J., Doey, L. J., and Lantos, P. (1997) The same prion strain causes vCJD and BSE. *Nature* **389,** 448-50, 526.

Hornemann, S., Korth, C., Oesch, B., Riek, R., Wider, G., Wuthrich, K., and Glockshuber, R. (1997) Recombinant full-length murine prion protein, mPrP(23-231): purification and spectroscopic characterization. *FEBS Lett* **413,** 277-281.

Horton, J. D. and Shimomura, I. (1999) Sterol regulatory element-binding proteins: activators of cholesterol and fatty acid biosynthesis. *Curr Opin Lipidol* **10,** 143-150.

Hsiao, K. K., Groth, D., Scott, M., Yang, S. L., Serban, H., Rapp, D., Foster, D., Torchia, M., DeArmond, S. J., and Prusiner, S. B. (1994) Serial transmission in rodents of neurodegeneration from transgenic mice expressing mutant prion protein. *Proc Natl Acad Sci U S A* **91,** 9126-9130.

Hua, X., Yokoyama, C., Wu, J., Briggs, M. R., Brown, M. S., Goldstein, J. L., and Wang, X. (1993) SREBP-2, a second basic-helix-loop-helix-leucine zipper protein that stimulates transcription by binding to a sterol regulatory element. *Proc Natl Acad Sci U S A* **90,** 11603-11607.

Hunter, N. (1997) PrP genetics in sheep and the applications for scrapie and BSE. *Trends Microbiol* **5,** 331-334.

Hwang, D., Lee, I. Y., Yoo, H., Gehlenborg, N., Cho, J. H., Petritis, B., Baxter, D., Pitstick, R., Young, R., Spicer, D., Price, N. D., Hohmann, J. G., DeArmond, S. J., Carlson, G. A., and Hood, L. E. (2009) A systems approach to prion disease. *Mol Syst Biol* **5,** 252.

Ikonen, E. (2008) Cellular cholesterol trafficking and compartmentalization. *Nat Rev Mol Cell Biol* **9,** 125-138.

Iwamaru, Y., Takenouchi, T., Ogihara, K., Hoshino, M., Takata, M., Imamura, M., Tagawa, Y., Hayashi-Kato, H., Ushiki-Kaku, Y., Shimizu, Y., Okada, H., Shinagawa, M., Kitani, H.,

and Yokoyama, T. (2006) Microglial cell line established from prion protein overexpressing mice is susceptible to various murine prion strains. *J Virol*.

Jakob, A. M. (1921) Über eingenartige Erkrankungen des Zentralnervensystems mit bemerkenswerten anatomischen Befunden (Spastische Pseudosklerose-Encephalomyelopathie mit disseminierten Degenerationsherden). *Dtsch Z Nervenheilk* **70,** 132-146.

Jarrett, J. T. and Lansbury, P. T., Jr. (1993) Seeding "one-dimensional crystallization" of amyloid: a pathogenic mechanism in Alzheimer's disease and scrapie? *Cell* **73,** 1055-1058.

Jewell, J. E., Conner, M. M., Wolfe, L. L., Miller, M. W., and Williams, E. S. (2005) Low frequency of PrP genotype 225SF among free-ranging mule deer (Odocoileus hemionus) with chronic wasting disease. *J Gen Virol* **86,** 2127-2134.

Julius, C., Hutter, G., Wagner, U., Seeger, H., Kana, V., Kranich, J., Klohn, P., Weissmann, C., Miele, G., and Aguzzi, A. (2008) Transcriptional stability of cultured cells upon prion infection. *J Mol Biol* **375,** 1222-1233.

Kaneko, K., Vey, M., Scott, M., Pilkuhn, S., Cohen, F. E., and Prusiner, S. B. (1997) COOH-terminal sequence of the cellular prion protein directs subcellular trafficking and controls conversion into the scrapie isoform. *Proc Natl Acad Sci U S A* **94,** 2333-2338.

Kempster, S., Bate, C., and Williams, A. (2007) Simvastatin treatment prolongs the survival of scrapie-infected mice. *Neuroreport* **18,** 479-482.

Klamt, F., Dal Pizzol, F., Conte da Frota ML JR, Walz, R., Andrades, M. E., da Silva, E. G., Brentani, R. R., Izquierdo, I., and Fonseca Moreira, J. C. (2001) Imbalance of antioxidant defense in mice lacking cellular prion protein. *Free Radic Biol Med* **30,** 1137-1144.

Klingenstein, R., Lober, S., Kujala, P., Godsave, S., Leliveld, S. R., Gmeiner, P., Peters, P. J., and Korth, C. (2006) Tricyclic antidepressants, quinacrine and a novel, synthetic chimera thereof clear prions by destabilizing detergent-resistant membrane compartments. *J Neurochem* **98,** 748-759.

Klohn, P. C., Stoltze, L., Flechsig, E., Enari, M., and Weissmann, C. (2003) A quantitative, highly sensitive cell-based infectivity assay for mouse scrapie prions. *Proc Natl Acad Sci U S A* **100,** 11666-11671.

Koh, C. H., Peng, Z. F., Ou, K., Melendez, A., Manikandan, J., Qi, R. Z., and Cheung, N. S. (2007) Neuronal apoptosis mediated by inhibition of intracellular cholesterol transport: microarray and proteomics analyses in cultured murine cortical neurons. *J Cell Physiol* **211,** 63-87.

Kretzschmar, H. A., Prusiner, S. B., Stowring, L. E., and DeArmond, S. J. (1986) Scrapie prion proteins are synthesized in neurons. *Am J Pathol* **122,** 1-5.

Kurschner, C. and Morgan, J. I. (1995) The cellular prion protein (PrP) selectively binds to Bcl-2 in the yeast two-hybrid system. *Brain Res Mol Brain Res* **30,** 165-168.

Kuwahara, C., Takeuchi, A. M., Nishimura, T., Haraguchi, K., Kubosaki, A., Matsumoto, Y., Saeki, K., Matsumoto, Y., Yokoyama, T., Itohara, S., and Onodera, T. (1999) Prions prevent neuronal cell-line death. *Nature* **400,** 225-226.

Ladogana, A., Puopolo, M., Croes, E. A., Budka, H., Jarius, C., Collins, S., Klug, G. M., Sutcliffe, T., Giulivi, A., Alperovitch, A., Delasnerie-Laupretre, N., Brandel, J. P., Poser, S., Kretzschmar, H., Rietveld, I., Mitrova, E., Cuesta, J. P., Martinez-Martin, P., Glatzel, M., Aguzzi, A., Knight, R., Ward, H., Pocchiari, M., Van Duijn, C. M., Will, R. G., and Zerr, I. (2005) Mortality from Creutzfeldt-Jakob disease and related disorders in Europe, Australia, and Canada. *Neurology* **64,** 1586-1591.

Lasmezas, C. I., Deslys, J. P., Demaimay, R., Adjou, K. T., Lamoury, F., Dormont, D., Robain, O., Ironside, J., and Hauw, J. J. (1996) BSE transmission to macaques. *Nature* **381,** 743-744.

Lasmezas, C. I., Deslys, J. P., Robain, O., Jaegly, A., Beringue, V., Peyrin, J. M., Fournier, J. G., Hauw, J. J., Rossier, J., and Dormont, D. (1997) Transmission of the BSE agent to mice in the absence of detectable abnormal prion protein. *Science* **275,** 402-405.

Lee, I. Y., Westaway, D., Smit, A. F., Wang, K., Seto, J., Chen, L., Acharya, C., Ankener, M., Baskin, D., Cooper, C., Yao, H., Prusiner, S. B., and Hood, L. E. (1998) Complete genomic sequence and analysis of the prion protein gene region from three mammalian species. *Genome Res* **8,** 1022-1037.

Lee, K. S., Magalhaes, A. C., Zanata, S. M., Brentani, R. R., Martins, V. R., and Prado, M. A. (2001) Internalization of mammalian fluorescent cellular prion protein and N-terminal deletion mutants in living cells. *J Neurochem* **79,** 79-87.

Lee, L. G., Connell, C. R., and Bloch, W. (1993) Allelic discrimination by nick-translation PCR with fluorogenic probes. *Nucleic Acids Res* **21,** 3761-3766.

Legname, G., Baskakov, I. V., Nguyen, H. O. B., Riesner, D., Cohen, F. E., DeArmond, S. J., and Prusiner, S. B. (2004) Synthetic mammalian prions. *Science* **305,** 673-676.

Li, A., Christensen, H. M., Stewart, L. R., Roth, K. A., Chiesa, R., and Harris, D. A. (2007) Neonatal lethality in transgenic mice expressing prion protein with a deletion of residues 105-125. *EMBO J* **26,** 548-558.

Li, A. and Harris, D. A. (2005) Mammalian prion protein suppresses Bax-induced cell death in yeast. *J Biol Chem* **280,** 17430-17434.

Liberski, P. P., Guiroy, D. C., Williams, E. S., Walis, A., and Budka, H. (2001) Deposition patterns of disease-associated prion protein in captive mule deer brains with chronic wasting disease. *Acta Neuropathol (Berl)* **102,** 496-500.

Livak, K. J., Flood, S. J., Marmaro, J., Giusti, W., and Deetz, K. (1995) Oligonucleotides with fluorescent dyes at opposite ends provide a quenched probe system useful for detecting PCR product and nucleic acid hybridization. *PCR Methods Appl* **4,** 357-362.

Livak, K. J. and Schmittgen, T. D. (2001) Analysis of relative gene expression data using real-time quantitative PCR and the 2(-Delta Delta C(T)) Method. *Methods* **25,** 402-408.

Llewelyn, C. A., Hewitt, P. E., Knight, R. S., Amar, K., Cousens, S., Mackenzie, J., and Will, R. G. (2004) Possible transmission of variant Creutzfeldt-Jakob disease by blood transfusion. *Lancet* **363,** 417-421.

Lopes, M. H., Hajj, G. N., Muras, A. G., Mancini, G. L., Castro, R. M., Ribeiro, K. C., Brentani, R. R., Linden, R., and Martins, V. R. (2005) Interaction of cellular prion and stress-inducible protein 1 promotes neuritogenesis and neuroprotection by distinct signaling pathways. *J Neurosci* **25,** 11330-11339.

Lueck, C. J., McIlwaine, G. G., and Zeidler, M. (2000) Creutzfeldt-Jakob disease and the eye. II. Ophthalmic and neuro-ophthalmic features. *Eye* **14 (Pt 3A),** 291-301.

Lugaresi, E., Medori, R., Montagna, P., Baruzzi, A., Cortelli, P., Lugaresi, A., Tinuper, P., Zucconi, M., and Gambetti, P. (1986) Fatal familial insomnia and dysautonomia with selective degeneration of thalamic nuclei. *N Engl J Med* **315,** 997-1003.

Ma, J., Wollmann, R., and Lindquist, S. (2002) Neurotoxicity and neurodegeneration when PrP accumulates in the cytosol. *Science* **298,** 1781-1785.

Maas, E., Geissen, M., Groschup, M. H., Rost, R., Onodera, T., Schatzl, H., and Vorberg, I. M. (2007) Scrapie infection of prion protein-deficient cell line upon ectopic expression of mutant prion proteins. *J Biol Chem* **282,** 18702-18710.

Mandavilli, A. (2006) The amyloid code. *Nat Med* **12,** 747-751.

Manetto, V., Medori, R., Cortelli, P., Montagna, P., Tinuper, P., Baruzzi, A., Rancurel, G., Hauw, J. J., Vanderhaeghen, J. J., Mailleux, P., and . (1992) Fatal familial insomnia: clinical and pathologic study of five new cases. *Neurology* **42,** 312-319.

Mange, A., Nishida, N., Milhavet, O., McMahon, H. E., Casanova, D., and Lehmann, S. (2000) Amphotericin B inhibits the generation of the scrapie isoform of the prion protein in infected cultures. *J Virol* **74,** 3135-3140.

Manson, J., West, J. D., Thomson, V., McBride, P., Kaufman, M. H., and Hope, J. (1992) The prion protein gene: a role in mouse embryogenesis? *Development* **115,** 117-122.

Marella, M., Lehmann, S., Grassi, J., and Chabry, J. (2002) Filipin prevents pathological prion protein accumulation by reducing endocytosis and inducing cellular PrP release. *J Biol Chem* **277,** 25457-25464.

Marsh, R. F., Kincaid, A. E., Bessen, R. A., and Bartz, J. C. (2005) Interspecies transmission of chronic wasting disease prions to squirrel monkeys (Saimiri sciureus). *J Virol* **79,** 13794-13796.

Martinez, T. and Pascual, A. (2007) Identification of genes differentially expressed in SH-SY5Y neuroblastoma cells exposed to the prion peptide 106-126. *Eur J Neurosci* **26,** 51-59.

Masters, C. L., Gajdusek, D. C., and Gibbs, C. J., Jr. (1981) Creutzfeldt-Jakob disease virus isolations from the Gerstmann-Straussler syndrome with an analysis of the various forms of amyloid plaque deposition in the virus-induced spongiform encephalopathies. *Brain* **104,** 559-588.

Mathiason, C. K., Powers, J. G., Dahmes, S. J., Osborn, D. A., Miller, K. V., Warren, R. J., Mason, G. L., Hays, S. A., Hayes-Klug, J., Seelig, D. M., Wild, M. A., Wolfe, L. L., Spraker, T. R., Miller, M. W., Sigurdson, C. J., Telling, G. C., and Hoover, E. A. (2006) Infectious prions in the saliva and blood of deer with chronic wasting disease. *Science* **314,** 133-136.

Matthews, J. C., Hori, K., and Cormier, M. J. (1977) Purification and properties of Renilla reniformis luciferase. *Biochemistry* **16,** 85-91.

Maxfield, F. R. and Tabas, I. (2005) Role of cholesterol and lipid organization in disease. *Nature* **438,** 612-621.

McGowan, J. P. (1914) Investigation into the disease of sheep called "scrapie" with special reference to its association with sarcospoidiosis. *Rept* 232.

McGowan, J. P. (1922) Scrapie in sheep. *Scottish J Agric* 356-375.

Miura, T., Hori-i A, Mototani, H., and Takeuchi, H. (1999) Raman spectroscopic study on the copper(II) binding mode of prion octapeptide and its pH dependence. *Biochemistry* **38,** 11560-11569.

Mok, S. W., Thelen, K. M., Riemer, C., Bamme, T., Gultner, S., Lutjohann, D., and Baier, M. (2006) Simvastatin prolongs survival times in prion infections of the central nervous system. *Biochem Biophys Res Commun* **348,** 697-702.

Momoi, T., Ando, S., and Magai, Y. (1976) High resolution preparative column chromatographic system for gangliosides using DEAE-Sephadex and a new porus silica, Iatrobeads. *Biochim Biophys Acta* **441,** 488-497.

Morrison, T. B., Weis, J. J., and Wittwer, C. T. (1998) Quantification of low-copy transcripts by continuous SYBR Green I monitoring during amplification. *Biotechniques* **24,** 954-962.

Mouillet-Richard, S., Ermonval, M., Chebassier, C., Laplanche, J. L., Lehmann, S., Launay, J. M., and Kellermann, O. (2000) Signal transduction through prion protein. *Science* **289,** 1925-1928.

Muramoto, T., DeArmond, S. J., Scott, M., Telling, G. C., Cohen, F. E., and Prusiner, S. B. (1997) Heritable disorder resembling neuronal storage disease in mice expressing prion protein with deletion of an alpha-helix. *Nat Med* **3,** 750-755.

Naslavsky, N., Stein, R., Yanai, A., Friedlander, G., and Taraboulos, A. (1997) Characterization of detergent-insoluble complexes containing the cellular prion protein and its scrapie isoform. *J Biol Chem* **272,** 6324-6331.

Neuhoff, H., Sassoe-Pognetto, M., Panzanelli, P., Maas, C., Witke, W., and Kneussel, M. (2005) The actin-binding protein profilin I is localized at synaptic sites in an activity-regulated manner. *Eur J Neurosci* **21,** 15-25.

Nieznanski, K., Nieznanska, H., Skowronek, K. J., Osiecka, K. M., and Stepkowski, D. (2005) Direct interaction between prion protein and tubulin. *Biochem Biophys Res Commun* **334,** 403-411.

Nishida, N., Harris, D. A., Vilette, D., Laude, H., Frobert, Y., Grassi, J., Casanova, D., Milhavet, O., and Lehmann, S. (2000) Successful transmission of three mouse-adapted scrapie strains to murine neuroblastoma cell lines overexpressing wild-type mouse prion protein. *J Virol* **74,** 320-325.

Nishida, N., Katamine, S., Shigematsu, K., Nakatani, A., Sakamoto, N., Hasegawa, S., Nakaoke, R., Atarashi, R., Kataoka, Y., and Miyamoto, T. (1997) Prion protein is necessary for latent learning and long-term memory retention. *Cell Mol Neurobiol* **17,** 537-545.

Ntambi, J. M. and Miyazaki, M. (2004) Regulation of stearoyl-CoA desaturases and role in metabolism. *Prog Lipid Res* **43,** 91-104.

Nunziante, M., Gilch, S., and Schatzl, H. M. (2003) Essential role of the prion protein N terminus in subcellular trafficking and half-life of cellular prion protein. *J Biol Chem* **278,** 3726-3734.

Oesch, B., Westaway, D., Walchli, M., McKinley, M. P., Kent, S. B., Aebersold, R., Barry, R. A., Tempst, P., Teplow, D. B., Hood, L. E., and . (1985) A cellular gene encodes scrapie PrP 27-30 protein. *Cell* **40,** 735-746.

Ohm, T. G., Treiber-Held, S., Distl, R., Glockner, F., Schonheit, B., Tamanai, M., and Meske, V. (2003) Cholesterol and tau protein--findings in Alzheimer's and Niemann Pick C's disease. *Pharmacopsychiatry* **36 Suppl 2,** S120-S126.

Owen, F., Poulter, M., Lofthouse, R., Collinge, J., Crow, T. J., Risby, D., Baker, H. F., Ridley, R. M., Hsiao, K., and Prusiner, S. B. (1989) Insertion in prion protein gene in familial Creutzfeldt-Jakob disease. *Lancet* **1,** 51-52.

Pai, J. T., Brown, M. S., and Goldstein, J. L. (1996) Purification and cDNA cloning of a second apoptosis-related cysteine protease that cleaves and activates sterol regulatory element binding proteins. *Proc Natl Acad Sci U S A* **93,** 5437-5442.

Pan, K. M., Baldwin, M., Nguyen, J., Gasset, M., Serban, A., Groth, D., Mehlhorn, I., Huang, Z., Fletterick, R. J., Cohen, F. E., and . (1993) Conversion of alpha-helices into beta-sheets features in the formation of the scrapie prion proteins. *Proc Natl Acad Sci U S A* **90,** 10962-10966.

Parchi, P., Castellani, R., Capellari, S., Ghetti, B., Young, K., Chen, S. G., Farlow, M., Dickson, D. W., Sima, A. A., Trojanowski, J. Q., Petersen, R. B., and Gambetti, P. (1996) Molecular basis of phenotypic variability in sporadic Creutzfeldt-Jakob disease. *Ann Neurol* **39,** 767-778.

Patterson, M. C. (2003) A riddle wrapped in a mystery: understanding Niemann-Pick disease, type C. *Neurologist* **9,** 301-310.

Pauly, P. C. and Harris, D. A. (1998) Copper stimulates endocytosis of the prion protein. *J Biol Chem* **273,** 33107-33110.

Peden, A. H., Head, M. W., Ritchie, D. L., Bell, J. E., and Ironside, J. W. (2004) Preclinical vCJD after blood transfusion in a PRNP codon 129 heterozygous patient. *Lancet* **364,** 527-529.

Pergami, P., Jaffe, H., and Safar, J. (1996) Semipreparative chromatographic method to purify the normal cellular isoform of the prion protein in nondenatured form. *Anal Biochem* **236,** 63-73.

Pfrieger, F. W. (2003) Cholesterol homeostasis and function in neurons of the central nervous system. *Cell Mol Life Sci* **60,** 1158-1171.

Prado, M. A., Alves-Silva, J., Magalhaes, A. C., Prado, V. F., Linden, R., Martins, V. R., and Brentani, R. R. (2004) PrPc on the road: trafficking of the cellular prion protein. *J Neurochem* **88,** 769-781.

Priller, J., Prinz, M., Heikenwalder, M., Zeller, N., Schwarz, P., Heppner, F. L., and Aguzzi, A. (2006) Early and rapid engraftment of bone marrow-derived microglia in scrapie. *J Neurosci* **26,** 11753-11762.

Prusiner, S. B. (1982) Novel proteinaceous infectious particles cause scrapie. *Science* **216,** 136-144.

Prusiner, S. B. (1998) Prions. *Proc Natl Acad Sci U S A* **95,** 13363-13383.

Prusiner, S. B. (2001) Shattuck lecture--neurodegenerative diseases and prions. *N Engl J Med* **344,** 1516-1526.

Prusiner, S. B., Groth, D. F., Bolton, D. C., Kent, S. B., and Hood, L. E. (1984) Purification and structural studies of a major scrapie prion protein. *Cell* **38,** 127-134.

Prusiner, S. B., Scott, M., Foster, D., Pan, K. M., Groth, D., Mirenda, C., Torchia, M., Yang, S. L., Serban, D., Carlson, G. A., and . (1990) Transgenetic studies implicate interactions between homologous PrP isoforms in scrapie prion replication. *Cell* **63,** 673-686.

Puglielli, L. (2008) Aging of the brain, neurotrophin signaling, and Alzheimer's disease: is IGF1-R the common culprit? *Neurobiol Aging* **29,** 795-811.

Quackenbush, J. (2002) Microarray data normalization and transformation. *Nat Genet* **32 Suppl,** 496-501.

Race, R. E., Fadness, L. H., and Chesebro, B. (1987a) Characterization of scrapie infection in mouse neuroblastoma cells. *J Gen Virol* **68 (Pt 5),** 1391-1399.

Race, R. E., Fadness, L. H., and Chesebro, B. (1987b) Characterization of scrapie infection in mouse neuroblastoma cells. *J Gen Virol* **68 (Pt 5),** 1391-1399.

Radonic, A., Thulke, S., Mackay, I. M., Landt, O., Siegert, W., and Nitsche, A. (2004) Guideline to reference gene selection for quantitative real-time PCR. *Biochem Biophys Res Commun* **313,** 856-862.

Rao, R. V., Ellerby, H. M., and Bredesen, D. E. (2004) Coupling endoplasmic reticulum stress to the cell death program. *Cell Death Differ* **11,** 372-380.

Reid, P. C., Sakashita, N., Sugii, S., Ohno-Iwashita, Y., Shimada, Y., Hickey, W. F., and Chang, T. Y. (2004) A novel cholesterol stain reveals early neuronal cholesterol accumulation in the Niemann-Pick type C1 mouse brain. *J Lipid Res* **45,** 582-591.

Riek, R., Hornemann, S., Wider, G., Billeter, M., Glockshuber, R., and Wuthrich, K. (1996) NMR structure of the mouse prion protein domain PrP(121-321). *Nature* **382,** 180-182.

Riek, R., Hornemann, S., Wider, G., Glockshuber, R., and Wuthrich, K. (1997) NMR characterization of the full-length recombinant murine prion protein, mPrP(23-231). *FEBS Lett* **413,** 282-288.

Riek, R., Wider, G., Billeter, M., Hornemann, S., Glockshuber, R., and Wuthrich, K. (1998) Prion protein NMR structure and familial human spongiform encephalopathies. *Proc Natl Acad Sci U S A* **95,** 11667-11672.

Riemer, C., Neidhold, S., Burwinkel, M., Schwarz, A., Schultz, J., Kratzschmar, J., Monning, U., and Baier, M. (2004) Gene expression profiling of scrapie-infected brain tissue. *Biochem Biophys Res Commun* **323,** 556-564.

Riemer, C., Queck, I., Simon, D., Kurth, R., and Baier, M. (2000) Identification of upregulated genes in scrapie-infected brain tissue. *J Virol* **74,** 10245-10248.

Rivera-Milla, E., Stuermer, C. A., and Malaga-Trillo, E. (2003) An evolutionary basis for scrapie disease: identification of a fish prion mRNA. *Trends Genet* **19,** 72-75.

Robakis, N. K., Devine-Gage, E. A., Jenkins, E. C., Kascsak, R. J., Brown, W. T., Krawczun, M. S., and Silverman, W. P. (1986) Localization of a human gene homologous to the PrP gene on the p arm of chromosome 20 and detection of PrP-related antigens in normal human brain. *Biochem Biophys Res Commun* **140,** 758-765.

Rothblat, G. H., Llera-Moya, M., Atger, V., Kellner-Weibel, G., Williams, D. L., and Phillips, M. C. (1999) Cell cholesterol efflux: integration of old and new observations provides new insights. *J Lipid Res* **40,** 781-796.

Roucou, X., Giannopoulos, P. N., Zhang, Y., Jodoin, J., Goodyer, C. G., and LeBlanc, A. (2005) Cellular prion protein inhibits proapoptotic Bax conformational change in human neurons and in breast carcinoma MCF-7 cells. *Cell Death Differ* **12,** 783-795.

Rubenstein, R., Carp, R. I., and Callahan, S. M. (1984) In vitro replication of scrapie agent in a neuronal model: infection of PC12 cells. *J Gen Virol* **65 (Pt 12),** 2191-2198.

Rubin, C. I. and Atweh, G. F. (2004) The role of stathmin in the regulation of the cell cycle. *J Cell Biochem* **93,** 242-250.

Runne, H., Kuhn, A., Wild, E. J., Pratyaksha, W., Kristiansen, M., Isaacs, J. D., Regulier, E., Delorenzi, M., Tabrizi, S. J., and Luthi-Carter, R. (2007) Analysis of potential transcriptomic biomarkers for Huntington's disease in peripheral blood. *Proc Natl Acad Sci U S A* **104,** 14424-14429.

Saeed, A. I., Sharov, V., White, J., Li, J., Liang, W., Bhagabati, N., Braisted, J., Klapa, M., Currier, T., Thiagarajan, M., Sturn, A., Snuffin, M., Rezantsev, A., Popov, D., Ryltsov, A., Kostukovich, E., Borisovsky, I., Liu, Z., Vinsavich, A., Trush, V., and Quackenbush, J. (2003) TM4: a free, open-source system for microarray data management and analysis. *Biotechniques* **34,** 374-378.

Sarnataro, D., Campana, V., Paladino, S., Stornaiuolo, M., Nitsch, L., and Zurzolo, C. (2004) PrP(C) association with lipid rafts in the early secretory pathway stabilizes its cellular conformation. *Mol Biol Cell* **15,** 4031-4042.

Schatzl, H. M., Da Costa, M., Taylor, L., Cohen, F. E., and Prusiner, S. B. (1995) Prion protein gene variation among primates. *J Mol Biol* **245,** 362-374.

Schatzl, H. M., Laszlo, L., Holtzman, D. M., Tatzelt, J., DeArmond, S. J., Weiner, R. I., Mobley, W. C., and Prusiner, S. B. (1997) A hypothalamic neuronal cell line persistently infected with scrapie prions exhibits apoptosis. *J Virol* **71,** 8821-8831.

Schettler, E., Steinbach, F., Eschenbacher-Kaps, I., Gerst, K., Muessdoerffer, F., Risch, K., Streich, W. J., and Frolich, K. (2006) Surveillance for prion disease in cervids, Germany. *Emerg Infect Dis* **12,** 319-322.

Schmitt-Ulms, G., Legname, G., Baldwin, M. A., Ball, H. L., Bradon, N., Bosque, P. J., Crossin, K. L., Edelman, G. M., DeArmond, S. J., Cohen, F. E., and Prusiner, S. B. (2001) Binding of neural cell adhesion molecules (N-CAMs) to the cellular prion protein. *J Mol Biol* **314,** 1209-1225.

Schneider, B., Mutel, V., Pietri, M., Ermonval, M., Mouillet-Richard, S., and Kellermann, O. (2003) NADPH oxidase and extracellular regulated kinases 1/2 are targets of prion protein signaling in neuronal and nonneuronal cells. *Proc Natl Acad Sci U S A* **100,** 13326-13331.

Sevin, M., Lesca, G., Baumann, N., Millat, G., Lyon-Caen, O., Vanier, M. T., and Sedel, F. (2007) The adult form of Niemann-Pick disease type C. *Brain* **130,** 120-133.

Sharma, A., Lambrechts, A., Hao, l. T., Le, T. T., Sewry, C. A., Ampe, C., Burghes, A. H., and Morris, G. E. (2005) A role for complexes of survival of motor neurons (SMN) protein with gemins and profilin in neurite-like cytoplasmic extensions of cultured nerve cells. *Exp Cell Res* **309,** 185-197.

Shmerling, D., Hegyi, I., Fischer, M., Blattler, T., Brandner, S., Gotz, J., Rulicke, T., Flechsig, E., Cozzio, A., von Mering, C., Hangartner, C., Aguzzi, A., and Weissmann, C. (1998) Expression of amino-terminally truncated PrP in the mouse leading to ataxia and specific cerebellar lesions. *Cell* **93,** 203-214.

Simons, K. and Ikonen, E. (1997) Functional rafts in cell membranes. *Nature* **387,** 569-572.

Skinner, P. J., Abbassi, H., Chesebro, B., Race, R. E., Reilly, C., and Haase, A. T. (2006) Gene expression alterations in brains of mice infected with three strains of scrapie. *BMC Genomics* **7,** 114.

Smith, P. G. and Bradley, R. (2003) Bovine spongiform encephalopathy (BSE) and its epidemiology. *Br Med Bull* **66,** 185-198.

Smith, P. K., Krohn, R. I., Hermanson, G. T., Mallia, A. K., Gartner, F. H., Provenzano, M. D., Fujimoto, E. K., Goeke, N. M., Olson, B. J., and Klenk, D. C. (1985) Measurement of protein using bicinchoninic acid. *Anal Biochem* **150,** 76-85.

Solforosi, L., Criado, J. R., McGavern, D. B., Wirz, S., Sanchez-Alavez, M., Sugama, S., DeGiorgio, L. A., Volpe, B. T., Wiseman, E., Abalos, G., Masliah, E., Gilden, D., Oldstone, M. B., Conti, B., and Williamson, R. A. (2004) Cross-linking cellular prion protein triggers neuronal apoptosis in vivo. *Science* **303,** 1514-1516.

Sparkes, R. S., Simon, M., Cohn, V. H., Fournier, R. E., Lem, J., Klisak, I., Heinzmann, C., Blatt, C., Lucero, M., Mohandas, T., and . (1986) Assignment of the human and mouse prion protein genes to homologous chromosomes. *Proc Natl Acad Sci U S A* **83,** 7358-7362.

Spielhaupter, C. and Schatzl, H. M. (2001) PrPC directly interacts with proteins involved in signaling pathways. *J Biol Chem* **276,** 44604-44612.

Stahl, N., Baldwin, M. A., Hecker, R., Pan, K. M., Burlingame, A. L., and Prusiner, S. B. (1992) Glycosylinositol phospholipid anchors of the scrapie and cellular prion proteins contain sialic acid. *Biochemistry* **31,** 5043-5053.

Stahl, N., Borchelt, D. R., Hsiao, K., and Prusiner, S. B. (1987) Scrapie prion protein contains a phosphatidylinositol glycolipid. *Cell* **51,** 229-240.

Sunyach, C., Jen, A., Deng, J., Fitzgerald, K. T., Frobert, Y., Grassi, J., McCaffrey, M. W., and Morris, R. (2003) The mechanism of internalization of glycosylphosphatidylinositol-anchored prion protein. *EMBO J* **22,** 3591-3601.

Svensson, P. A., Englund, M. C., Markstrom, E., Ohlsson, B. G., Jernas, M., Billig, H., Togerson, J. S., Wiklund, O., Carlsson, L. M., and Carlsson, B. (2003) Copper induces the expression of cholesterogenic genes in human macrophages. *Atherosclerosis* **169,** 71-76.

Tamguney, G., Giles, K., Bouzamondo-Bernstein, E., Bosque, P. J., Miller, M. W., Safar, J., DeArmond, S. J., and Prusiner, S. B. (2006) Transmission of elk and deer prions to transgenic mice. *J Virol* **80,** 9104-9114.

Taraboulos, A., Scott, M., Semenov, A., Avrahami, D., Laszlo, L., Prusiner, S. B., and Avraham, D. (1995) Cholesterol depletion and modification of COOH-terminal targeting sequence of the prion protein inhibit formation of the scrapie isoform. *J Cell Biol* **129,** 121-132.

Taylor, D. R. and Hooper, N. M. (2006) The prion protein and lipid rafts. *Mol Membr Biol* **23,** 89-99.

Temel, R. E., Tang, W., Ma, Y., Rudel, L. L., Willingham, M. C., Ioannou, Y. A., Davies, J. P., Nilsson, L. M., and Yu, L. (2007) Hepatic Niemann-Pick C1-like 1 regulates biliary cholesterol concentration and is a target of ezetimibe. *J Clin Invest* **117,** 1968-1978.

Turley, S. D., Burns, D. K., and Dietschy, J. M. (1998) Preferential utilization of newly synthesized cholesterol for brain growth in neonatal lambs. *Am J Physiol* **274,** E1099-E1105.

Turley, S. D., Burns, D. K., Rosenfeld, C. R., and Dietschy, J. M. (1996) Brain does not utilize low density lipoprotein-cholesterol during fetal and neonatal development in the sheep. *J Lipid Res* **37,** 1953-1961.

Tusher, V. G., Tibshirani, R., and Chu, G. (2001) Significance analysis of microarrays applied to the ionizing radiation response. *Proc Natl Acad Sci U S A* **98,** 5116-5121.

Valenza, M. and Cattaneo, E. (2006) Cholesterol dysfunction in neurodegenerative diseases: is Huntington's disease in the list? *Prog Neurobiol* **80,** 165-176.

Valenza, M., Rigamonti, D., Goffredo, D., Zuccato, C., Fenu, S., Jamot, L., Strand, A., Tarditi, A., Woodman, B., Racchi, M., Mariotti, C., Di Donato, S., Corsini, A., Bates, G., Pruss, R., Olson, J. M., Sipione, S., Tartari, M., and Cattaneo, E. (2005) Dysfunction of the cholesterol biosynthetic pathway in Huntington's disease. *J Neurosci* **25,** 9932-9939.

Vance, J. E. (2006) Lipid imbalance in the neurological disorder, Niemann-Pick C disease. *FEBS Lett* **580,** 5518-5524.

Vaya, J. and Schipper, H. M. (2007) Oxysterols, cholesterol homeostasis, and Alzheimer disease. *J Neurochem* **102,** 1727-1737.

Vey, M., Pilkuhn, S., Wille, H., Nixon, R., DeArmond, S. J., Smart, E. J., Anderson, R. G., Taraboulos, A., and Prusiner, S. B. (1996) Subcellular colocalization of the cellular and scrapie prion proteins in caveolae-like membranous domains. *Proc Natl Acad Sci U S A* **93,** 14945-14949.

Vilette, D., Andreoletti, O., Archer, F., Madelaine, M. F., Vilotte, J. L., Lehmann, S., and Laude, H. (2001) Ex vivo propagation of infectious sheep scrapie agent in heterologous epithelial cells expressing ovine prion protein. *Proc Natl Acad Sci U S A* **98,** 4055-4059.

Vincent, I., Bu, B., Hudson, K., Husseman, J., Nochlin, D., and Jin, L. (2001) Constitutive Cdc25B tyrosine phosphatase activity in adult brain neurons with M phase-type alterations in Alzheimer's disease. *Neuroscience* **105,** 639-650.

Vorberg, I., Raines, A., Story, B., and Priola, S. A. (2004) Susceptibility of common fibroblast cell lines to transmissible spongiform encephalopathy agents. *J Infect Dis* **189,** 431-439.

Wadsworth, J. D. and Collinge, J. (2007) Update on human prion disease. *Biochim Biophys Acta* **1772,** 598-609.

Wadsworth, J. D., Joiner, S., Hill, A. F., Campbell, T. A., Desbruslais, M., Luthert, P. J., and Collinge, J. (2001) Tissue distribution of protease resistant prion protein in variant Creutzfeldt-Jakob disease using a highly sensitive immunoblotting assay. *Lancet* **358,** 171-180.

Wang, J. M., Liu, L., Irwin, R. W., Chen, S., and Brinton, R. D. (2008) Regenerative potential of allopregnanolone. *Brain Res Rev* **57,** 398-409.

Wang, X., Sato, R., Brown, M. S., Hua, X., and Goldstein, J. L. (1994) SREBP-1, a membrane-bound transcription factor released by sterol-regulated proteolysis. *Cell* **77,** 53-62.

Weissmann, C. (1991) A 'unified theory' of prion propagation. *Nature* **352,** 679-683.

Weissmann, C., Fischer, M., Raeber, A., Bueler, H., Sailer, A., Shmerling, D., Rulicke, T., Brandner, S., and Aguzzi, A. (1996) The use of transgenic mice in the investigation of transmissible spongiform encephalopathies. *Int J Exp Pathol* **77,** 283-293.

Westaway, D., Cooper, C., Turner, S., Da Costa, M., Carlson, G. A., and Prusiner, S. B. (1994) Structure and polymorphism of the mouse prion protein gene. *Proc Natl Acad Sci U S A* **91,** 6418-6422.

Westergard, L., Christensen, H. M., and Harris, D. A. (2007) The cellular prion protein (PrP(C)): its physiological function and role in disease. *Biochim Biophys Acta* **1772,** 629-644.

Whitfield, J. F. (2006) Can statins put the brakes on Alzheimer's disease? *Expert Opin Investig Drugs* **15,** 1479-1485.

Wickner, R. B. (1994) [URE3] as an altered URE2 protein: evidence for a prion analog in Saccharomyces cerevisiae. *Science* **264,** 566-569.

Wilesmith, J. W., Wells, G. A., Cranwell, M. P., and Ryan, J. B. (1988) Bovine spongiform encephalopathy: epidemiological studies. *Vet Rec* **123,** 638-644.

Will, R. G. (1998) New variant Creutzfeldt-Jakob disease. *Dev Biol Stand* **93,** 79-84.

Will, R. G., Ironside, J. W., Zeidler, M., Cousens, S. N., Estibeiro, K., Alperovitch, A., Poser, S., Pocchiari, M., Hofman, A., and Smith, P. G. (1996) A new variant of Creutzfeldt-Jakob disease in the UK. *Lancet* **347,** 921-925.

Wille, H., Michelitsch, M. D., Guenebaut, V., Supattapone, S., Serban, A., Cohen, F. E., Agard, D. A., and Prusiner, S. B. (2002) Structural studies of the scrapie prion protein by electron crystallography. *Proc Natl Acad Sci U S A* **99,** 3563-3568.

Williams, E. S. (2005) Chronic wasting disease. *Vet Pathol* **42,** 530-549.

Williams, E. S. and Miller, M. W. (2002) Chronic wasting disease in deer and elk in North America. *Rev Sci Tech* **21,** 305-316.

Williams, M. A. and McCluer, R. H. (1980) The use of Sep-Pak C18 cartridges during the isolation of gangliosides. *J Neurochem* **35,** 266-269.

Wong, B. S., Venien-Bryan, C., Williamson, R. A., Burton, D. R., Gambetti, P., Sy, M. S., Brown, D. R., and Jones, I. M. (2000) Copper refolding of prion protein. *Biochem Biophys Res Commun* **276,** 1217-1224.

Wood, K. V., de Wet, J. R., Dewji, N., and DeLuca, M. (1984) Synthesis of active firefly luciferase by in vitro translation of RNA obtained from adult lanterns. *Biochem Biophys Res Commun* **124,** 592-596.

Wopfner, F., Weidenhofer, G., Schneider, R., von Brunn, A., Gilch, S., Schwarz, T. F., Werner, T., and Schatzl, H. M. (1999) Analysis of 27 mammalian and 9 avian PrPs reveals high conservation of flexible regions of the prion protein. *J Mol Biol* **289,** 1163-1178.

Wu, M. X. (2003) Roles of the stress-induced gene IEX-1 in regulation of cell death and oncogenesis. *Apoptosis* **8,** 11-18.

Wyatt, J. M., Pearson, G. R., Smerdon, T. N., Gruffydd-Jones, T. J., Wells, G. A., and Wilesmith, J. W. (1991) Naturally occurring scrapie-like spongiform encephalopathy in five domestic cats. *Vet Rec* **129,** 233-236.

Xiang, W., Hummel, M., Mitteregger, G., Pace, C., Windl, O., Mansmann, U., and Kretzschmar, H. A. (2007) Transcriptome analysis reveals altered cholesterol metabolism during the neurodegeneration in mouse scrapie model. *J Neurochem* **102,** 834-847.

Xiang, W., Windl, O., Wunsch, G., Dugas, M., Kohlmann, A., Dierkes, N., Westner, I. M., and Kretzschmar, H. A. (2004) Identification of differentially expressed genes in scrapie-infected mouse brains by using global gene expression technology. *J Virol* **78,** 11051-11060.

Yang, Y. H., Dudoit, S., Luu, P., Lin, D. M., Peng, V., Ngai, J., and Speed, T. P. (2002) Normalization for cDNA microarray data: a robust composite method addressing single and multiple slide systematic variation. *Nucleic Acids Res* **30,** e15.

Yao, J. K. and Rastetter, G. M. (1985) Microanalysis of complex tissue lipids by high-performance thin-layer chromatography. *Anal Biochem* **150,** 111-116.

Yokoyama, C., Wang, X., Briggs, M. R., Admon, A., Wu, J., Hua, X., Goldstein, J. L., and Brown, M. S. (1993) SREBP-1, a basic-helix-loop-helix-leucine zipper protein that controls transcription of the low density lipoprotein receptor gene. *Cell* **75,** 187-197.

Zahn, R., Liu, A., Luhrs, T., Riek, R., von Schroetter, C., Lopez, G. F., Billeter, M., Calzolai, L., Wider, G., and Wuthrich, K. (2000) NMR solution structure of the human prion protein. *Proc Natl Acad Sci U S A* **97,** 145-150.

Zanata, S. M., Lopes, M. H., Mercadante, A. F., Hajj, G. N., Chiarini, L. B., Nomizo, R., Freitas, A. R., Cabral, A. L., Lee, K. S., Juliano, M. A., de Oliveira, E., Jachieri, S. G., Burlingame, A., Huang, L., Linden, R., Brentani, R. R., and Martins, V. R. (2002) Stress-inducible protein 1 is a cell surface ligand for cellular prion that triggers neuroprotection. *EMBO J* **21,** 3307-3316.

Zeidler, M., Johnstone, E. C., Bamber, R. W., Dickens, C. M., Fisher, C. J., Francis, A. F., Goldbeck, R., Higgo, R., Johnson-Sabine, E. C., Lodge, G. J., McGarry, P., Mitchell, S., Tarlo, L., Turner, M., Ryley, P., and Will, R. G. (1997) New variant Creutzfeldt-Jakob disease: psychiatric features. *Lancet* **350,** 908-910.

Zhang, C. C., Steele, A. D., Lindquist, S., and Lodish, H. F. (2006) Prion protein is expressed on long-term repopulating hematopoietic stem cells and is important for their self-renewal. *Proc Natl Acad Sci U S A* **103,** 2184-2189.

Zigas, V. and Gajdusek, D. C. (1957) Kuru: clinical study of a new syndrome resembling paralysis agitans in natives of the Eastern Highlands of Australian New Guinea. *Med J Aust* **44,** 745-754.

6. Abbreviations

μ	micro (10^{-6})
7-AAD	7-AminoActinomycin D
A	adenine, ampere
Fig.	figure
Ab	antibody
APS	ammonium persulfate
aa	amino acid
ATP	adenosine 5′-triphosphate
b	base
bp	base pare
BSA	bovine serum albumin
BSE	bovine spongiform encephalopathy
C	cytosine
CJD	Creutzfeldt-Jakob-Disease
vCJD	variant Creutzfeldt-Jakob-Disease
CNS	central nervous system
Cyp51	cytochrome p450 family 51
Da	dalton
DMSO	dimethyl sulfoxide
DNA	deoxyribonucleic acid
DNase	desoxyribonuclease
DOC	sodium deoxycholate
dsDNA	double strand DNA
dNTP	desoxyribonucleosid-5´-Triphosphat
EDTA	ethylene diamine tetraacetat, sodium salt
ER	endoplasmatic reticulum
EST	expressed sequence tag
EtBr	ethidium bromide
EtOH	ethanol
Et-SH	β-mercapto-ethanol
Fdft1	farnesyl diphosphate farnesyl transferase 1
FFI	fatale familial insomnia

FCS	fetal calve serum
g	gram
G	guanine
GndHCl	guanidine hydrochloride
GPI anchor	glycosyl phosphatidyl inositol anchor
h	hour
$H_2O_{dest.}$	distilled water
$H_2O_{bidest.}$	double distilled, de-ionised und filtered water
Hmgcr	3-hydroxy-3-methylglutaryl-Coenzyme A reductase
Hmgcs1	3-hydroxy-3-methylglutaryl-Coenzyme A synthase 1
Idi1	isopentenyl-diphosphate delta-isomerase 1
kb	kilo base pair
kDa	kilo dalton
l	litre
Ldlr	low density lipoprotein receptor
m	meter, milli (10^{-3}),
M	molar
MESA	MOPS-EDTA-sodium acetate buffer
min	minute
MM	molar mass
Mvk	mevalonate kinase
n	nano (10^{-9})
N	nitrogen
OD	optic density
p	piko (10^{-12})
PAA	polyacrylamide
PAGE	polyacrylamide gel electrophoresis
PBS	phosphate buffered saline
PCR	polymerase chain reaction
PVDF membrane	polyvinylidin-difluorid-membrane
PrP^C	cellular prion protein
PrP^{Sc}	pathological isoform of PrP^C
RML	mouse adapted scrapie strain from the Rocky Mountain Laboratory
RNA	ribonucleic acid

RNase	ribonuclease
RPII	RNA polymerase II
rpm	rounds per minute
RT	room temperature
RT-PCR	reverse transcription-PCR
Sc4mol	C-4 methyl sterol oxidase
SDS	sodium dodecylsulfate
sec	second
SRE	sterol regulatory element
Srebf2	sterol regulatory element binding factor 2
Srebp2	sterol regulatory element binding protein 2
Strep	streptomycin
T	thymine
TAE	Tris/ Acetate/ EDTA
Taq	Thermus aquaticus
TE	Tris/ EDTA
TEMED	N,N,N´,N´-Tetramethylethylendiamine
Tris	tris(hydroxymethyl)aminomethane
TSE	Transmissible spongiform encephalopathy
U	unit
UV	ultraviolet
V	Volt
% (v/v)	volume per volume
% (w/v)	weight pre volume

7. Publications and conventional presentations

Publications

1. Stengel A, **Bach C**, Vorberg I, Frank O, Gilch S, Lutzny G, Seifarth W, Erfle V, Maas E, Schätzl H, Leib-Mösch C, Greenwood AD: (2006) Prion infection influences murine endogenous retrovirus expression in neuronal cells. Biochem Biophys Res Commun 343, 825-831.

2. Gilch S., **Bach C**., Lutzny G., Vorberg I., and Schatzl H. M. (2009) Inhibition of cholesterol recycling impairs cellular PrP(Sc) propagation. Cell Mol Life Sci 66, 3979-3991.

3. **Bach, C**., Gilch, S., Rost, R., Greenwood, A. D., Horsch, M., Hajj, G. N., Brodesser, S., Facius, A., Schadler, S., Sandhoff, K., Beckers, J., Leib-Mosch, C., Schatzl, H. M., and Vorberg, I. (2009) Prion-induced activation of cholesterogenic gene expression by a sterol regulatory element binding protein (SREBP2) in neuronal cells. J Biol Chem. 284, 31260-31269.

Oral presentations

1. Final symposium of the Bayrischer Forschungsverbund FORPRION; oral presentation: "Prion infection alters gene expression in mouse neuroblastoma cells and leads to an up-regulation of the cholesterol pathway"; Munich, May 2007

2. Annual Meeting of the Institute of Virology; oral presentation: "Prion-induced activation of Srebp2-regulated gene expression in neuronal cells", abstract book 5th session, 4th talk; Tutzing, February 2008

Poster presentations

3. Annual Meeting of the Gesellschaft für Virologie; poster presentation: "Differential gene expression in prion infected cell culture versus uninfected and pentosan polysulfate treated cells"; Hannover, 2005

4. Annual Meeting of the Institute of Virology; poster presentation: "Differential gene expression in prion infected cell culture versus uninfected and cured cells"; Hohenkammern, 2005

5. Annual Meeting of the Bayrischer Forschungsverbund FORPRION; poster presentation: "Differential gene expression in prion infected cell culture versus uninfected cells"; Munich, 2006

6. Annual Meeting of the Gesellschaft für Virologie; poster presentation: "Differential gene expression in prion infected cell culture versus uninfected cells"; Munich, 2006

7. Annual Meeting of the Gesellschaft für Virologie; poster presentation: "Prion induced activation of Srebp2-regulated gene expression in neuroblastoma cells"; Nürnberg, 2007

8. Annual Meeting of the Gesellschaft für Virologie; poster presentation: "Prion induced activation of cholesterogenic gene expression by a sterol regulatory binding protein (Srebp2) in neuronal cells"; Leipzig, 2009

8. Acknowledgement